2012-08-07

Characterization of the Cellular and Organellar Dynamics that Occur with a Partial Depletion of Mitochondrial DNA when Arabidopsis Organellar DNA Polymerase IB is Mutated

John D. Cupp
Brigham Young University - Provo

Characterization of the Cellular and Organellar Dynamics that Occur with a Partial Depletion of Mitochondrial DNA when *Arabidopsis* Organellar DNA Polymerase IB Is Mutated

John David Cupp

A dissertation submitted to the faculty of
Brigham Young University
in partial fulfillment of the requirements for the degree of

Doctor of Philosophy

Brent L. Nielsen, Chair
Laura C. Bridgewater
William R. McCleary
Craig E. Coleman
Jeff J. Maughan

Department of Microbiology and Molecular Biology

Brigham Young University

December 2012

ABSTRACT

Characterization of the Cellular and Organellar Dynamics that Occur with a Partial Depletion of Mitochondrial DNA when *Arabidopsis* Organellar DNA Polymerase IB Is Mutated

John David Cupp
Department of Microbiology and Molecular Biology, BYU
Doctor of Philosophy

Plant mitochondrial genomes are large and complex, and the mechanisms for maintaining mitochondrial DNA (mtDNA) remain unclear. *Arabidopsis thaliana* has two DNA polymerase genes, polIA and polIB, that have been shown to be dual localized to mitochondria and chloroplasts but are unequally expressed within primary plant tissues involved in cell division or cell expansion. PolIB expression is observed at higher levels in both shoot and root apexes, suggesting a possible role in organelle DNA replication in rapidly dividing or expanding cells. It is proposed that both polIA and polIB are required for mtDNA replication under wild type conditions. An *Arabidopsis* T-DNA polIB mutant has a 30% reduction in mtDNA levels but also a 70% induction in polIA gene expression. The polIB mutant shows an increase relative to wild type plants in the number of mitochondria that are significantly smaller in relative size, observed within hypocotyl epidermis cells that have a reduced rate of cell expansion. These mutants exhibit a significant increase in gene expression for components of mitorespiration and photosynthesis, and there is evidence for an increase in both light to dark (transitional) and light respiration levels. There is not a significant difference in dark adjusted total respiration between mutant and wild type plants. Chloroplast numbers are not significantly different in isolated mesophyll protoplasts, but mesophyll cells from the mutant are significantly smaller than wild type. PolIB mutants exhibit a three-day delay in chloroplast development but after 7dpi (days post-imbibition) there is no difference in relative plastid DNA levels between the mutant and wild type. Overall, the polIB mutant exhibits an adjustment in cell homeostasis, which enables the maintenance of functional mitochondria but at the cost of normal cell expansion rates.

Keywords: polymerase gamma, PolIA, PolIB, TWINKLE, mitochondria, DNA replication

ACKNOWLEDGEMENTS

I would like to thank my wife, four children, and my parents for their patience, encouragement, and support in taking this journey with me. I would like to thank Dr. Brent Nielsen for accepting me as his student and for the generous amount of time he has provided for my graduate education. I would also like to thank the members of my committee: Drs. William McCleary, Laura Bridgewater, Chin-Yo Lin, Craig Coleman, and Peter Maughan for their patience and direction provided to me throughout this educational experience. I thank Dr. Leslie Sieburth (Univ. of Utah) for training me in plant genetic and molecular methodology, sharing with me the cycB1:1::GFP transgenic reporter line, providing me with bench space to conduct my experiments, and providing me with growth chamber space so I could obtain consistent phenotypic results from *Arabidopsis* mutants. I thank Dr. Weiping Zhang (Univ. of Utah) for providing me with cDNA generated from selected *Arabidopsis* (Col-0) tissues (Zhang et al., 2010) and for sharing unpublished primers for analysis of gene expression from the plastid genome. I thank Dr. David Logan (Univ. of Saskatchewan, Canada) for sharing the *Arabidopsis* mtGFP transgenic line (Columbia background). I also thank Dr. Dong-Keun Lee (Univ. of Utah) for his advice in plant genetics and molecular techniques. I thank Drs. Sam St. Clair and Richard Gill (Brigham Young Univ.) for allowing me to use their Li-Cor equipment. I would like to thank the following undergraduate and graduate students that I had the opportunity to train in various lab techniques: Ashley Wright, Bennjamin Fronk, Dr. Bilquees Gul, Bryan Payne, Cindee Perry, David Hawkins, Elizabeth Haws, James Schmitt, Jeff Brammer, Kallie Tibbitts, Hsin-Tze Lu, Logan Hazard, Madeleine Bailey, Meagan Wyllie, Peter Hawkins, Ramesh Tiwari, Scott Jones, Shiva Pandey, Tatiana Alarcón, Travis Hunt, Tyler Hedin, Van Willis, Whitney Davison, and Mary Rennick.

TABLE OF CONTENTS

LIST OF FIGURES

INTRODUCTION

Mitochondria are essential to higher eukaryotic cells because they provide intracellular energy in the form of ATP by the process of oxidative phosphorylation (Hatefi, 1985). In addition to energy production, mitochondria are involved in a number of metabolic processes that include, but are not limited to, cell retrograde signaling, cell division, and cell death (McBride et al., 2006). In plants, chloroplasts coordinate with mitochondria by harvesting and converting light energy, forming glucose and providing oxygen for oxidative phosphorylation by both mitorespiration and chlororespiration (Aluru and Rodermel, 2004; Rumeau et al., 2007; Hausler et al., 2009). The plastid is also involved in the production of fatty acids (Joyard et al., 2010; Chen et al., 2012), heme synthesis by the C_5 pathway (Hamel et al., 2009), biosynthesis of terpenes (Aharoni et al., 2003), and starch production and storage (Ponce et al., 2008). The maintenance of genetic information and communication between the nucleus, plastid, and mitochondria are required for normal plant growth and development (Okada and Brennicke, 2006).

The majority of the genes required for organelle functions are located within the cell nucleus, while some genes are encoded in the mitochondrial and plastid genomes (Elo et al., 2003; de Grey, 2005; Armisen et al., 2008). Genomes are multi-copy in both mitochondria and plastids, but the copy number is variable. Recent publications indicate that the mitochondrion (Butow and Avadhani, 2004; Rhoads and Subbaiah, 2007; Schwarzlander et al., 2012) and the plastid (Kropat et al., 1997; Pfannschmidt, 2003) have the ability to control nuclear gene expression of organelle-targeted genes through retrograde signaling. In addition to nuclear control of organelle function, signaling from the mitochondria has been observed to control plastid function and vice versa (Hamel et al., 2009; Toshoji et al., 2011). Cross-talk between

these three compartments generally occurs via transcriptional control (Sekito et al., 2000), RNA editing (Tang et al., 2010), metabolite sensing (Leister, 2005), or substrate limitation responses (Hamel et al., 2009). This dynamic and functional balance between these three compartments is essential for cell viability.

Adjustments in cellular dynamics and communication are observed when housekeeping genes that target these organelles are disrupted (Conley and Hanson, 1995; Pesaresi et al., 2006; Juszczuk et al., 2012). The majority of housekeeping genes responsible for organelle genome maintenance are found in the nucleus. The mechanisms involved in plastid DNA (ptDNA) maintenance are better understood than those for plant mitochondrial DNA (mtDNA) maintenance, yet there are still many details that are not understood (Nielsen et al., 2010). Gene redundancy and dual targeting of housekeeping gene products to both organelles have been reported (Elo et al., 2003; Wall et al., 2004; Shedge et al., 2007), including two DNA polymerase genes (polIA and polIB) and a TWINKLE-helicase gene found in *Arabidopsis* (Christensen et al., 2005; Carrie et al., 2009). Recently, the characterization of the two organellar localized DNA polymerase genes has shown a reduction in both mitochondrial and plastid relative genome abundance when either of these genes is knocked out (Parent et al., 2011). It appears that because of the redundancy of having two DNA polymerases that target both organelles, *Arabidopsis* is capable of maintaining a sub-lethal phenotype when either gene is mutated. Generally, severe to lethal phenotypes can occur when the mitochondrial genome is fully depleted (Dimmock et al., 2010; Schaller et al., 2011).

Parent et al. (2011) observed that when the expression of the full-length polIB gene is knocked down the plant exhibits a slow growth phenotype. No plant phenotype was observed when polIA expression was depleted. Single mutants for either gene showed a similar reduction

in both ptDNA and mtDNA levels. One of the novel differences reported was that polIB has a functional 3' to 5' exonuclease domain for DNA proofreading. But it remains unclear why the polIB mutant has a slow growth phenotype. We hypothesize that PolIB is essential for normal mtDNA replication, as PolIA cannot fully compensate for the loss of PolIB. The cell monitors expression of polIB, and when depleted, both physiological and cellular dynamics are adjusted to compensate for the loss of polIB expression.

Literature Review: Introduction to Organelles

Mitochondria consist of a network of individual organelles, which are constantly undergoing fission and fusion events (Westermann, 2010). Hence, the overall morphological structure of these organelles differs based on organelle movement dynamics (Logan, 2006). Historically, these organelles have not demonstrated any developmental differences based on their individual morphology or function. Generally, the numbers of mitochondria per cell are dependent on tissue type and cell location. Gene expression patterns affecting mitochondrial genome maintenance and overall function are directly affected by tissue type and cell location within an individual organism (Reddy et al., 2004; Monticone et al., 2010; Marin-Garcia et al., 2012). Both cellular and environmental cues monitored by the mitochondria are observed to trigger retrograde signaling to the nucleus which alters cellular gene expression patterns to maintain both mitochondrial and cellular homeostasis (Jandova et al., 2012).

Recently, a mitochondrial cage-like structure surrounding the cell nucleus has been observed within the meristem region of plants and animal stem cells (Segui-Simarro et al., 2008; Antico Arciuch et al., 2012). This centralized structure is maintained throughout the cell cycle and has been observed to divide with the cell upon anaphase and cytokinesis. Smaller mitochondria are observed to bud out from the centralized mitochondrion to form peripheral

mitochondria during the cellular growth phases of the cell cycle. Upon entry into M phase of the cell cycle, these peripheral mitochondria are recalled back and fuse again with the centralized structure. It is unknown if the centralized mitochondrion is developmentally different from peripheral mitochondria or if this structure is similar in function to protoplasts found in plastid differential development. As with protoplasts (Bendich, 2004), it has been proposed that this centralized mitochondrion is where the majority of the mitochondrial genome is replicated and or maintained (Logan, 2010). Interestingly, once plant cells divide out of the meristematic zone and undergo differential development, the cage-like mitochondrial structure is no longer observed surrounding the nucleus. Studies on the mechanisms controlling mitochondrial dynamics in relation to cell division have led to significant advancements over the last decade, but a complete understanding has not been obtained.

Like mitochondria, chloroplasts have been observed to undergo fission and fusion events. These organelles also move throughout the cell but at a much slower rate than mitochondria. It is speculated that the observed differences in the rate of movement between these two types of organelles is because the chloroplasts are significantly larger in physical size when compared to mitochondria. Unlike the mitochondrial network, chloroplasts have a distinctly specific morphological structure. The chloroplast network consists of defined borders between individual organelles. Borders between individual mitochondria are difficult to determine because of the dynamic nature of mitochondrial morphology. Similar to mitochondria, the numbers of individual chloroplasts per cell are directly dependent upon tissue and cell type and where the cell is located within the tissue.

Another major difference between chloroplasts and mitochondria is that chloroplasts are part of a group of organelles called plastids. Plastid members are developmentally different from

one another and have specific cellular functions, even though each plastid contains the same genome. The plastid developmental program, mechanisms, and genes required for differential plastid development are poorly understood. It is known that the plastid genome must be maintained for biological function regardless of plastid type. As with mitochondria, genes expressed from both the nucleus and the organelle genome are required for plastid genome maintenance. Many examples have been demonstrated in model organisms (like *Arabidopsis*) where nuclear encoded genes required for organellar genome maintenance are dual-targeted to both the mitochondria and chloroplast (to be discussed in greater detail) (Peeters and Small, 2001).

Literature Review: Organellar Function and Evolution

Mitochondria are the site of oxidative phosphorylation and are involved in cellular respiration. Plastid functions, and more specifically chloroplasts, are required for photosynthesis in plants. These two essential functions are just a narrow description of the overall biological functions these organelles provide for the cell. Genetic and molecular analysis of mutants have greatly influenced these two fields of study in the determination of organellar biological function. These tools have aided in the determination of functional genes from non-coding open reading frames within their respective organellar genomes. Organelle targeted nuclear encoded genes required for biological function have also been identified using these same techniques. Genetic, biochemical, and molecular analysis have led to a greater understanding of organellar phenotypic and functional differences. Through these experiments, different types of plastids were found to be developmentally distinct with both evolutionary and genetic similarities. The following are plastids with specific functions (Mullet, 1988).

Proplastids are undifferentiated non-photosynthetic organelles located within the plant meristematic stem cells (Vothknecht and Westhoff, 2001). All plastids are derivatives from proplastids. These organelles possess a complete copy of the plastid genome. In addition, Bendich (2006) and associates have proposed the majority of plastid DNA is replicated within this organelle prior to plastid development. Experiments have demonstrated that as a cell begins to migrate away from the meristematic region and the plastids proceed to undergo development and continue to age, the relative DNA abundance levels within these specialized plastids proceeds to decline until eventually the DNA is undetectable or leaf senescence occurs.

Plant leucoplasts are a subcategory of non-photosynthetic plastids that consists of amyloplasts, elaioplasts, and proteinoplasts (Charuvi et al., 2012). Amyloplasts synthesize and store starch (Fernie et al., 2002). Statocytes are a specialized amyloplast linked to gravitropism and are located within both the root tip and the shoot apical meristem (Driss-Ecole et al., 2003). Elaioplasts produce and store sterol esters and tapetosomes, which are required for pollen maturation and pollen tube elongation (Ishiguro et al., 2010). Proteinoplasts have large protein inclusion bodies. The functional role of this organelle remains unknown (Kohler and Hanson, 2000; Wise, 2007).

Sieve-element plastids develop from the proplastid, as do the leucoplasts, etioplasts, and the chloroplasts. These organelles are found in the phloem cells and consist of S-type (starch storage) and P-type (protein storage). These organelles are also found in spermatophytes (van Bel, 2003).

Etioplasts are transitional organelles between protoplasts and fully formed chloroplasts. These organelles are found in hypocotyl tissue and cotyledons prior to chloroplast differentiation upon white light detection (Rodriguez-Villalon et al., 2009). The major function of etioplasts is

to synthesize gibberellic acids (GA), which are growth hormones that stimulate hypocotyl elongation under etiolated growth (Neff et al., 2000). GA also influences the plant developmental program switch from skotomorphogenesis to photomorphogenesis (Alabadi et al., 2004). Much like etioplasts the chromoplasts have the ability to switch to or from chloroplasts. In general, chromoplasts are carotenoid-rich organelles that are directly involved in fruit development, ripening, color, and aroma (Klee, 2010; Barry et al., 2012).

Chloroplasts are mainly involved in photosynthesis and are found in algae, C_3 pathway plants, and C_4 pathway plants. The C_3 carbon fixation pathway extracts carbon directly from atmospheric carbon dioxide whereas the C_4 carbon fixation pathway retrieves carbon dioxide from malate. These organelles are also involved in the following biological functions: fatty acid lipid synthesis (Nobusawa and Umeda, 2012), aromatic amino acid synthesis (Schmid and Amrhein, 1995), nitrogen and sulfate assimilation (Fischer and Klein, 1988; Kopriva, 2006), light sensing and gene expression regulation by cell signaling (Ruckle et al., 2012), cell signaling (Foyer and Noctor, 2005; Koussevitzky et al., 2007; Nomura et al., 2012), cellular CO_2 / O_2 concentration sensing and stomata control (Assmann, 1999; Miller et al., 2010). Chlororespiration and photorespiration occur as secondary functions of the chloroplast photosynthesis machinery. Chloroplasts also differentiate into gerontoplasts when leaves begin to enter the senescence phase (Wise, 2007).

Evolutionary derivatives of plastids are found in animal and protozoan organisms. These organelles contain genomes with similar gene content as plant plastids. These organelles are divided into the following categories: muroplasts, rhodoplasts, kleptoplasts, and apicoplasts. Muroplasts are photosynthetic organelles that are found in Glaucocystophytic algae (Wise and Hoober, 2006). Rhodoplasts are found in *Rhodophytes* (specifically Gracilaria tenuistipitata).

They harvest red light by photosynthesis (Hagopian et al., 2004). Apicoplasts are organelle derivatives from amyloplasts that are found in *Plasmodium falciparum* (Lim and McFadden, 2010). Kleptoplasts are remnants of chloroplasts that have been removed from green algae cells by digestion from sea slugs (*Sacoglossan*). Once removed these chloroplasts remain undigested and are incorporated into the cells of the new host's gut lumen. These chloroplasts remain photosynthetically functional up to six months (Wagele et al., 2011).

These plastid derivatives provide supporting evidence for the endosymbiotic theory. Genetic and phylogenetic analysis indicates these organelles are similar to present day cyanobacteria. An ancient relative to cyanobacteria is proposed to have initiated a symbiotic relationship with an early eukaryotic host. There remains a debate if the initiation of this relationship occurred once or up to three specific times throughout evolutionary history. Regardless, the endosymbiotic event did occur and has led to the current plastid organelles we observe. The linking of plastid genomes to cyanobacteria has aided the field of plastid research in the ability to predict and propose genes responsible for mechanisms involved in both plastid function and genome maintenance.

Similar to plastids, the mitochondria are believed to have evolved from an earlier and singular symbiotic event where an ancient relative to the current day alpha-proteobacterium (aerobic bacterium) was engulfed by another anaerobic bacterium. With evolutionary time came the current-day mitochondria. As with plastids, many of the original genes from the symbiotic organisms were either lost over time or transferred to the nucleus leaving a required organellar genome. Through genetic analysis, many gene similarities are found between mitochondrial, plastid, prokaryotic, nuclear, and bacteriophage genomes. In addition, many functional genes have been successfully identified and characterized from mutational analysis of gene

homologues found between these genomes. In summary, the endosymbiotic theory in combination with biosystematics and molecular tools has led to the identification and characterization of gene homologs that are essential to mitochondrial biological function.

Mitochondria are involved in numerous metabolic and cellular activities. Typically if mitochondrial functions become disrupted without compensation, detrimental or potential lethal effects to the cell shortly come to pass. The majority of the following biological processes are directly linked to all functioning mitochondrial networks.

Mitochondria transcribe and translate many of the protein complex precursors for respiratory complexes I-V and cytochrome c. These protein complexes are required to maintain ATP and NADH cellular levels in homeostasis (Brookes et al., 2004). Apoptosis is initiated by the cytosolic release of cytochrome c from the mitochondrial membrane when these organelles fail to regulate the accumulation of reactive oxidative species (Smith and Schnellmann, 2012). Apoptosis is also initiated when mitochondria fail to regulate intracellular calcium homeostasis (Poburko and Demaurex, 2012).

Mitochondria are directly involved in maintaining various forms of cellular homeostasis. Intracellular iron homeostasis is controlled by mitochondrial uptake of iron from the cytosol. Iron within the inner mitochondria matrix is then synthesized into heme, Fe-S clusters, or cofactors (Levi and Rovida, 2009; Hederstedt, 2012). Lipid homeostasis is also controlled by mitochondrial absorption of excess cytosolic lipids, lipid beta oxidation catabolism, and mitophagy (Glick et al., 2012). Interestingly the mitochondrial network is not directly connected to the vascular transport system (van Meer et al., 2008). Alternatively, specific mitochondrial lipids are synthesized when mitochondrial-associated membranes of the endoplasmic reticulum fractionate with mitochondria and create a new compartment for lipid biosynthesis (Raturi and

Simmen, 2012). In addition to the mitochondrial control of cellular homeostasis these organelles are also involved in the inter-conversion of amino acids. More specifically these organelles serve as an intermediate step in plant photorespiration conversion of glycine to serine.

Mitochondria have additional general functions, including the following. Mitochondrial ribozymes function in mitochondrial protein folding as molecular chaperones (Das et al., 2011). These organelles produce precursors of a number of steroids. Mitochondria are involved in nucleotide metabolism (Elo et al., 2003). DNA repair enzymes, replication machinery, RNA polymerase, transcription machinery, and RNA editing machinery are incorporated from nuclear encoded gene products to function within the inner mitochondria matrix. Through retrograde signaling these mitochondria have the ability to control gene expression in the nucleus. In plants, cross-talk between mitochondria and plastids is also common.

The majority of the mitochondrial functions described occur in all eukaryotic organisms except for *Giardia intestinalis*. This eukaryote has a mitochondrial-like structure called a mitosome. This unique organelle evolved from mitochondria but no long contains a genome (Tovar et al., 2003). A better understanding of mitosomes may provide greater insight into the relationship between mitochondria and the peroxisomes.

In summary, functional mitochondria and plastids are essential to higher plants. As described in this section, organelles are involved in a number of metabolic and cellular activities that when disrupted without compensation lead to detrimental or potentially lethal effects on the cell. Nuclear encoded genes provide the majority of molecular components required within these organelles to sustain and regulate specific biological homeotic functions. In addition, the few organellar-encoded genes within these genomes are required to sustain function of the organellar network (Logan, 2006). Despite the functional similarities between the majority of mitochondria

and plastids across a wide range of organisms, there are major differences in the overall genomic content and genomic structures when comparing organellar genomes between animal, plant, protozoan, and fungal organisms.

Literature Review: Characterization of Molecular Phenotypes Observed in Organellar Genomes

The following five points are common between all mitochondrial and plastid genomes. Organelles contain genomes that are replicated under the control of nuclear encoded genes. DNA replication of these genomes is independent of nuclear DNA replication and the cell cycle. Organelle genomes contain essential genes for eukaryotic life and host cell fitness. These genes are transcribed within the matrix of the respective organelle. Organellar genome depletion eventually leads to fewer organelles per cell. In contrast to the observed functional similarities between organelles, there are extreme differences in genome structure and dynamics when comparing organellar genomes between species.

Historically, the majority of mitochondrial and plastid genomes were believed to be composed of a singular circular DNA chromosome. This very simplistic view of organellar genomes was primarily based on DNA sequencing and restriction mapping. This dogma has begun to change over the last decade with the addition of many non-metazoan fully sequenced organellar genomes and the use of molecular techniques with higher precision and greater resolution. The majority of non-metazoan species have organellar genomes that are linear chromosomes. Ploidy number of chromosomes is not an acceptable term when discussing the relative number of genome copies per organelle. In the simplest form, a single genetic unit (or chromosome) exists in multiple copies within the organelle. The number of chromosomal copies is dependent on the distance of the organelle from the nucleus (Mignotte et al., 1987; Davis and

Clayton, 1996), the fission and fusion dynamic rates of the organelle, the location of the cell within a tissue, and the tissue type. Differences in chromosomal copy number under normal conditions have little to no effect on the overall genome size and gene content. Variable copy numbers of organellar chromosomes is the most consistent form of genome complexity between these organelles. The next level of complexity is found in the overall differences in genomic sizes and structures between organellar genomes of different groups of organisms.

Organellar Genome Sizes and Structures

To date, there are 2663 metazoan mitochondrial genomes that have been fully DNA sequenced (NCBI Organelle Genome Resource). In contrast, only 109 fungal and 69 viridiplantae mitochondrial genomes have been fully sequenced. There are also 277 fully sequenced plastid genomes. Interestingly, there are 16 fully sequenced mitochondrial plasmids that have been identified from the following groups of organisms: Amoebozoa (1 plasmid), Opisthokonta (10 plasmids), and Viridiplantae (5 plasmids). The majority of these plasmids consist of linear DNA molecules that are between 1-2 kilobases (kb) in size (containing 1 – 3 genes), 9 to 14 kb (containing 3 -10 genes), 22 kb (containing 5 genes), and 31 kb in size (containing 13 genes). The term genome "size" with regard to mapped genome sequences is purposely used instead of the term genome "length". The reason for the distinction between genome "size" and "length" will be discussed when comparing sizes of fungal mitochondrial genomes.

Metazoan mitochondrial genomes can be split into two phylogenetic groups: eumetazoan and placozoan. Eumetazoa have the smallest and simplest mitochondrial genomes with an average size range of 14 -20 kb. However, the slender duck louse (*Anaticola crassicornis*) has the smallest mitochondrial genome size of 8 kb. The pacific ridley (*Lepidochelys olivacea*) and

the walleye pollock (*Gadus chalcogrammus*) are two animals that contain the largest mapped mitochondrial genomes of 33 kb.

In general, all organisms within the eumetazoan subgroup contain a single circular mitochondrial chromosome except for the two largest genomes listed above. Mitochondrial genomes from both the pacific ridley and the walleye pollock contain two distinct chromosomes. Therefore our definition of a chromosome as a single copy of the complete organellar genome needs to be modified. In these specific cases a chromosome refers to the more traditional definition. These two specific organisms having two chromosomes is not to be confused with the previous description of variable copy numbers of single genomic units within mitochondria.

Members of the placozoan subgroup have larger mitochondrial genomes compared to their eumetazoan relatives. Only five of these genomes have been fully sequenced. These genomes produce circular maps ranging between 32-43 kb in size. Mitochondria from eumetazoa and placozoa generally have genomes containing 37 to 42 functional genes regardless of the actual genome size.

Only 90 protozoan mitochondrial genomes have been fully sequenced to date. It is difficult to make comparisons between these genomes because of the limited data set. With the sequences provided, these organisms can be divided into two groups based on the polarity in their mitochondrial genome sizes. Many of the genomes are smaller than the metazoan eumetazoan genomes. The remaining protozoan genomes are similar in size to the metazoan placozoa genomes. All of these genomes map circular independent of genome size.

Fully DNA sequenced fungal mitochondrial genomes are more diverse in size than metazoan and protozoan mitochondrial genomes. Mitochondrial genomes within these organisms range from 19-127 kb in size (19 kb: *Harpochytrium* sp *JEL94* and 127 kb:

Chaetomium thermophilum). Like the metazoan mitochondrial genomes, the majority of fungal genomes have circular genome maps. But unlike metazoan genomes, the predicted genome sizes and circular structures are rarely observed in most fungal mitochondrial genomes. Circular DNA molecules observed within these genomes by either electron microscopy, fluorescent in situ hybridization, or by size determination by migration comparisons after agarose gel-electrophoresis generally indicate these mitochondrial DNA (mtDNA) molecules are much longer or shorter in physical length than the genome sized chromosomes predicted from traditional mapping. This explains the distinction between the physical "length(s)" of DNA molecules (or chromosome(s)) and their differences from the predicted genomic "size(s)" of organellar chromosomes.

In addition to the observable differences in DNA circular structure, the majority of fungal mtDNA is observed to be composed of linear DNA molecules. As with the circular mtDNA, these linear strands of mtDNA are variable in length. In addition, both circular and linear DNA molecules have been observed simultaneously in mtDNA extractions of fungi. Overall the actual lengths of mitochondrial chromosomal structures in fungal organisms rarely correspond to the predicted genomic structures and sizes as observed in metazoan mitochondrial chromosomes. This is just another example of mitochondrial genome complexity and divergence between phylogenetically different organisms. That said, the overall differences in mtDNA chromosomal structure within fungal mitochondria remains mutually exclusive to the average number of genes these genomes encode. On average slightly more genes are found within fungal mitochondrial genomes when compared to metazoan mitochondrial genomes (average of 48 fungal to 37 metazoan mitochondrial genes). The overall range of genes found in fungal mitochondrial genomes (24 genes in *Arthroderma obtsusum* to 84 genes in *Moniliophthora roreri*) is also wider

than in metazoan mitochondrial genomes. These differences observed between metazoan and fungal averages in the numbers of mitochondrial genes and the relative genome sizes may suggest that genome size and the number of encoded organellar genes are somewhat related.

Viridiplantae organisms have the fewest number of fully sequenced mitochondrial genomes. This group of organisms can be split into two groups: Chlorophyta (lower plants) and Streptophyta (higher plants and land plants). Chlorophyta has 17 fully sequenced mitochondrial genomes that range from 12-95 kb in size. Most of these genomes contain a single circular chromosome. *Polytomella parva* and *Polytomella sp*. SAG 63-10 are the exception to this rule by containing two chromosomes each. In general mitochondrial genomes of chlorophyta contain between 20-89 open reading frames (orf). Many homologous genes to those identified in metazoa and fungi have also been identified in these chlorophyta mitochondrial genomes. Both chlorophyta and streptophyta mitochondrial genomes contain many open reading frames that are either pseudo genes or genes that are expressed but have not been fully characterized for their function. Proposed mechanisms explaining why plant mitochondrial genomes have on average more genes and open reading frames than metazoan organisms will be discussed later in this section.

Streptophyta has 52 fully sequenced genomes, which range from 42 kb to 11 mega-bases (mb) in size (42 kb: *Mesostigma viride* and 11 mb: *Silene conica*). The majority of these genomes contain a single chromosome with the exceptions of *Cucumis sativus* and *Silene vulgaris* containing 3 chromosomes, *Silene conica* containing 128 chromosomes, and *Silene noctiflora* containing 59 chromosomes. *Streptophyta* mitochondrial genomes contain the highest number of genes and open reading frames in comparison to the mitochondrial genomes from the groups discussed previously. These genomes have a range of 13-196 orf and identified genes (13

orf: *Silene vugaris* and 196 orf: *Silene conica*). Like metazoan and fungal genomes these genomes contain the two inverted repeat sequences used for mapping these genomes as circles. As observed with many fungal genomes, higher plant mtDNA chromosomes are never observed as master circles but instead as linear DNA molecules that have variable lengths. In addition, circular sub-genomes of variable lengths are also observed. Finally, rare linear branch-like structures and circular sigma-like mtDNA molecules have been observed in plant mitochondrial genomes. None of the observed linear, branched, circular, or sigma like mtDNA structures exist with a length that matches the predicted chromosomal sizes.

Plastids on average contain the largest organelle genomes. Unlike mitochondrial genomes, all sequenced plastid genomes have a single chromosome. When sequenced the majority of these genomes map circular because of the presence of an inverted DNA repeat sequence. There are 277 plastid genomes that have been fully DNA sequenced. Like the protozoan mitochondrial group previously discussed, more plastid genomes need to be fully sequenced from non-plant organisms to be able to determine trends in plastid genome sizes, structure, and gene content.

Plastid genomes are found in specific organisms within all the groups discussed, including alveolata, cryptophyta, euglenozoa, glaucocystophyceae, haptophyceae, rhizaria, and rhodophyta. Plastids within these organisms range from 29 kb to 1.02 mb in size and contain between 56 - 915 open reading frames (26 kb: *Plasmodium falciparum HB3 apicoplast* and 1.02 mb: *Paulinella chromatophora chromatophore*). The majority of sequenced plastid genomes are found in viridiplantae. These genomes range from 37-521 kb in size and contain a range of 37-313 open reading frames (37 kb: *Helicosporidium sp* and 521 kb: *Floydiella terrestris*).

Internal Repeat Sequences & Homologous Recombination

In addition to the inverted repeat sequences for recombination of the master circle chromosome, these genomes contain shorter DNA direct and inverted repeat sequences. These additional DNA repeat sequences are proposed to be directly linked to DNA recombination within these genomes. Metazoan mitochondrial genomes have few or no shorter repeat sequences. Hence the low variability observed in metazoan mitochondrial genome structure and length. Even though many of the metazoan genomes contain a few DNA repeat sequences it is believed because of the limited size of their chromosome that recombination is mostly inhibited. In addition, the metazoan genomes are gene dense molecules with little to no space that distances neighboring genes from one another. Recombination events within these genomes render a significant chance of gene mutations. Mutations like these are often perpetuated by the replication of mtDNA and frequently lead to mitochondrial related diseases.

Recombination is more common in fungal and especially plant mitochondrial genomes. There is direct evidence indicating that plant plastid genomes readily undergo recombination events as well. Organellar recombination events have been proposed to be the primary reason for smaller sub-genomic circular structures observed in plant organelle genomes. The probability of higher rates of recombination within fungal, plant mitochondrial, and most plant plastid genomes are significantly greater than metazoan mitochondrial genomes because of the greater amounts of noncoding DNA between neighboring genes. Even though recombination of organellar genomes is widely accepted, the actual mechanisms involved within these recombination events are not well understood.

Recombination events can occur either intra- or inter-chromosomally. These two processes occur in plant mitochondrial genomes in high frequencies. For example,

recombination of the *Arabidopsis* mitochondrial genome occurs simultaneously at 33 individual sites of short inverted repeats when these plants are placed under specific environmental stresses (Arrieta-Montiel et al., 2009). When these recombination events occur both gene structure and chromosomal lengths are affected. Genes that were once functional often become non-functional open reading frames (Feng et al., 2009). It is speculated that recombination events like these are either a form of gene expression control or an attempt for gene optimization and evolution (Shedge et al., 2010). Regardless, these recombination events are not always beneficial to the organelle or the organism.

Inter-molecular recombination events can cause genomic deletions in combination with the formation of recombinant sub-genomic circles. Genomic deletions have proven to be deleterious to most organellar genomes. Sub-genomic circular molecules are replicated with the linear mtDNA. During mtDNA replication the smaller circular molecules can be favored for replication. When favoritism occurs these molecules are referred to as "selfish elements" or depending upon their size "selfish genomes" (Lavrov, 2010). Mutant selfish genomes are often observed in yeast and result from the described rearrangements, deletions, and insertions in mtDNA. In yeast selfish genomes often result in increased cell senescence, decreased cell senescence, or slowing of hyphal growth (Bertrand et al., 1980; Griffiths, 1992; Nakagawa et al., 1998; Barr et al., 2005). Overall, these mutant genomes are a result of recombination and exceedingly selective mtDNA replication.

Mitochondrial genomes of fungi contain multiple origins of replication (MacAlpine et al., 2001). Selfish DNA elements contain at least one or more ori sequences that allow for the molecule to become over-replicated (MacAlpine et al., 2001; Barr et al., 2005). As mitochondria with this mutation continue to undergo fusion and fission, these selfish DNA molecules spread

throughout the mitochondrial network. Eventually the wild type-like DNA molecules are diluted and the organellar genome is depleted. The amount of mitochondria that remain functional is directly dependent upon the gene content of these "selfish elements". Eventually mutations like these lead to loss of function mutants because all mitochondrial genes are required to sustain mitochondria function. Yeast can contain mitochondria that lack a functional genome for a short time because of their ability to undergo fermentation (petite mitochondrial mutant). In addition, yeast can also contain mitochondria that are completely void of a genome (petite null mitochondrial mutants) (Williamson, 2002). These mutants are often generated from the failure of chromosomes to segregate into daughter organelles during mitochondrial fission.

Organellar fusion is required for maintaining mitochondrial genomes and for metabolic function. In addition, fusion between organelles permits membrane-bound protein to exchange between individual organelles and for chromosomal mixing. Overall, mitochondrial dynamics are essential to maintaining a balance between wild type, mutated, damaged, and recombinant genomes. Excessive mitochondrial fission has been reported in biological mutants where mtDNA damage has occurred. These smaller mitochondria generated by fission are predicted to either isolate damaged mtDNA for repair or to hold the damaged mtDNA in preparation to be recycled by mitophagy.

Genome Inheritance, Heteroplasmy, and Selfish DNA

Metazoan mitochondrial genomes are inherited primarily from the maternal parent (Birky, 2001). There are a few cases reported of paternal leakage (Laser et al., 1997) and uniparental inheritance of mitochondrial genomes (Breton et al., 2007). Generally, paternal mitochondria are transferred from the sperm to the egg at the time of fertilization to create a heterogeneous mixture of mitochondria. On average there are fewer paternal mitochondria

within the germ cells than maternal mitochondria. It has been reported that shortly after fertilization there is a 10-fold reduction in mitochondrial numbers when comparing levels from the primary oocytes to germ cells (Jansen, 2000). In effect, this total reduction of mitochondria causes a "bottleneck effect" where the maternal mitochondrial genome has a greater probability of being retained as the inherited genome.

Biparental inheritance of mitochondria is common in plants. The effects of biparental inheritance result in the coexistence of two distinguishably different mitochondrial genomes or "two mitotypes" that are both maintained within the mitochondrial network (Barr et al., 2005). A "mitotype" is a single mitochondrial genome from an individual. The mixing of the two mitotypes creates a condition termed length heteroplasmy.

Paternal mitochondrial genome leakage is another form of length heteroplasmy. This occurs when both maternal and paternal mitotypes are present after both maternal and paternal mitochondria have fused together. These two mitotypes can undergo recombination to create a hybrid genome or intermediate mitotype (Tsukamoto et al., 2000; Hattori et al., 2002; Aksyonova et al., 2005).

Heteroplasmy is generally defined as an individual organism that contains a genetically distinct mitochondrial genome (Barr et al., 2005). Heteroplasmy is split into two groups: length heteroplasmy and site heteroplasmy. Length heteroplasmy involves large-scale insertion or deletion of the original genome. Site heteroplasmy is when site-specific nucleotide mutations alter the nucleotide composition of a relatively short segment of the genome. Overall site heteroplasmy is difficult to detect within a single species. This phenomenon is mostly observed in animal species and is directly related to tandem repeats generated within the mtDNA control

region after mtDNA replication (Townsend and Rand, 2004; Munwes et al., 2011). More often length heteroplasmy is observed within plant and fungal mitochondria.

Another example of length heteroplasmy occurs when sub-genomic circles containing parental mtDNA insertions are formed within a mitochondrial genome. These sub-circular genomes are generally kept in low abundance (or substoichiometric) and replicated with the rest of the mtDNA (Woloszynska, 2010). Substoichiometric mitochondrial DNA molecules are referred to as "sublimons" (Woloszynska, 2010). Sublimons can also originate from intra-molecular recombination of short inverted or palindromic mtDNA repeat sequences. Generally, sublimons are maintained within the mitochondrial genome by DNA replication over many reproduction generations and are transferred to the progeny. The genes encoded within sublimons are normally expressed at low levels. In contrast and by unknown mechanisms, mtDNA replication can increase the relative copy numbers of sublimons from substoichiometric levels to the normal mtDNA levels of the predominant genomic molecules (Small et al., 1989; Janska et al., 1998). The expression of sublimon genes is directly related to the numbers of sublimons present.

Sublimons can be beneficial or detrimental to the overall fitness of the organism. These molecules have the ability to recombine back into the major molecules of the genome. Recombination is mostly irreversible when occurring from intra-molecular recombination generated sublimons (Kubo and Newton, 2008). The reintegration of substoichiometric molecules containing paternal mtDNA is most common in plants. Depending on gene content these molecules can serve as a "molecular band aid" by replacing homologous genes that have become damaged. In contrast, sublimons can function as a "molecular time bomb" if they encode a gene for cytoplasmic male sterility (cms, a plant mitochondrial disease). This gene can

be incorporated from the sublimon to the main genomic molecules, replicated with the mtDNA, and expressed at normal levels after being transferred through many generations of progeny and remain expressed at low levels.

Introns, Concatamers, and "Everything Else"

Fungal and plant mitochondrial genomes contain introns that were vertically transmitted from a common ancestor. Plants have both group I and group II introns while fungi only have group II introns in their mitochondrial genomes (Oda et al., 1992; Ohta et al., 1993). These introns are found within different genes depending upon the species. Not all mitochondrial encoded genes contain introns. Many intronic DNA sequences have been found to be similar between adjacent DNA exon sequences within the same gene (Ohta et al., 1993; Yamato et al., 1993). In addition, many similarities have been found between intronic sequences in adjacent genes (Lippok et al., 1994). It has been proposed that the similarities observed between intronic sequences result from duplication by recombination. Intron sequences homologous to those observed in the organellar genomes are also found in nuclear encoded mitochondrial genes.

Plant genomes contain several common characteristics, including cis- and trans-splicing of group II introns (Francs-Small et al., 2012). RNA editing occurs in both plant mitochondrial and plastid genomes (Verbitskiy et al., 2011). These genomes contain transposable elements and retro-transposable elements (Zhang et al., 2011). Gene migration has occurred in both mitochondrial and plastid genomes. Specific portions of the plastid genome have been duplicated and transferred to the mitochondrial genome and portions of the mitochondrial genome are proposed to have been transfered to the cell nucleus. A section of chromosome 2 in *Arabidopsis* has been duplicated and transferred into the mitochondrial genome (Marienfeld et al., 1999).

As discussed previously, circular and linear mtDNA molecules are the major structures observed within the mitochondrial genome of plants. In addition to these structures, minor structures are found in low abundance. These include sigma-like lariats with linear tails, rosette-like structures, catenane-like molecules, and linear molecules with branching (Backert et al., 1996; Bendich, 1996; Backert and Borner, 2000). These structures provide direct evidence of recombination intermediates and may suggest that multiple mtDNA replication strategies are involved when replicating plant mitochondrial genomes (Nosek and Tomaska, 2003).

In summary, plant organellar genomes are complicated. By mechanisms not well understood, the cell is capable of balancing mtDNA and ptDNA (plastid DNA) replication and organellar gene expression. The minimum form of organellar genome complexity is found in mtDNA copy numbers within an organelle. All cells replicate multiple copies of their organellar single genomic unit or mitotype. These organelles utilize many mechanisms by which their genomes become diversified. Regardless of genome diversity, dynamics, and complexity all components of the genome (i.e. mitotypes, heteroplasmy, and sublimons) need to be replicated for the system to remain functional.

Literature Review: Models for Organellar DNA Replication

The molecular machinery used to replicate organellar genomes is found to be somewhat dependent on the phylogenetic kingdom in which the organism resides. As discussed previously, mitochondria are believed to have evolved from an alpha-proteobacteria ancestor prior to when plastids evolved from a cyanobacterium ancestor. It has been proposed that the T7 bacteriophage was incorporated into these organellar genomes either by the lytic pathway or as a linear plasmid early in the evolution of these organelles (Holt et al., 2000; Shutt and Gray, 2006).

Regardless of the mode of entry, the T7 phage DNA possesses genes homologous to those that are required for organellar DNA replication.

Metazoan mitochondrial RNA polymerase, DNA polymerase gamma (polG), and TWINKLE helicase (T7 gp4-like protein with intra-mitochondrial nucleoid localization (Spelbrink et al., 2001)) are more homologous to their equivalent orthologs found in T7 bacteriophage than in bacteria. In contrast, both mitochondrial single-stranded DNA-binding proteins and organellar DNA polymerases in plants, fungi, and protozoa are more similar to DNA polymerase I found in monera. Also, variants of the TWINKLE primase-helicase are found in animals, plants, and protozoa but are not found in fungi. Hence, the required components for organellar DNA replication differ between metazoa, plants, and protozoa.

Metazoan mitochondrial genomes have the most comprehensive mtDNA replication and genome maintenance model to date, but there still remain many questions. The current metazoan replication model is fashioned after both viral and prokaryotic DNA replication systems. Metazoan organellar mtDNA replication models currently serve as a starting point in the attempt to discover replication models for larger and more complex organellar genomes.

T7 Bacteriophage Model for Phage DNA Replication

The T7 bacteriophage has a linear genome that encodes seven proteins required for its DNA replication (Shutt and Gray, 2006). The RNA polymerase (gp1), primase-helicase (gp4), DNA polymerase (gp5), single-stranded DNA-binding protein (gp2.5) (SSB), and thioredoxin (Bedford et al., 1997) from the host organism are essential for the initiation and elongation phases of T7 DNA replication.

The initiation phase for T7 bacteriophage DNA replication requires the RNA polymerase to initiate transcription at the origin of replication on the leading strand of the molecules. The

DNA polymerase then displaces the RNA polymerase by binding next to the nascent RNA transcript. The DNA polymerase uses the 3'-OH of the RNA transcript as a primer where the newly synthesized DNA strand is elongated by the addition of deoxyribonucleotides (Sugimoto et al., 1987).

For DNA elongation to occur in both directions the gp4 primase-helicase is required. This bifunctional fusion protein contains both DNA primase and helicase functions. In addition this protein is capable of simultaneously unwinding DNA and synthesizes a primer for the lagging strand. T7 phage SSB is required for both primase activity of the gp4 primase-helicase and for phage DNA polymerase activity (He and Richardson, 2004). Thioredoxin (found in *Escherichia coli*) functions as a T4 DNA polymerase processivity factor (Fan et al., 1999). Once the elongation phase is complete, DNA repeat sequences at the terminal ends of the linear replicated molecules are recognized for homologous recombination and the synthesis of concatemers (Hwang and Kornberg, 1992). By generating concatemers the T7 bacteriophage avoids the shortening of its linear DNA molecule after each pass of DNA replication (Shutt and Gray, 2006).

Animal Mitochondrial DNA Replication Model

The initiation of metazoan mtDNA replication is similar to the initiation of T7 bacteriophage DNA replication. The initiation of DNA replication of the circular mitochondrial chromosome begins with the transcription of promoters (by nuclear encoded mitochondrial RNA polymerase (Tiranti et al., 1997)) for non-coding DNA control regions within the origins of DNA replication for the leading strand (O_H) and the (11 kb (Clayton, 1982)) upstream origin of replication for the lagging strand (O_L). Transcription of the O_H initiates a replication bubble or D-loop (Robberson et al., 1972) where leading strand synthesis is initiated upon the generation of

a complementary RNA primer and the formation of the mitochondrial DNA replisome complex. This replisome complex consists of the mitochondrial DNA polymerase gamma (PolG) (Ropp and Copeland, 1996), mitochondrial TWINKLE helicase (Spelbrink et al., 2001), and the mitochondrial single-stranded DNA-binding (mtSSB) proteins (Edmondson et al., 2005). RNA primers for both leading and lagging-strand DNA synthesis are generated from transcription of the non-coding control region within the lagging strand origin of replication (O_L) (Xu and Clayton, 1996; Matsunaga et al., 2003). The mtRNA polymerase has been observed to terminate transcription spontaneously within the O_L region and hence generates short RNA molecules of variable lengths to be used as short semi-random RNA primers for mtDNA replication (Pham et al., 2006). The D-loop is stabilized by the hybridization of these small RNA molecules to the lagging-strand single-stranded DNA. This ssDNA/RNA hybridization in effect creates a partially single-stranded molecule. The short RNA molecules are used instead of single-stranded DNA binding proteins to protect the lagging strand (Yang et al., 2002; Yasukawa et al., 2006).

Previous models for metazoan mitochondrial DNA replication proposed either a strand-displacement (Clayton, 1982) or the conventional coupled leading- and lagging-strand mechanism for DNA synthesis (Holt et al., 2000). Portions of these two models have been merged together with the recently proposed replication model of "RNA Incorporation Throughout the Lagging Strand" or RITOLS replication to form a more comprehensive model (Yasukawa et al., 2006; Holt, 2009). The RITOLS model implicates that short RNA molecules take the place of mtSSB in the displacement of the template strand (Holt, 2009). The RITOLS model alone does not completely represent animal mtDNA replication because RITOLS replication is only observed in one direction and only during lagging strand synthesis (Yasukawa

et al., 2006). It is well documented that animal mtDNA replication proceeds in both directions of the initial replication bubble (Bowmaker et al., 2003; Reyes et al., 2005).

Metazoan mitochondria follow a two-step process for Okazaki fragment maturation and long-patch base excision repair (Rossi et al., 2008). A short segment of the 5' end of hybridized RNA primers is displaced by the mtPolG forming a 5' end flap. Three protein complexes bind to the flap: nuclear hPIF (helicase) (Futami et al., 2007), RPA (ncSSB) or mtSSB, and Dna2 (nuclease/helicase) (Zheng et al., 2008). hPIF, RPA, and Dna2 have dual function in both nuclear and mitochondrial DNA replication. The helicase function of Pif1 displaces the flap to a distance greater than 25 bases. RPA then proceeds to bind to the single stranded RNA molecule and blocks Fen1 (Flap endonuclease 1 (Liu et al., 2004)) from attacking the 5' flap. Dna2 binds to the flap and proceeds to displace RPA and Pif1. Then Dna2 continues to cleave the long flap and displace the single-stranded molecule (Copeland and Longley, 2008). The second step consists of Fen1 endonuclease removing the remaining short DNA flap (Liu et al., 2008) left behind from Dna2 cleavage. Finally, ligase III fills the gap created by Fen1 (Lakshmipathy and Campbell, 1999; Ruhanen et al., 2011).

Telomeres are not a concern for most metazoan mitochondrial genomes because of their circular structures. Ciliates are the only animal known to have linear mitochondrial genomes. The mechanism for maintaining telomeres of linear mtDNA appears to be similar to those used in the steps of Okazaki fragment maturation (Paeschke et al., 2010). There remains much to be determined in how the telomeres are maintained on these linear molecules without a functional mitochondrial telomerase. Recombination and non-homologous strand invasion are the two working models for telomere elongation and maintenance of linear mtDNA molecules (Nosek et al., 2006).

Plant Mitochondrial DNA Replication

A specific model for plant mitochondrial DNA replication has not been proposed. Many biochemical studies and in vitro experiments have been conducted to isolate and characterize replication protein homologues from plant mitochondrial extracts. Many genes that encode proteins isolated from mitochondrial extracts have been successfully identified within model organisms. In contrast, very few of these genes have been characterized for their function within the plant. In summary, there is more direct evidence provided by in vitro studies and very little direct evidence linking these genes to actual function within the plant.

Higher plant mitochondrial genomes are very complex. The diversity of mtDNA structures would suggest that higher plants have multiple strategies for mtDNA replication. In contrast, lower plant mitochondrial genomes are relatively simple. It is proposed that the circular mtDNA of lower plants is replicated by similar mechanisms found either in metazoan or fungal mtDNA replication. Unfortunately, a similar proposal cannot be made for higher plants. The most direct, but also most difficult way to determine if higher plant mitochondrial genomes possess multiple mechanisms for DNA replication is to examine these replicative processes and components directly within the mitochondria of plants.

Plastid Genome DNA Replication Model

Less direct evidence is available regarding DNA replication of plastid genomes as compared to mtDNA replication of animal mitochondria. There remains a long-standing model proposed for plastid genome replication that is somewhat similar to portions of current mtDNA replication models for animals. The plastid model involves the initiation of replication at two origins of replication (oriA and oriB) and the formation of a double D-loop structure (Manchekar et al., 2006; Nielsen et al., 2010). The two replication forks fuse to form a Cairns replication

intermediate structure that proceeds around the circlar plastid DNA. Replication continues until the replication forks converge. When replication is nearly complete initiation of rolling circle replication at the nick can serve to continue replication to generate additional copies of the genome (Kolodner and Tewari, 1975). Bidirectional rolling circle replication is initiated 180 degrees from the D-loop origins of replication (Hedrick et al., 1993).

This described method for plastid DNA replication only works if the DNA is a circular model. It is likely that ptDNA can replicate by more than one mechanism (Nielsen et al., 2010). Recent evidence suggests that the majority of plastid genomes are linear molecules that attach to a nucleoid-like structure (Bendich, 2004). Nucleoids are also found in animals (Bogenhagen, 2010), fungi (Miyakawa et al., 2009), and most recently in plant (Xu et al., 2011) mitochondria. These plastid nucleoid structures are very similar to those observed in bacteria like *Escherichia coli* (Macvanin and Adhya, 2012). A nucleoid provides a scaffolding structure where multiple copies of the genome are attached and can undergo DNA replication and recombination. It has been proposed that the nucleoid structures also provide a hub for DNA recombination-mediated control over mitochondrial gene expression.

Higher plant plastids are found to have predominantly linear ptDNA with a low frequency of mini-circular structures (Oldenburg and Bendich, 2004; Koumandou and Howe, 2007). The linear plastid genomes attach in multiple copies to a nucleoid-like structure similar to that found in mammalian mitochondria (Zoschke et al., 2007). But unlike the mammalian nucleoid structures, the attached ptDNA molecules are not circular catenated structures. These molecules are linear and have putative origins of replication at the 5' and 3' ends (Scharff and Koop, 2006).

Bendich et al (2004) provided direct evidence that linear catenated molecules are generated at the nucleoid-like structures. These linear catenated structures are proposed to have been generated from inter-molecular recombination at the large inverted repeat sequences contained within the plastid genome (Oldenburg and Bendich, 2004, 2004). The catenation of these linear ptDNA molecules is very similar to DNA replication strategies found within the T4 bacteriophage and the proposed telomere formation strategies in the absence of telomerase (Mosig, 1998; Nosek et al., 2006). It has also been proposed that the plastid genomes of higher plants are primed for DNA replication by single-stranded DNA invasion and hybridization at the large internal repeat sequences (including the origins of replication) found on the ends of these linear molecules.

As a final note, greater quantities of ptDNA are found in the shoot apical meristem of plants. The relative levels of plastid DNA diminish in tissue that is further away from the meristematic region (Rowan and Bendich, 2009). In addition, the relative copy number of ptDNA also is observed to diminish in the chloroplast as the plant ages (Rowan et al., 2007). It has been proposed that a limited number of copies of ptDNA are generated within the proplastids of the meristem. As plastids develop and age the ptDNA is diluted over time through DNA damage, degradation, or recycling of plastid organelles without increased ptDNA replication (Rowan et al., 2004). Plastid depletion may function as a control for plant senescence.

Literature Review: Description of Proteins Required for the Mitochondrial DNA Replisomal Model

Organellar DNA Polymerase

Arabidopsis has two DNA polymerases (polIA and polIB) that have been shown to target both the mitochondria and the plastids (Elo et al., 2003). These two polymerases are between 30-35% similar in protein identity to bacterial DNA polymerase I than to DNA polymerase

gamma (PolG) (Garcia-Diaz and Bebenek, 2007). PolG is found to target animal mitochondria. One of the major differences in protein identity between PolG, PolIA, and PolIB is the location of the DNA binding fingers located within the palm domain or polymerase catalytic site (Moriyama et al., 2008). Another major difference is that animal PolG has a small accessory protein that attaches to PolG to enhance polymerase function and procesivity (Jazayeri et al., 2003; Moriyama et al., 2011).

Another major difference between DNA polymerase gamma and the plant organellar DNA polymerases found in *Arabidopsis* is that PolIA has a putative ribonuclease domain and PolIB has a 3' to 5' exonuclease proof-reading domain whereas PolG does not have either of these two domains (Moriyama et al., 2008). Animal DNA polymerase gamma has been shown to interact with both mitochondrial single-stranded DNA-binding protein and TWINKLE-helicase to form a DNA replicase (Korhonen et al., 2003). It remains unclear if either of the two *Arabidopsis* organellar polymerases interacts with either TWINKLE or mtSSB plant homologs found in plants (Moraes, 2001). In addition, it also remains unclear if the two *Arabidopsis* plant organellar DNA polymerases form a similar DNA replisomal mechanism model as observed in most metazoans.

TWINKLE-Helicase

Arabidopsis has a nuclear encoded putative TWINKLE gene that is homologous to the animal TWINKLE-helicase previous discussed. The *Arabidopsis* TWINKLE homolog is predicted to be more similar to the T7 bacteriophage in possessing both functional helicase and primase domains (Spelbrink et al., 2001). Animal TWINKLE protein homologs do not exhibit dual function as observed in the T7 bacteriophage TWINKLE, which has a functional primase domain in addition to retaining their 5' to 3' DNA helicase activity (Korhonen et al., 2003).

Alternatively, most metazoan TWINKLE genes retain in part the protein motifs that make up the primase domain. Although there is no evidence supporting primer synthesis from these primase domain fragments there is growing evidence that suggests the remaining motifs function in loading primer onto the single-stranded DNA during replication. Even though the primase domain is not fully functional it has been shown to be required for a functional animal TWINKLE-helicase (Shutt and Gray, 2006).

T7 bacteriophage, animal, and plant TWINKLE proteins all retain a short protein linker domain that remains highly conserved. This linker domain is encoded near the middle of the gene and is between the helicase and primase encoded DNA sequences. The purpose of this protein linker region is to allow for the formation of a hexamer or heptamer helicase barrel structure. Mitochondrial DNA depletion to embryo-lethality is observed in animals depending upon the type and severity of gene mutations generated within this linker region (Elpeleg et al., 2002; Echaniz-Laguna et al., 2010).

Arabidopsis TWINKLE has been observed to target both mitochondria and chloroplasts (Carrie et al., 2009). It remains unclear if TWINKLE is required for plant organellar DNA replication (Tyynismaa et al., 2004). It also remains unclear if this protein is essential in the formation of a plant organellar DNA replisomal mechanism.

Mitochondrial Single-Stranded DNA-Binding (mtSSB) Proteins

The final component of the animal mitochondrial DNA replisomal mechanism is the single-stranded DNA-binding protein. These proteins bind to the single-stranded DNA within the replication bubble during mitochondrial DNA replication (Korhonen et al., 2003). The N-terminal domain of TWINKLE-helicase aids in the binding of mtSSB proteins (Farge et al., 2008). *Arabidopsis* contain at least one mtSSB protein that localizes to the mitochondria

(Edmondson et al., 2005). It remains unclear if multiple mtSSB genes are required for *Arabidopsis* mtDNA replication. It also remains unclear how mtSSB may contribute to the plant mitochondrial DNA replisomal mechanism.

CHAPTER 1: Research Questions and Hypothesis

The metazoan model for mtDNA replication requires three essential components that constitute the replisome: DNA polymerase gamma (PolG), TWINKLE-helicase, and mtSSB (Korhonen et al., 2004). When either the DNA polymerase gamma or the TWINKLE-helicase is mutated or depleted within a metazoan organism the depletion of the mtDNA is directly observed (Sarzi et al., 2007; Correia et al., 2011; Stumpf and Copeland, 2011). Both PolG and TWINKLE-helicase come from single copy genes in metazoan nuclear genomes. In addition, metazoan cells do not have the ability to compensate for the loss of either of these genes. Therefore, homozygous mutations within either gene result in an embryo-lethal phenotype (Spelbrink et al., 2001; Hance et al., 2005).

Plant mitochondrial and plastid genomes are much more complex than organellar genomes observed in most metazoans. Despite these differences observed in organelle genome structures, both animal and most plant nuclear genomes encode an organellar DNA polymerases, a single full length TWINKLE-helicase, and mtSSB proteins. One of the main differences between these two genomes is that animals only have one organellar DNA polymerase while most plants, including *Arabidopsis*, have two organellar DNA polymerases (Elo et al., 2003; Kaguni, 2004). Another contrast is that most fungi do not have an equivalent homolog to the TWINKLE-helicase. Other helicases than TWINKLE have been identified for mtDNA replication in most fungi. Overall, fungal organelle genomes and structures are more similar to plant organelle genomes and complexity (Burger et al., 2003; Bullerwell and Gray, 2004). This leads to the overall major question, are plant organelle genomes maintained more like metazoans, more like fungi, are they maintained by a combination of strategies similar to both groups of organisms, or could they have their own unique mechanism(s) for DNA replication?

The difference observed in plant organellar genome structures would indicate that multiple replication strategies are used for mtDNA and ptDNA replication (Bendich, 2004; Nielsen et al., 2010). Specifically, one strategy could be used to replicate long lengths of linear DNA while another strategy may be used to replicate sublimons and other circular sub-genomic molecules (Bendich, 1996; Woloszynska, 2010). In addition, there are DNA recombination and repair events that occur at predicted high frequencies that require a DNA polymerase function in plants(Dowton and Campbell, 2001; Davila et al., 2011; Galtier, 2011). Because the plastid and mitochondrial genomes have similar linear and circular DNA structures it may be possible that both polymerases may be needed to maintain all of the genomic structures. Hence the question, are both DNA polymerases required for the maintenance of *Arabidopsis* organellar genomes, or are they functionally redundant?

The two DNA polymerases found in *Arabidopsis* are believed to be redundant isoforms of one another (Elo et al., 2003; Parent et al., 2011). Both of these isoforms have been localized to the mitochondria and the chloroplast by techniques using transgenic GFP reporters and transient expression after biolistic bombardment of leaf tissue (Elo et al., 2003; Christensen et al., 2005; Ono et al., 2007; Moriyama et al., 2008). In addition, similar experiments have been conducted with *Arabidopsis* TWINKLE-helicase, which indicates TWINKLE is localized to both plant organelles (Carrie et al., 2009). This leads to the question, does the plant organellar DNA replication model "require" TWINKLE-helicase as does the metazoan model, or is *Arabidopsis* TWINKLE just available as a "potential" component of organellar genome maintenance?

One of the major differences between *Arabidopsis* PolIA and PolIB is that PolIB contains a DNA exonuclease proofreading domain which is homologous to domains observed in bacterial DNA polymerase I (Moriyama et al., 2011; Parent et al., 2011). Structurally both organellar

DNA polymerase genes are more homologous to bacterial DNA polymerase I than to metazoan DNA polymerase gamma and T7 DNA polymerase (Baldauf, 2003). Unlike bacterial DNA polymerase I these two polymerases are believed to function more like bacterial DNA polymerase III (Moriyama et al., 2008). This raises the question, because polIB has additional function, is this gene preferentially expressed?

Many examples from the introduction demonstrated the various roles that mitochondria have in maintaining intracellular homeostasis (Chan et al., 2009). In addition to cellular homeostasis, organellar homeostasis is tightly maintained by nuclear gene expression and organellar dynamics (Monastyrska and Klionsky, 2006; Kang et al., 2007; Nowikovsky et al., 2007; Kessler and Schnell, 2009). Mitochondria and chloroplasts have the capacity to directly signal the nucleus and alter nuclear gene expression when under stress (Liu and Butow, 2006). It remains unknown if these organelles have the capacity to monitor DNA levels and influence nuclear gene expression of organellar machinery components.

It has been shown that mitochondria begin to fractionate by fission when under genotoxic stress (Sato et al., 2006; Knott et al., 2008). Interestingly, between 25 - 40% of mitochondrial fission events under normal conditions leave a daughter organelle without mtDNA (Legros et al., 2004). This could explain why mtDNA depletion rapidly occurs when essential components required for mtDNA maintenance lose function. The occurrence of functional organelles that lack a functional genome provides support for the idea that organelles are somewhat resilient or resistant to reactive oxidative species (ROS) damaging (Mancuso et al., 2006; Mancuso et al., 2007; Dlaskova et al., 2008). Surprisingly, there are few reports of gene mutations observed within organelle genomes due to DNA damage by ROS generated from mitorespiration, chlororespiration, and photosynthesis. Most likely, organelles elevate their DNA copy numbers

so the quantity of functional genomes outnumbers the quantity of nonfunctional genomes (Clay Montier et al., 2009; Preuten et al., 2010). Hence the question, could organellar DNA replication be linked to mitochondrial homeostasis and could the DNA polymerases be linked not only to replication but also in monitoring organellar DNA levels?

It is proposed that plant organelle genomes are tightly monitored for genome maintenance and relative DNA copy numbers. It is also proposed that plant organellar DNA replication is unique compared to metazoan mtDNA replication. Finally it is hypothesized that both *Arabidopsis* organellar DNA polymerases are required to monitor and maintain plant mtDNA copy levels. These two DNA polymerase genes are proposed to be dynamically expressed and if mutated, mtDNA levels will drop causing sub-lethal phenotypes because of the compensation capacity from the redundant gene.

CHAPTER 2: Establishing Transgenic Plant Mutants

Summary

Arabidopsis homozygous allelic T-DNA insertion mutations were successfully isolated for organellar DNA polymerase IA (polIA), DNA polymerase IB (polIB), and TWINKLE-helicase genes. As discussed in more detail in Chapter 3, polIB was the only gene mutant that demonstrated a clear phenotype. The main purpose of this chapter is to establish and confirm gene knockout mutants. In addition, the reasoning for generating transgenic crosses with mtGFP and cycB1;1::GFP reporter genes is provided in this chapter.

Methodology

Strategies for Characterizing Plant Genes by Mutational Analysis

Unlike many classical microbiological and tissue culture experiments to generate mutations within a targeted gene, obtaining specific gene mutations in plants is not as straightforward. Currently there are only two reliable methods for generating stable gene mutations in plants. These methods involve either creating a transgenic insertion (Clough and Bent, 1998; Bent, 2006) or generating a single base mutation within a gene (Andersen and Lubberstedt, 2003). Both of these approaches initially generate multiple mutations throughout the genome (Alonso et al., 2003). Often the progeny from these initial mutants are backcrossed to eliminate additional and undesired non-specific gene mutations (Tax and Vernon, 2001). Generally multiple backcrosses are conducted while continuing to screen for retention of the mutation within the targeted gene.

Plant transgenic lines are generated from a transferred DNA (T-DNA) segment from modified species of *Agrobacterium* into the female germ cells (Gelvin, 2003). Traditionally, this

process works well within *Arabidopsis* and many other dicotyledonous and monocot plant species (Liu et al., 1992; Curtis, 2005; Wroblewski et al., 2005; Agarwal et al., 2009). On average there are 2-3 random T-DNA genomic insertions for every mutant generated (Alonso et al., 2003). Depending upon the experimental purpose for mutagenesis these T-DNA inserts can be used to knockout or knock-down gene expression or they can be used to introduce new genes (Curtis and Grossniklaus, 2003). Most T-DNA molecules carry a constitutively expressed gene for antibiotic resistance (Gelvin, 2003). Therefore, primary screening for T-DNA mutants is often conducted on selective media followed by both PCR and DNA sequencing methods to determine the location of T-DNA mutations in the nuclear genome of the plant (Azpiroz-Leehan and Feldmann, 1997).

T-DNA molecules can also be delivered by a biolistic gene gun into specific plant tissues to observe the transient effects of gene expression from the introduced gene (Finer et al., 1999). In addition to engineering specific genes into T-DNA molecules, specific promoters for either constitutive or inducible gene expression can also be cloned into these molecules (Curtis and Grossniklaus, 2003). Many times T-DNA mutants like these are used to rescue gene knock-out mutants, to characterize a gene's effect on plant development or cellular function, and for localization experiments with the addition of reporter constructs.

In contrast to generating T-DNA mutants to examine gene mutation, sub-lethal single-base mutations can be generated within genes by using chemicals like ethyl methanesulphonate (EMS) or by using gamma irradiation (van der Veen and Wirtz, 1968; Christensen et al., 1998; Bohmdorfer et al., 2011). Like initial T-DNA insertions, these types of mutations generate random mutations but with a significantly higher frequency. On average, EMS mutants need to be backcrossed at least 5 times to eliminate most of the undesired additional mutations. The

major advantage to using this approach is to determine sensitive coding sites within a gene.

T-DNA insertion mutant lines were used to conduct the following experiments because of the availability of previously generated polIa, polIb, and TWINKLE-helicase mutant lines from seed stock centers (such as the *Arabidopsis Biological Resource Center* (ABRC)) (Samson et al., 2002; Rhee et al., 2003). The majority of seeds obtained from the resource centers have additional T-DNA insertions within the genome even though the mutant seed lines are identified with a specific gene insertion (Krysan et al., 1999). It was expected that at least two backcrosses would need to be conducted to segregate potential additional T-DNA insertions not within the specified target gene. In addition, the genotypes of allelic T-DNA insertions of the stock seeds are unknown until PCR screening is conducted on the first generation of plants. Genotypic analysis would need to be conducted to identify primary mutant lines with either a heterozygous or homozygous T-DNA allelic insertion. Finally, the ratios generated from segregating phenotypes of mutants could help predict if the mutant has insertions affecting additional genes besides the target. This analysis can also help determine if additional backcrosses need to be conducted prior to obtaining stronger confidence that the specific phenotypes observed are representative of the specific gene mutated.

Determining Loss or Gain of Function of the Mutant Gene

Once a stable phenotype is obtained after at least two generations of backcrosses, the confirmed homozygous T-DNA insertion mutant should be examined for a gain or loss of gene function (Chalfun-Junior et al., 2003; Ko et al., 2006). It is possible to have a gain of function mutation depending upon the location where the T-DNA has inserted into the mutated gene. This is primarily because of the promoter and gene structure that has been molecularly engineered into these T-DNA molecules. Generally, if a mRNA transcript is successfully

generated from a T-DNA mutant, because of the T-DNA sequence the resulting transcript becomes unstable and undergoes RNA degradation (Park et al., 2002; Parent et al., 2011). This said, there remains a low probability that a functional and truncated gene product will be produced from these mutants.

The simplest way to determine if a T-DNA insertion has disrupted the expression of a gene is to generate cDNA by reverse transcription of total RNA followed by a quantitative PCR experiment to determine the relative gene expression levels of the mutant in relation to the wild type. Before these experiments can be conducted a reference sample (or negative control) must be chosen that remains consistently expressed between wild type and mutant samples. In addition, another level of experimental control is if the gene expression levels within the wild type sample have similar expression levels (or CT-values) between the reference group and the experimental group (Livak and Schmittgen, 2001; Sieburth et al., 2006). Therefore, in an ideal experiment only the gene expression values for the mutant sample experimental group are predicted to change (single variable analysis) (Udvardi et al., 2008).

When conducting these experiments it is essential that RNA is extracted from equal amounts of the same tissue type. RNA is then converted to cDNA by reverse transcription. The cDNA is representative of the relative levels of RNA that were present at the time of sampling. The cDNA is then amplified by PCR using a specialized thermal-cycler that has the ability to measure light density. Simply, through specialized reactions newly synthesized DNA molecules emit a signal that is detected by the machine. The strength of the signal is given as a value that is representative of the quantity of DNA that has been replicated. In addition, this thermal-cycler is capable of determining a signal threshold where DNA levels from all samples are equal. A cycle value (or CT-value) is generated for each sample that indicates when the amplified sample

reaches the threshold value. Hence a sample that contains less target will take more cycles to generate the same DNA levels than a sample that contains more target. Therefore, reference samples should have the same CT-values indicating that the starting material for both the mutant and wild type were the same. If there is no significant differences between reference groups of wild type and mutant, then observable differences in CT-values will have greater significance when comparing experimental groups between wild type and mutants (Livak and Schmittgen, 2001). Hence, it is predicted for the following experiments that the relative expression levels for the T-DNA homozygous mutants will drop.

Generally, a T-DNA insertion destabilizes RNA molecule secondary structure and the transcript is degraded with little or no expression detected (Holec et al., 2006). In addition, a T-DNA insertion can also interfere with RNA editing and intron removal. Results generated from RNA reverse transcription quantitative PCR experiments are somewhat limiting because a phenotype cannot be directly linked to a loss of function mutation generated from a T-DNA insertion. These experiments will confirm the expression levels of the gene and whether the knock-out mutation was successful. In contrast, a mutant plant phenotype can be directly determined to be a result of a knock-out gene mutation if the mutant plant returns to a wild type phenotype upon reintroducing the functional gene back into the mutant by the transformation of another T-DNA molecule with the gene under the control of its native promoter. Alternatively, if multiple allelic mutants for the same gene share the same mutant phenotypes and have similar gene expression patterns, then there is a greater chance that the mutant phenotype is related to the mutated gene. Therefore, for the following experiments multiple T-DNA allelic mutants were examined to correlate the observed phenotypes to the mutant genotypes.

Additional Crosses and Transgenic Reporter

Once mutant lines are determined to be clear or "clean" of additional mutational inserts, these lines can be crossed with additional "clean" transgenic lines that either contain reporter systems or other mutated genes. The term "clean" refers to mutants that have segregated all additional T-DNA insertions except insertions that lay within a short physical distance from the targeted mutation that cannot undergo segregation. Crossing mutants is the quickest and the cleanest way to generate double mutants. If using a transgenic GFP reporter, depending upon its expression profile, the genotype of these reporter mutants can be predicted by examining the GFP expression phenotype (not by PCR) and segregation ratios. When examining GFP or other phenotypes a larger sample size will bring greater confidence of significance when conducting a chi-squared analysis (Zhao et al., 2000). The approaches described were used when crossing and screening mtGFP and cycB1;1::GFP transgenic lines into the polIb mutants (Colon-Carmona et al., 1999; Takada and Jurgens, 2007). In addition single allelic T-DNA mutants were crossed to generate double mutants of polIa x polIb and polIa x TWINKLE-helicase.

Results

DNA Polymerase IB

A reverse genetic screening was conducted to isolate allelic T-DNA insertion mutations for the *Arabidopsis* polIB gene from four seed lines (Fig. 1A). Three of these mutant seed lines had a T- DNA insertion in an exon upstream from the DNA polymerase active site palm domain (Swan et al., 2009; Yamtich and Sweasy, 2010) (See introductory literature review for properties of organellar DNA polymerase). Both seed lines WiscDsLoxHs02109D and Flag_463C09 are predicted to retain their proofreading capability but lose polymerase activity because of T- DNA insertions that are downstream from the exonuclease domain but upstream from the polymerase

palm domain. As discussed previously this is assuming that the T-DNA insertion does not destabilize the RNA resulting in RNA degradation. This is also assuming that transcription will terminate shortly after entering the T-DNA sequence. T-DNA elements contain transcription termination sequences for their encoded genes but not necessarily on their 5' and 3' ends.

Plants germinated from all four original seed stocks had similar slow growth phenotypes (Fig. 1A) (More detailed information is given in Chapter 3). The genotypes for these plants were determined using a PCR based technique to establish the allelic conformation of T-DNA insertions. When screening the root lengths from young seedlings (< 5 dpi) a significant 1:2:1 segregation ratio was observed (X^2=1.34, n=277, at the 95% confidence level). As a follow-up, genotypic results indicated that each individual within each phenotypic (root length) group (1:2:1) had the same genotype: polIb$^{(+/+)}$ (wild type root length), polIb$^{(+/-)}$ (intermediate range root length), and polIb$^{(-/-)}$ (short root length) (Fig. 2).

Before further phenotypic (Chapters 3), physiological (Chapter 4), and molecular analysis the homozygous polIB mutants from all four seed lines were backcrossed to wild type (Col-0) plants at least two times. All seedlings of the F1 generation from each backcrossed generation had an intermediate range of root length when compared to wild type. The self-crossed F2 plants always displayed a root length segregation phenotype of 1:2:1 as described previously. In addition, genotypic confirmation of each F2 seedling indicated all plants with an intermediate root length (~50% of the population) had a heterozygous allelic T-DNA insertion and plants with a short root length (~25% of the population) had a homozygous allelic T-DNA insertion within the polIB gene (Fig. 4). These results in addition to the chi-squared analysis provide evidence that the polIB gene is haploinsufficient.

All four homozygous and heterozygous T-DNA insertion polIb mutant lines had similar

phenotypes. Therefore, the following DNA polymerase IB experiments were primarily focused on the polIb-2 mutant.

By assuming that both polIA and polIB genes are redundantly expressed in wild type plants, it was predicted that polIA gene expression levels would increase to compensate for a decrease in polIB expression. RT-QPCR (with technical duplicates and biological triplicates) analysis showed that the polIb-2 mutant had a 70% increase in polIA expression when compared to wild type polIA expression levels (Fig. 3). These results suggest that the increase in polIA expression is a response by the plant to compensate for the knockdown of polIB expression or the loss of polIB polymerase activity. The induction of polIA expression levels may also suggest that this gene is regulated under some type of feedback mechanism in response to either polIB expression dynamics.

To confirm that the polIb-2 mutant had a decrease in polIB gene expression a similar experiment was conducted by RT- qPCR to compare relative expression in both wild type and the polIb-2 background. It was determined that polIb-2 has a 90% reduction in polIB expression when analyzing transcript levels for the palm domain at the 3' end of the gene (normalized to Actin 2 gene expression) (Fig. 3). The remaining 10% expression of polIB in the polIb-2 mutant can likely be explained as experimental background.

DNA Polymerase IA

A reverse genetic screening was conducted to isolate allelic T-DNA insertion mutations for the *Arabidopsis* polIA gene from two seed lines (Fig. 1B). Similar approaches were taken as described previously. Primary mutants contained a 3:1 root length phenotype (wild type length root to short length root) (Fig. 5). Genotypes were also confirmed in relation to root length phenotypes. Both wild type segregates and heterozygous plants contained the same root length

phenotype and homozygous mutants had a shorter root length phenotype. These mutants needed to be backcrossed at least 5 times to eliminate additional T-DNA insertions that were confounding phenotypic results of older plants (Fig. 6, 47). Gene expression levels of polIa mutant lines, determined by RT-qPCR, indicate a significant decrease in polIA gene expression within the mutant when compared to wild type expression levels of polIA (Fig. 7). In addition, the polIa mutants had an induction of polIB gene expression.

TWINKLE-Helicase

A reverse genetic screening was conducted to isolate allelic T-DNA insertion mutations for the *Arabidopsis* TWINKLE-helicase gene and a TWINKY (primase pseudogene) gene from two seed lines each (Fig. 1C). No phenotypic differences were observed between wild type and either heterozygous or homozygous confirmed mutants (Fig. 8). Two backcrosses of TWINKLE mutants were conducted regardless of there being no observable growth or developmental differences. Gene expression analysis by RTqPCR of TWINKLE-helicase mutants indicated a significant reduction in transcript levels using a target 3' of the linker region of the gene (Data not shown). Gene expression results for the TWINKY gene were conflicting.

Discussion

Because polIb-3 and polIb-4 exhibited the same plant growth phenotypic differences as previously reported mutant lines polIb-1 and polIb-2 (Parent et al., 2011) we decided to focus our analysis by conducting additional phenotypic, physiological, and molecular analysis exclusively with the backcrossed polIb-2 mutants. Minimal additional experimental results can be reported at this time regarding polIa mutants because of the time involved to backcross and segregate additional T-DNA insert mutations out of these lines. Interestingly, early polIa mutants and polIb mutants have a similar root length phenotype, but when comparing older

mutants the polIa mutants have a wild type like phenotype while the polIb mutants continue to have a slow growth phenotype (Fig. 9, 14). Strong phenotypic evidence was obtained that polIA is haplo-sufficient while polIB is haplo-insufficient. This would suggest that both polIA and polIB are redundant isoforms of one another and that the role of polIB may have priority or is required for organellar genome maintenance.

It remains possible that these two genes are expressed differently within the cell. The promoter regions for these genes are significantly different (Fig. 10). These two DNA polymerases have a protein identity of 71.33% and there is significant homology when the polymerase palm domain is compared across several other plant species (Fig. 11). Interestingly, gene expression of both polIA and polIB did not significantly differ when comparing levels from wild type seedlings (not tissue specific) at 5 dpi (Fig. 3). It is possible that both genes are expressed at about the same levels and at the same time in the same plant tissues. Alternatively, each polymerase may have preference to mitochondria or plastid DNA replication and therefore would be expressed at greater levels within tissues that contain a greater amount of the preferred targeted organelle. To test these predictions, an RTqPCR approach was used to quantify the relative gene expression of both polIA and polIB within selected wild type plant tissues (Chapter 3)

Reports indicate that plant, fungal, and protozoan organellar DNA polymerases are more homologous to bacterial DNA polymerase I than to T7 DNA polymerase or DNA polymerase gamma found within metazoan species (Moriyama et al., 2011). This may suggest an evolutionary divergence between plant and animal mitochondrial and plastid DNA polymerases and potential difference in methods and mechanisms within plants that are required for organellar genome maintenance. *Arabidopsis* TWINKLE has also been reported to have a

divergent sequence when compared to other eukaryotic homologues (Shutt and Gray, 2006). The failure of plant TWIKLE mutants to exhibit a phenotype may also suggest that plant DNA replication of the organellar genomes in plants differs from the metazoan mtDNA replication model. It appears that plants do not require TWINKLE for function of the organellar DNA replisomal complex.

Mitochondrial DNA depletion occurs in metazoan mitochondria when TWINKLE is not expressed or when TWINKLE mutants lose functionality (Elpeleg et al., 2002). It has been reported that two additional T7-like TWINKLE homologs are encoded within the *Arabidopsis* genome (Shutt and Gray, 2006). The actual gene identifications were not given in this report and DNA sequence BLAST searches reveal only the two T7-like TWINKLE homologs within the *Arabidopsis* genome that have already been mentioned. When conducting protein BLAST searches of the *Arabidopsis* proteome there is only one known full-length TWINKLE (gene: At1g30680) protein that contains a primase domain, linker domain, and helicase domain. There is pseudo or truncated TWINKLE (or TWINKY gene: At3g30660) protein sequence that contains significant homology to the primase domain. There are also three other protein sequences that have a low identity to the full length TWINKLE protein: At2g24834 (primase domain only), At1g19240 (section of helicase domain), and At5g09720 (significant portion of the primase domain). Preliminary evidence suggests that TWINKE mutations do not have the same effects on plants as in metazoa. In summary, the plant mitochondrial and plastid genomes can replicate without the expression of the organellar TWINKLE gene (At1g30680).

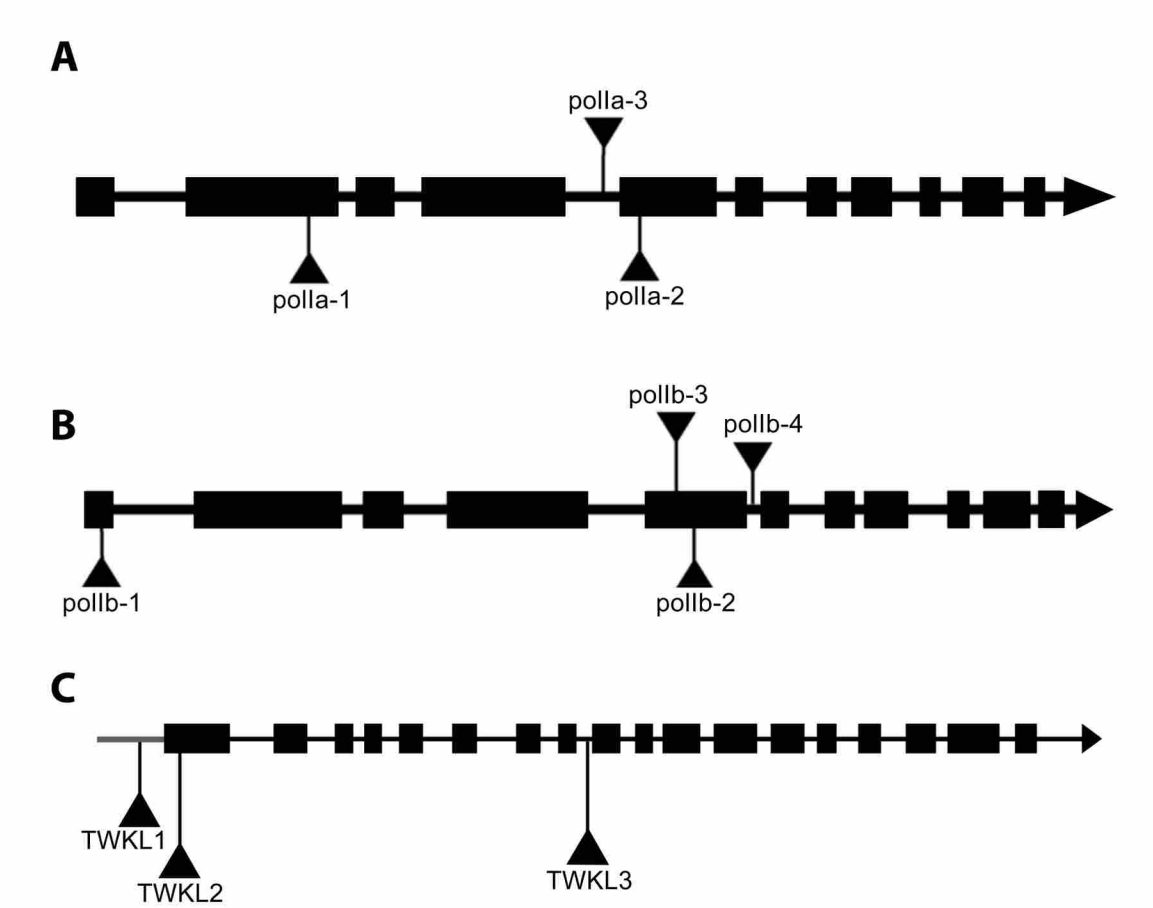

Figure 1. Gene Maps of T-DNA Insertion Mutants
Map of mutant T-DNA allelic insertions. Black boxes represent gene exons and grey line (C) represents the promoter region. A) DNA polymerase IA with T-DNA insertion mutant seed lines SALK_150322 (polIa-1), SALK_022624 (polIa-2), and SALK_022638 (polIa-3); B) DNA Polymerase 1B with T-DNA insertion mutant lines SALK_134274 (polIb-2), WiscDsLoxHs021_09D (polIb-2), Flag_463C09 (polIb-3), and Flag_419G10 (polIb-4); C) TWINKLE-helicase with T-DNA insertion mutant seed lines SALK_038039 (Promoter insertion line TWKL1), SALK_152246 (TWKL2), and SLAK_049818 (TWKL-3).

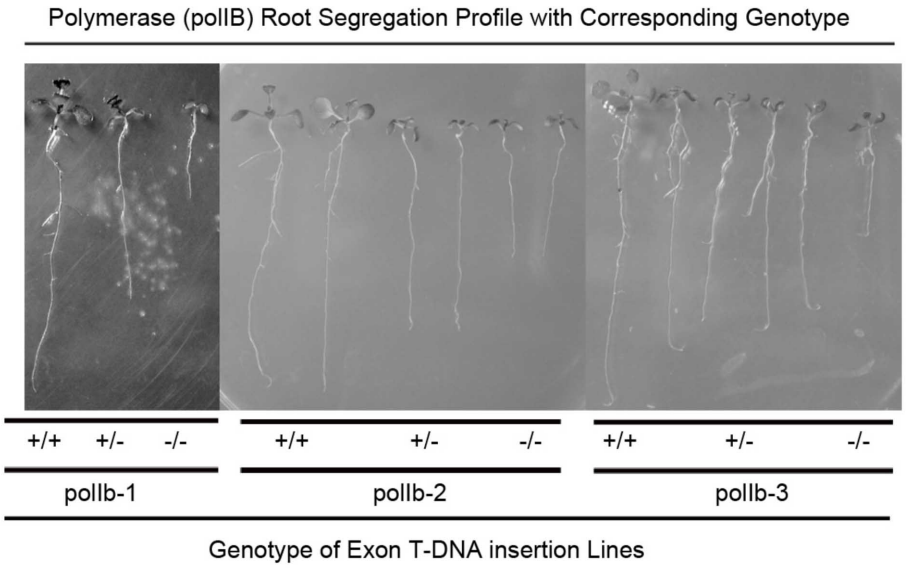

Figure 2. Primary polIB Root Length Segregation Groups
Root segregation phenotype from phenotypic screening of root length with leaf area. Root segregation phenotype of polIb-1, polIb-2, and polIb-3 allelic mutations show a long, intermediate, and short root phenotype. Only the mutants with an intermediate and short root length phenotype were placed into groups if they also exhibited a reduced leaf size or area.

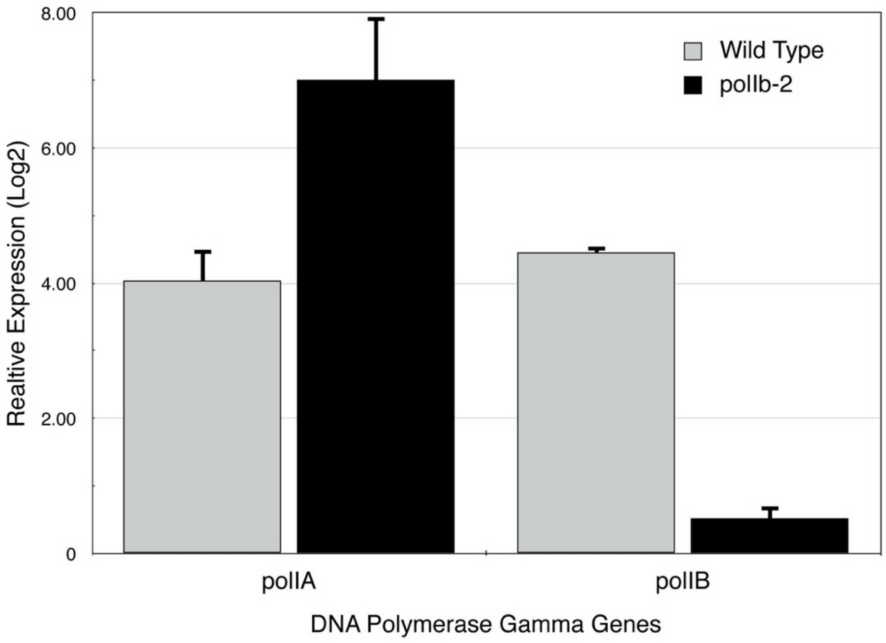

Figure 3. Relative Gene Expression of polIb-2 Mutants
Relative gene expression of both polIA and polIB in the wild type and polIb-2 backgrounds. Samples at 5 dpi. In the polIb homozygous mutant there is a 70% increase in polIA gene expression and a 90% reduction in polIB gene expression when compared to wild type polIA and polIB gene expression. Error bars represent positive SEM.

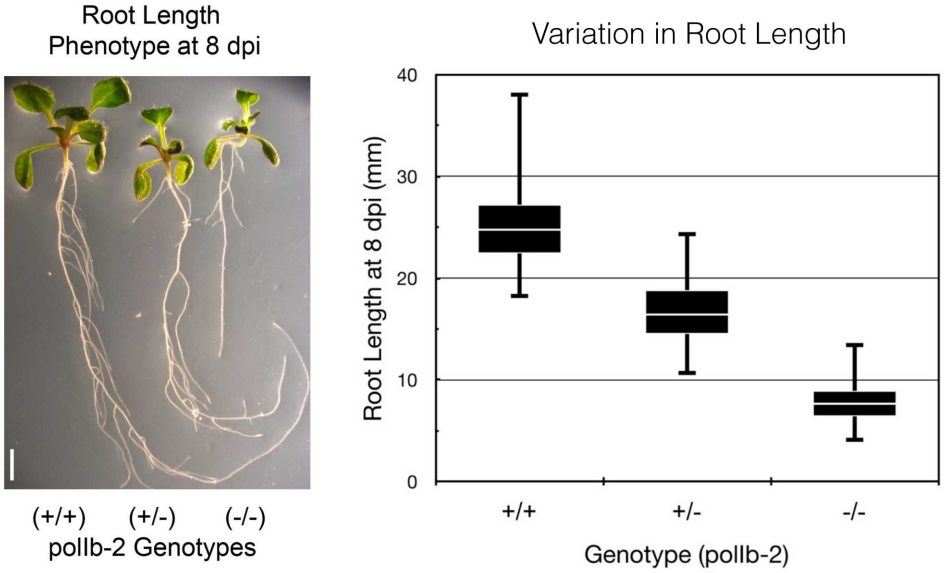

Figure 4. polIB Root Segregation Groups
Box plot representing variation of root length grouped by root and leaf growth phenotype. Roots segregate in a 1:2:1 ratio of long to intermediate to short root lengths.

Figure 5. polIa-2 Mutants Exhibit a 3:1 Ratio Root Segregation Phenotype (Preliminary Results) Genotype was confirmed for each polIa-2 mutant. Heterozygous mutants have a similar root length growth phenotype to that observed in the wild type plants.

Figure 6. polIA Mutant Bushy Phenotype (Preliminary Results)
This plant phenotype is a result of multiple allelic T-DNA genomic insertion mutations. Five backcrosses were required to eliminate this bushy phenotype while retaining a homozygous T-DNA allelic insertion within the polIA gene. Photographed at 35 dpi.

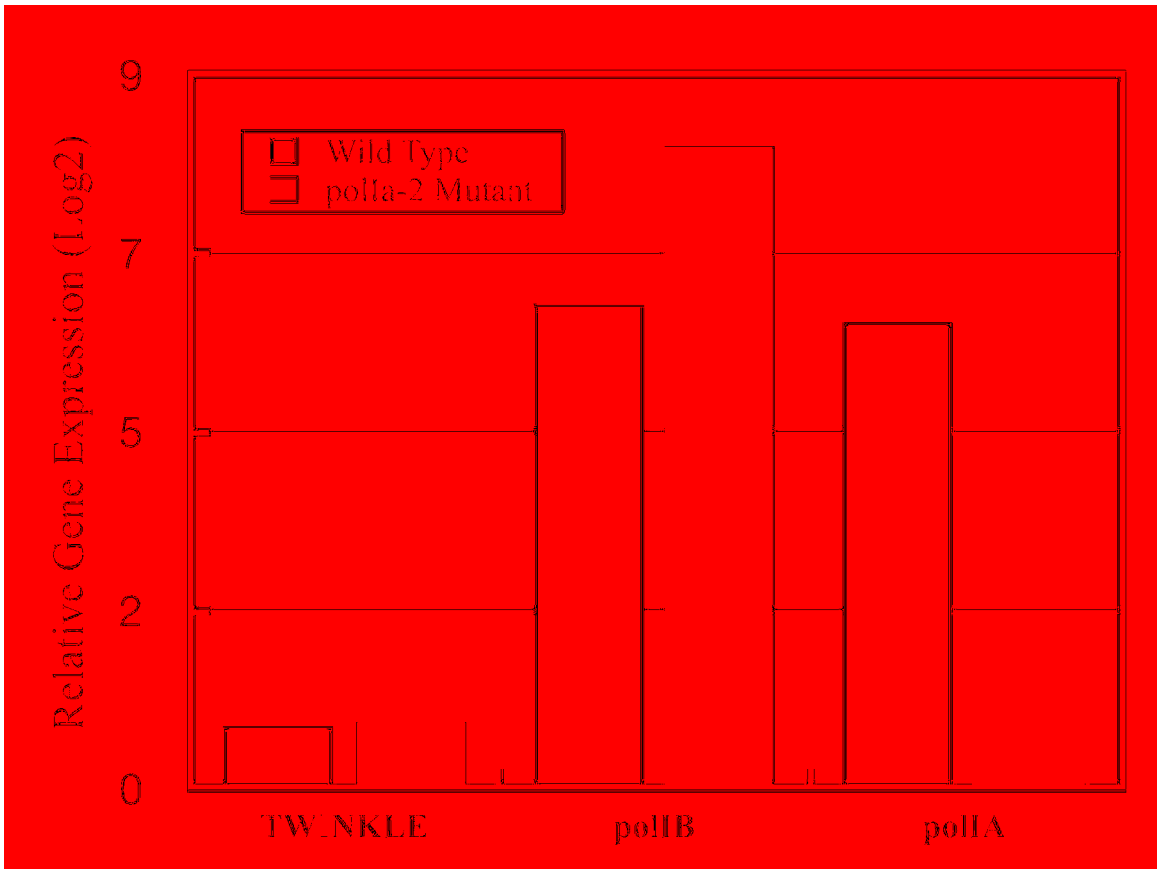

Figure 7. Relative Gene Expression of polIa-2 Mutants (Preliminary Results)
Relative gene expression of both polIA and polIB in the wild type and polIa-2 backgrounds. Samples at 5 dpi. In the polIa homozygous mutant there is an increase in polIA gene expression and a 99% reduction in polIA gene expression when compared to wild type polIA and polIB gene expression. Average of three biological replicates. Normalized to Actin 2 gene expression.

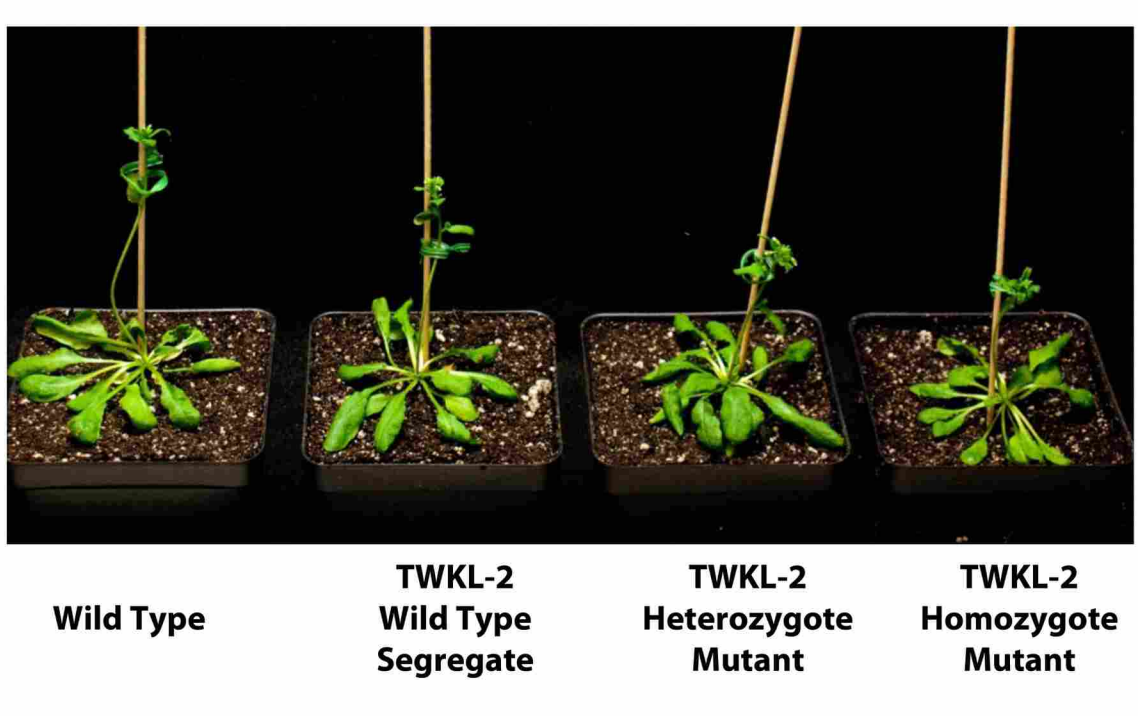

Figure 8. Growth Phenotype of TWKL-2 Mutants
TWINKLE mutants (TWKL-2) do not exhibit a significant growth or plant phenotype that differs from wild type of the same biological age.

Figure 9. Organellar DNA Polymerase Mature Plant Slow Growth Phenotypes
Left plant is wild type and right plant is the slow growing polIb-2 homozygous mutant. Both plants were photographed at the same biological age of 6 weeks.

Figure 10. Predicted Promoter Regions for *Arabidopsis* DNA Polymerases
Map indicating unique DNA sequences and regions within the promoter regions of *Arabidopsis* polIA and polIB genes. Generated with Athena (O'Connor et al., 2005). Blue boxes within the promoter region are CpG islands. **polIA** promoter region predictions: ARF binding site motif at -2439; AtMYC2 BS in RD22 at -1022; CARGCW8GAT at -1001, -760, -347, -347, -760, -1001; CCA1 binding site motif at -2390; CDA1ATCAB2 at -2786; E2F binding site motif at -2779; GAREAT at -1363, -340; I box promoter motif at -2827; MYB binding site promoter at -845, -721; MYB1AT at -2538, -2469, -2403, -2205, -920, -848, - 843, -724, -719, -1344 at -1646; MYB2AT at -1931, -418, -1316; MYB4 binding site motif at - 845, -721; MYCATERD1 at -1022; RAV1-B binding site motif at -2752; T-box promoter motif at -2621, -334; TATA-box Motif at -348; W-box promoter motif at -643, -272, -1200. **polIB** promoter prediction: ARF binding site motif at -1876; AtMYC2 BS in RD22 at -961; BoxII promoter motif at -1435, -2276; CARGCW8GAT at -321; DRE core motif at -2498; DREB1A/CBF3 at -2496; I box promoter motif at -2512; L1-box promoter motif at -2560; MYB1AT at -2335, -2275, -814, -754, -201, - 728, -742, -1414, -1472, -2143; MYB4 binding site motif at -436, -985, -1443, -2189; MYCATERD1 at -961; SV40 at -1471; T-box at -456; TATA-box at -1188, -2558, -2821; and W-box promoter motif at -2950, -2662, -271.

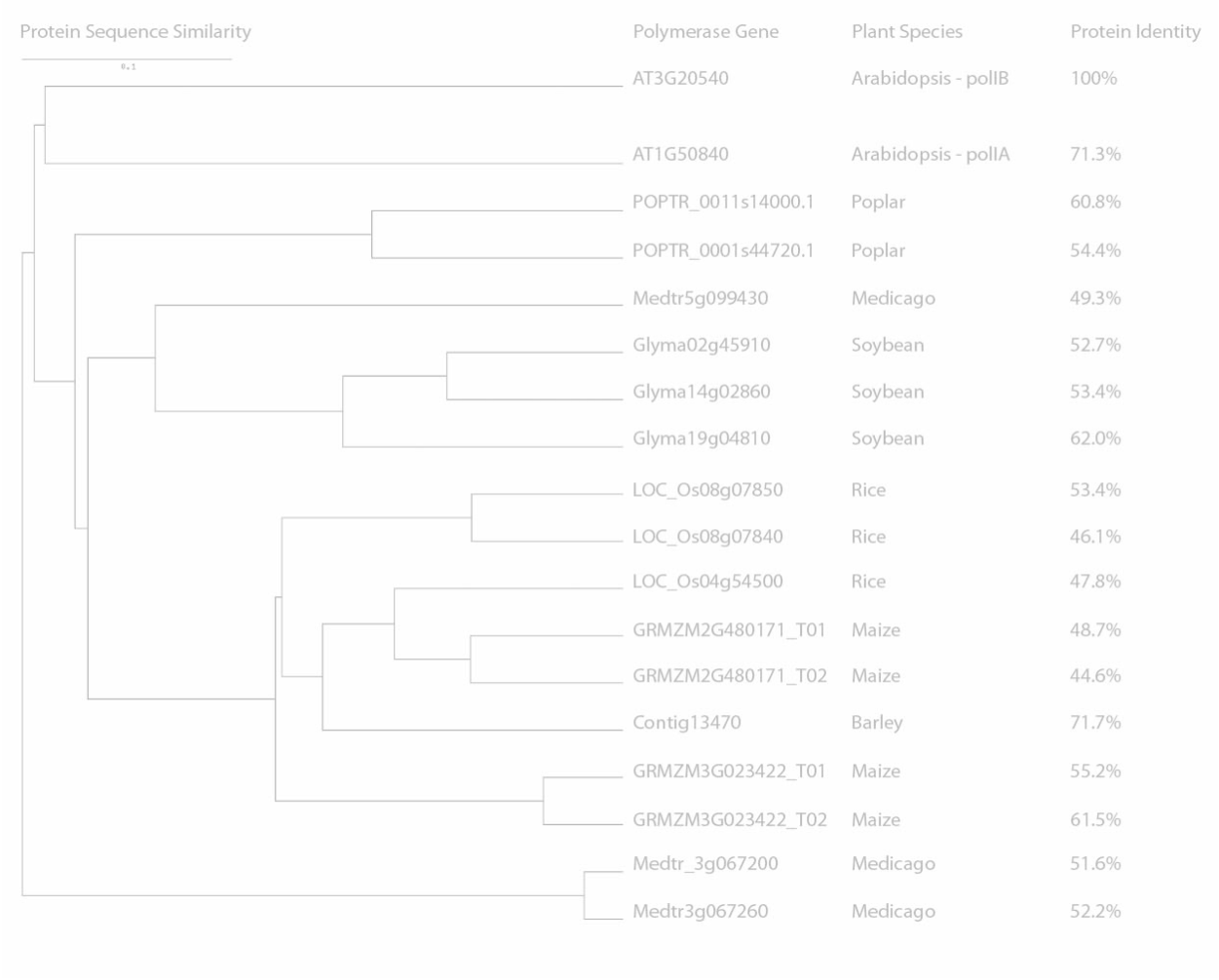

Figure 11. Phylogenetic Tree of Plant Organellar DNA Polymerase
Phylogenetic analysis of plant organellar DNA polymerases with similar palm domain protein identities. *Arabidopsis* polIA and polIB proteins have a 71.3% identity between their catalytic palm domains. (Tree generated using web tool: http://bar.utoronto.ca/expressolog_treeviewer/cgi- bin/expressolog_treeviewer.cgi).

CHAPTER 3: Phenotypic Analysis of the polIb-2 Mutant

Summary

Preliminary results indicated that *Arabidopsis* DNA polymerase IB mutants have a reduced rate of growth compared to wild type plants of the same biological age. The main phenotypic differences observed with polIb-2 mutants include the following growth and developmental defects. Root growth rate and hypocotyl extension rates are reduced in the DNA polymerase mutants. The rate of hypocotyl epidermis cell elongation is also reduced in the mutant. These mutants have a reduced seed set that is most likely caused by a mechanical delay in pistil elongation prior to pollination. These mutants germinate at the same time as wild type seedlings except that the mutant seedlings have a delayed greening effect and a partial loss of gravitropism. Plant greening recovery and negative gravitropism are restored to the mutant by 5 days post germination.

Methodology

Not all T-DNA insertion mutations result in a plant phenotype (Shedge et al., 2007; Parent et al., 2011). This can occur when the mutated gene tested has an unknown duplicate gene with homologous function, or the cell is able to compensate for the loss of one gene's function by using alternative cellular pathways and mechanisms. Many times phenotypes generated from gene mutation are difficult to detect because of both environmental and growth conditions. For example, a plant may not exhibit a phenotype when germinated under optimal growth conditions, but when a single variable like light intensity, growth temperature, or media supplement are adjusted then a phenotypic difference may become detectable.

Hypocotyl extension mutation analysis is a classic example of changing a single variable to obtain a phenotype. Under normal growth conditions *Arabidopsis* hypocotyl epidermis cells elongate at the same rate after germination and when in the presence of light (Le et al., 2005). This process of development is called photomorphogenesis (Li et al., 2011). Light is sensed by the plastids located within the epidermis cells of both the hypocotyl and the cotyledon (Vandenbussche et al., 2005). In contrast, when a seedling is germinated under etiolated conditions (dark growth) the development program of the hypocotyl is much different. This developmental program is called skotomorphogenesis (Josse and Halliday, 2008). Under these conditions the hypocotyl epidermis cells elongate much differently. The hypocotyl epidermis cells at position 1 that are at the shoot root junction begin to elongate first. After the first cells have begun to elongate then the cells at position 2 begin to elongate. This process continues until cell 20 at the hypocotyl and cotyledon junction or until the plastids sense light (Gendreau et al., 1997; Feng et al., 2008). The purpose of this developmental process is to extend to seedling out of the soil and into the light where photosynthesis may begin. Under dark growth conditions the chloroplast and the photosystems required for photosynthesis and chlororespiration fail to develop. Under these conditions cellular energy is provided strictly by the mitochondria.

Plant Meristematic Regions

Plants have two primary meristematic regions which are rich in mitochondrial density (Logan, 2010). These two regions contain stem cells and are found within the shoot apex and the root apex of the plant. The shoot apical meristem generates leaf primordia through the processes of cell division, cell elongation, and cell differentiation. Leaf primordia eventually develop into true leaves and continue to undergo cell expansion as their cell vacuoles fill with water and various solutes (Kang et al., 2003). Leaves generated by the shoot apical meristem form a

structure called the rosette. The timing of leaf development, number of leaves generated, and the position of the leaves generated are under strict control from the meristematic region (Grbic and Bleecker, 2000; Autran et al., 2002). Mutations resulting in a decreased number of leaves generated within the rosette may be linked to either a meristem or cell division defect.

The root apical meristem is located at the root tip and is comprised of three district zones (Dolan et al., 1993). The first zone is named the "zone of cell division". Like the shoot apical meristem, root cell division occurs within this "zone of cell division". This region contains around 22 cells from the quiescent center (QC) to the "zone of cell elongation". The junction between the "zone of cell division" and the "zone of cell elongation" is distinguished by the half volume cortex cells found within the "zone of cell division" compared to cells within the "zone of cell expansion". The third zone is called the "zone of cell differentiation". Within this zone the cells have fully expanded and often root hairs and lateral root branches are found. At the end of the root is the root tip which is composed of columnar cells. The root tip is dense in mitochondria. In addition the root will fail to grow without a root cap (Blancaflor et al., 1998). Root growth defects are found to result from a defect in cell division when the conserved numbers of cortex cells within the "zone of cell division" differs from wild type plants of the same biological age (Dolan et al., 1993).

In addition, the zone of cell division is a good location within the plant to determine pauses or defects in the cell cycle. For example, a GFP reporter gene under the control of the native cyclin B promoter can be used to determine the relative amount of cells that are transitioning from G2 to M phase of the cell cycle (Francis, 2011; Nowack et al., 2012). Most of the cells within this region progress through the cell cycle at the same time and at the same rate. Engineered within these reporter constructs is the ability for GFP to become degraded after each

turn of the cell cycle and transition into M phase (Antico Arciuch et al., 2012). This way GFP does not continue to accumulate and give false results. CycB1;1:: GFP results are dependent upon where in the cell cycle the root tip is at (Colon-Carmona et al., 1999). Therefore multiple wild type and mutant root tips need to be observed to determine if there are delays or a halt in the transition from G2 to M phase affecting mitosis.

Results

Tissue Specific Relative Gene Expression

Both organellar DNA polymerase genes were expressed in all tissues examined and the relative expression of both polymerases varied depending on tissue type (Fig. 12). The polIB relative expression levels were higher in tissues where cell density is higher (pistils and anthers, for example). Also, polIB expression levels were greater in tissue regions that contained a meristem (root and shoot apex) and where both cell division and cell expansion occurs. In contrast, gene expression levels for both genes were most similar in tissues where only cell expansion occurs, such as the hypocotyl and petal. Overall, the relative gene expression of polIB was observed to be more dominant in tissues that do not have photosynthesis as their primary function. In contrast, polIA expression levels were higher in total rosette leaf tissue, which is primary tissue for photosynthesis (Fig. 13). These results suggest that a balance exists between the expression levels of polIA and polIB. Based on expression levels within mitochondrial rich tissue this data may suggest that polIB is involved in mtDNA maintenance. In addition, tissue specific relative gene expression of TWINKLE was similar to the relative expression of polIB. This suggests that TWINKLE and polIB may function together inside the same tissue.

Analysis for Defects in Plant Development

Total plant growth rates are reduced when polIB gene expression is knocked down in the polIb mutant (Fig. 8). It was predicted that plant developmental defects should be observable within tissue regions where wild type polIB relative gene expression is high. No phenotypic differences were observed in temporal development at germination, at the onset of the first primordial leaves, the number of rosette leaves generated, in the numbers and morphology of tricomb cells generated per given leaf area, or at the onset of the primary stem bolting. In contrast, it was observed that shortly after germination there was a partial loss of root gravitropism and a reduction in the amount of starch granules within the root tip columnar cells (Fig. 15, 16). In addition, when germinated on media containing 1% sucrose we observed a delayed greening effect in the mutant, which resolved itself between 3 to 4 days post germination (5-6 dpi) (Fig. 16). Shortly after greening (6-7 dpi) the root columnar cell starch levels increased (data not shown) and negative gravitropism was restored.

The polIb-2 mutant routinely generated a lower seed set when compared to wild type plants, regardless of optimized water, soil, and growth chamber conditions (Christensen, 1997) (data not shown). Reciprocal crosses were conducted (Christensen et al., 1998) with wild type plants to determine if the observed low seed set was a result of either a male or female gametophyte defect. Successful pollination occurred in both directions with wild type-like siliques and seed sets generated. To determine if the low seed set was a result of an embryo defect, anthers from polIb-2 mutants were used to manually self-pollinate the mutant pistils (Christensen et al., 2002). Siliques generated from the manually self-crossed mutants were phenotypically normal and produced a similar seed set as wild type siliques. When observing the polIb-2 pistil prior to pollination it was found that the mutant pistils were on average shorter

when compared to wild type. Both flowers had anthers that were fully extended and had already begun to shed their pollen (Fig. 17). It was proposed that the polIb-2 low seed set results from a mechanical defect or a developmental delay in pistil extension rate[1] and not from either an embryo or gametophyte defect.

Analysis of Root Growth and Hypocotyl Expansion Rate

Knowing that wild type polIB is expressed highly within root tissue, additional characterization of the root length phenotype was generated by developing root growth curves. When comparing growth rates of polIb-2 mutants to wild type seedlings on modified growth medium (that was not supplemented with 1% sucrose), we found the mutants had a significantly slower root growth rate (Fig. 18) and only survived up to 21 dpi. In addition, when seedlings were transferred from the modified growth medium to soil (between 7 – 10 dpi) all mutants died within 10 days of the transfer, while both polIb-2 heterozygotes and wild type plants survived. The rate of root growth for the mutant was also significantly lower (47.5% less) than wild type when germinated on growth media (containing 1% sucrose) (Fig. 19). From this we determined that the polIb-2 mutant needs media containing at least 1% sucrose at germination to survive to maturity and produce seeds. At seven days post germination and after the onset of greening, seedlings could be transferred to soil and were no longer dependent upon sucrose.

Changes in plant starch levels, sucrose levels (Smith and Stitt, 2007), and the loss of gravitropism all have the ability to affect plant growth. Interestingly, the polIb-2 mutant roots exhibit phenotypic effects involving all three of these factors. These three factors mostly affect cell elongation but it remained unclear whether cell division could be also affected. Thus, the

[1] The actual rate of pistil extension was not measured and proven to have a statistically significant rate reduction. This statement was made from qualitative observations when emasculating and manually pollinating over 50 mutants and wild type individual crosses.

meristematic zone of root tips was observed to determine if the polIb-2 mutant had delays in cell division. When observing propidium iodide stained (Weigel, 2002) root tips by confocal microscopy there were no differences found in cell numbers or relative cell sizes of cortex cells, which extended up from the quiesent center (QC) to the zone of cell expansion (n=10, 5 dpi) (Fig. 20). Within the same region no differences were observed in the G2/M phase transition of the cell cycle when observing (n=15) polIb-2 x cycB1;1::GFP seedlings at either 5 or 7 dpi (Colon-Carmona et al., 1999) (Fig. 21). Hence, we found no supporting evidence of a cell division defect within the root tip.

Analysis for a Cell Expansion Defect

Hypocotyl epidermis cell numbers were examined to determine if polIb-2 had a cell division or cell expansion defect. The hypocotyl was selected to detect any cell division defects because the majority of the hypocotyl epidermis should have already divided prior to germination (Gendreau et al., 1997). If the mutant had a cell division defect then it was predicted that fewer epidermal cells would be present in the mutant than in wild type. There were no significant differences found in the number of hypocotyl epidermis cells extending from the root shoot junction to the cotyledons (n=6, 2 dpi; n=3 at each 3, 4, and 5 dpi). However, the mutant hypocotyls were observed to extend at a 31.8% slower rate when compared to wild type plants at the same biological ages and germinated under the same dark growth conditions (Fig. 22). The mutant hypocotyls never reached the same lengths as the wild type hypocotyls when germinated under light or dark growth conditions (n=100) (Fig. 23A,B)

The polIb-2 mutants did not have a temporal difference in the order in which hypocotyl epidermis cells expanded. Hence, at 2 dpi cells near the root/shoot junction (position 1) up to hypocotyl epidermis cells at position 12 had begun to expand in the mutant, similar to those

observed in the wild type. A major difference was found in cell size (viewed planer area) between the wild type and mutant cells. The expanding mutant cells were significantly smaller than the wild type cells of the same biological age (Fig. 24). The cells that had not begun to expand within either the mutant or wild type hypocotyls remained to have similar cell sizes. It is proposed that the observed differences in hypocotyl epidermis expansion provide direct evidence that the polIb-2 mutant has a delay in cell elongation.

Discussion

Gene Expression

The polIB mutant exhibits a slow growth plant phenotype. The relationship between mechanisms involved in organellar DNA replication and plant growth are not well understood. Potentially, slow growth can result from either defects in plant development, defects in plant cell division, or defects in plant cell elongation. Growth phenotypes are often observed as secondary effects from gene mutations. For example, mutations that increase the levels of photorespiration in the plastid, or gene mutations that increase reactive oxidative species in mitochondria, or gene mutations that effect overall cellular homeostasis. Hence there are many possibilities that can affect a general category like plant growth.

Gene expression analysis of both polIA and polIB was conducted in an effort to find a focal region where either of the two organellar DNA polymerase genes had significant differences or similarities in expression levels. These locations could serve as primary sites of investigation for phenotypic analysis. Interestingly the polIB gene is expressed with greater relative abundance in almost all non-photosynthetic tissues examined. More specifically polIB gene expression was greatest in both the shoot and root apex in addition to the pistil. The majority of plant development and cell division take place within these three organ types. In

contrast the expression of both DNA polymerases was observed to be most similar within the hypocotyl. The hypocotyl is not considered to be a tissue that undergoes developmental changes or cell division after germination, but this is an organ that can undergo extreme rates of cell expansion during etiolated plant growth (Vandenbussche et al., 2005). In addition, cell expansion is significant in the three other plant organs previously discussed.

Gene expression was greatest within the shoot apex tissues which also contain the meristematic stem cells. This region has a high cell density in addition to high mitochondria density. A previous assumption was that mitochondria within this region are more active in cellular respiration than within other tissue types. The basis for this assumption is because cells need energy to divide. In addition, mitochondria observed in previous studies indicate that a unique cage-like structure forms around the nucleus of meristematic cells within this region (Segui-Simarro et al., 2008). It has been proposed by others that this cage structure is where DNA replication and mitochondrial DNA is mixing after fusion of peripheral mitochondria (Logan, 2006). It is well accepted that larger mitochondria are required for metabolic function and it stands to reason the closer this organelle is to the nucleus the greater the probability that nuclear encoded mitochondrial targeted proteins will successful make their way to the organelle (Antico Arciuch et al., 2012).

One unknown is the level of DNA replication of the level of oxidative phosphorylation that takes place near the nuclease. Expression analysis of polIA would suggest that mitochondrial DNA replication or repair is greater within this area. When conducting a side project to determine the relative gene expression of mitochondrial encoded cox1, atp1, nad6, and rps4 genes it was determined that the pistil had the greatest expression of these genes (Fig. 25). Mitochondrial gene expression models have proposed that organellar gene expression is directly

proportional to the chromosomal content of the organelle. That said, why does the shoot apex which contains the meristematic stem cells, mitochondrial cage structures, the primary location for cell division and differentiation, and rapidly expanding tissue have lower levels of relative gene expression than the tissue found in the pistil[2]?

It is proposed that the model relating chromosomal or mitotype content needs more work. These gene expression analysis experiments need to be followed up by additional experiments to determine the membrane protein content of the larger organelle (Dubessay et al., 2007). It is possible that respiration is significant in the region because of the mixing of intra-membrane proteins upon mitochondrial fusion. Even if this is so, the fact remains that mitochondria-encoded genes appear to be expressed at a lower than predicted level within the meristematic tissue.

Mitochondrial or Plastid Phenotype?

Both the partial loss of gravitropism and the delayed greening phenotype suggest that the plastid may be affected within the polIB mutant. Developmental delay may result in a slowly replicating plastid genome, a slowly developing organelle, or possible indirect effects from mitochondrial defects. As discussed previously, the mitochondria are responsible in part for heme regulation of the cell. Heme is required by the plastid and the mitochondria in mechanisms of photosynthesis, chlororespiration, mitorespiration, and photorespiration. If the mitochondria fail in regulating heme then all of the listed functions will be affected. Alternatively, secondary pathways for heme metabolism are also found in many plant plastids (Woodson et al., 2011).

[2] The same cDNA samples at the same concentrations were used in both RTqPCR experiments to determine the relative gene expression of organellar DNA polymerase I and mitochondrial encoded genes.

Sucrose or starch levels are not adequate within the polIB mutants at germination. This is evident when characterizing plant growth rates on media supplemented with or without sucrose. Mutants do not survive without sucrose being provided at germination. Homozygous polIB mutants have not been observed to germinate directly in soil. The haplo-insufficient heterozygous polIb-2 mutant germinates and matures to seed on general growth medium without sucrose and when germinated directly in soil. This would also suggest that the sucrose need is a direct result from some deficiencies caused by the single polIb-2 mutation.

Sucrose is generated from the combining of glucose and fructose (Bieniawska et al., 2007). This disaccharide can be exported from cells and travel from the shoot to the roots where it can then enter distant cells and be metabolized (Hammond and White, 2008). This molecule is known to act as a regulator of transcription of at least 26 *Arabidopsis* nuclear encoded genes. Sucrose is a secondary product generated from photorespiration[3]. The two sugar monomers of sucrose are involved in starch formation, cell wall structure, and cellular respiration (Wang et al., 1993; Kohorn et al., 2006). In general, high levels of sucrose are inhibitory to plant growth (Barratt et al., 2009). In the case of the polIb-2 mutant sucrose is required at germination for the homozygous mutant plant to survive.

Cell Division

The polIb-2 mutant does not have a defective cell division phenotype. This was determined from the following. Rosette leaves generated from the shoot apical meristem at the same time as the wild type plants. This indicated that the temporal development of leaves is not affected. Cell division is required in the formation of leaf primordia. Both the mutant and the wild type plants bolt or put up stems at relatively the same time. The shoot apical meristem

[3] Photorespiration does not generate ATP.

remains at the top of the stem and eventually is differentiated into flowers and gametes (Williams and Fletcher, 2005; Wagner and Meyerowitz, 2011). Stem elongation is a result of both cell division and cell elongation.

Differences in cell division can be directly observed in the hypocotyl and the cortex cells of the root tip (Beemster and Baskin, 1998). The hypocotyl contains all of its replicated cells prior to germination. The number of hypocotyl epidermis cells remains conserved between *Arabidopsis* plants. Once the seedling germinates, the hypocotyl cells continue to expand until the cotyledons detect light. Therefore, a difference in hypocotyl epidermis cell numbers would indicate a cell division defect prior to germination. The hypocotyls from wild type and polIb-2 mutants have the same number of epidermis cells and therefore provide no evidence for a cell division defect.

The root tip is another conserved region where differences in cell division can be detected. As discussed previously, there were no detectable differences in the number of cortex cells extending up from the QC to the "zone of cell elongation" of the root tip. The cortex cells within the root tip "zone of cell division" of the polIb-2 mutant may have a greater planer area. Analysis to measure and compare the area between these cell has not been completed.

The cycB1;1::GFP reporter line provided strong evidence that the cell cycle within the mutant lines is progressing from G2 to M phase at relatively the same time. The cells within this region remain relatively in sync with each other and divide at relatively the same time. In summary, there is no supporting evidence that the polIb-2 mutant has a cell division defect.

Cell Elongation Defect

Strong evidence has been obtained that demonstrates the slow growth phenotype observed in the polIb-2 mutant is a result of a cell elongation defect. Elongation differences are

observed in the planer area of hypocotyl epidermis cells. These epidermis cells begin to expand according to their temporal developmental program, but they extend at a slower rate. This is evident in hypocotyl expansion from mutant and wild type samples of the same biological age and regardless of growth in the light or the dark. In addition the mutant hypocotyl extends the same regardless of fluridone treatment[4]. These results would suggest that chloroplasts are not a direct factor affecting the growth phenotype.

Factors Involved in Cell Expansion

Multiple factors can directly affect cell expansion. One of the major group of factors that control both cell division and cell expansion are plant hormones. There are six plant hormones that have been well studied in root growth. They are auxin, abscisic acid (ABA), brassinosteroids (BRs), cytokinin (CK), ethylene, and gibberellins (GA). Each of these hormones interacts with different receptors at different tissue locations within the plant. These hormones regulate gene expression for the following enzymes for cell wall cleavage and synthesis. Genes required for cell wall expansion encode the following enzymes: xyloglucan endotransglycosylases (XTHs), pectinmethylesteraseses (PMEs), expansins, extensins, Pro-rich proteins (PRPs), arabinogalactan proteins (AGPs), and peroxidase genes (De Grauwe et al., 2005; Ubeda-Tomas et al., 2012). A potential semi-direct connection between mitochondrial and plastid involvement in cell expansion is that both organelles have the ability to produce sterols and steroid precursors.

Cell expansion is initiated from turgor pressure within the cell. After the process of cell wall expansion has been initiated, this process continues and is not reversible. In short, the cell

[4] See Chapter 4 methodology for details regarding the mechanism of the fluridone herbicide.

wall is enzymatically cleaved, expanded by intracellular pressure, then reconnected together between cellulose microfibrils (Fry, 1992).

In cell division dynamin-related proteins have been linked to the formation of a cell plate. These proteins are also related to mechanisms involved in mitochondria and chloroplast division. The following is a simple model for dynamin-related protein organellar division. *Arabidopsis* dynamin-like proteins 1C and 1E aid in the formation of a spiral or ring-like structure around the organelle (Jin et al., 2003). First this ring structure begins to constrict forming an elongated hourglass-like structure. Second, these molecules pinch the organelle, release clathrin-coated vesicles, and reduce the area of the organellar membrane. Third, cytokinesis occurs. Fourth, the end product contains a planar fenestrated sheet (Collings et al., 2008).

Arabidopsis dynamin-like protein 1A mutants have extremely similar phenotypes to the polIb-2 mutants described in the results section of the chapter. These mutates have reduced growth rate in both the hypocotyl and the root. In addition these mutants exhibit a partial loss of gravitropism which is restored shortly after germination. The dynamin-like protein 1A mutants do not show a change in cell numbers within areas of cell division. In addition these mutants exhibited a slowed rate of individual cell expansion. The final results were that the *Arabidopsis* dynamin-like 1A null mutant had defects in endocytosis, cellulose synthesis, cytokinesis, and cell expansion (Collings et al., 2008). It remains unclear if *Arabidopsis* dynamin-like 1A gene is affected by a polIb-2 mutation. But it does remain plausible that defects may occur within mitochondrial division that could potentially affect organellar dynamics.

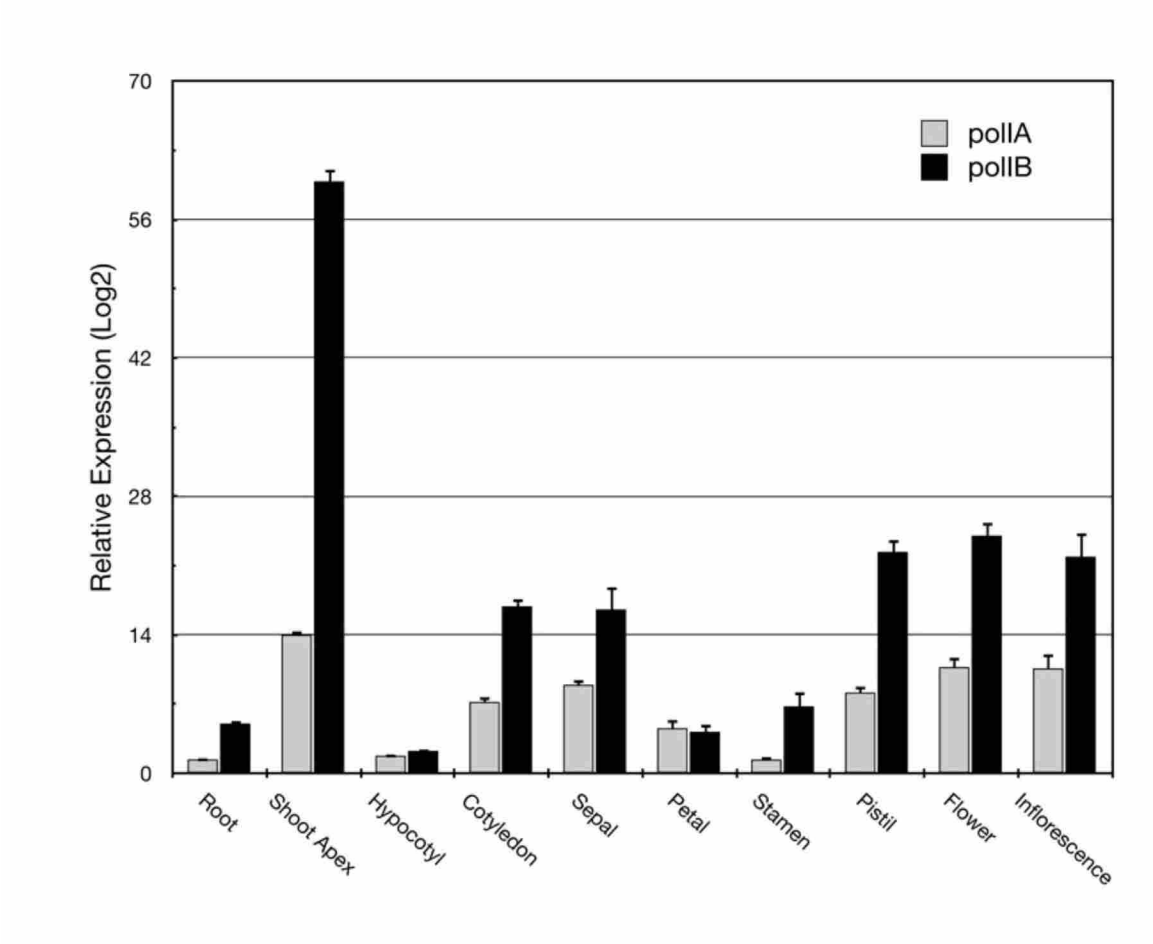

Figure 12. DNA Polymerase I Gene Expression in Non-Primary Photosynthetic Tissue
Gene expression profile of polIA and polIB in wild type tissues. All gene expression experiments were normalized to Actin 2 gene expression (biological triplicates). Error bars represent positive SEM.

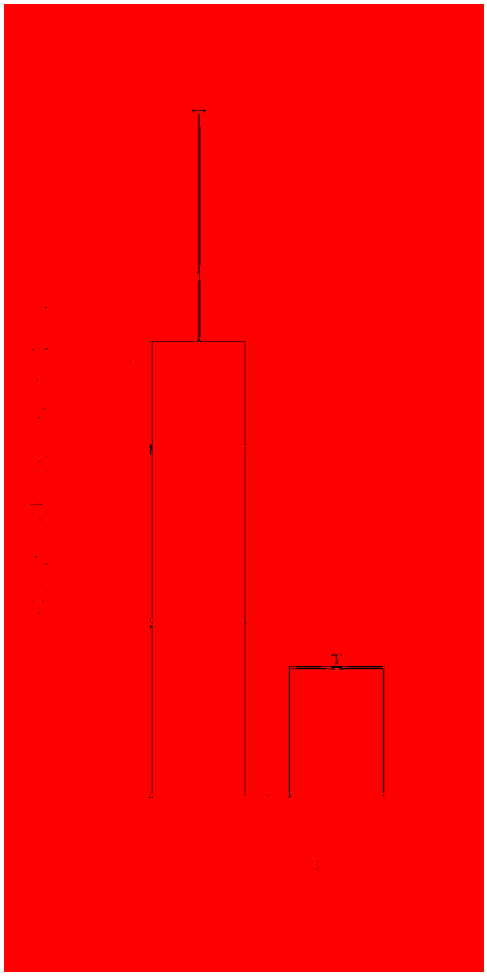

Figure 13. DNA Polymerase I Gene Expression in 14 dpi Total Rosette Leaf Tissue
Gene expression profile of polIA and polIB in wild type tissues. All gene expression experiments were normalized to Actin 2 gene expression (biological triplicates). Error bars represent positive SEM.

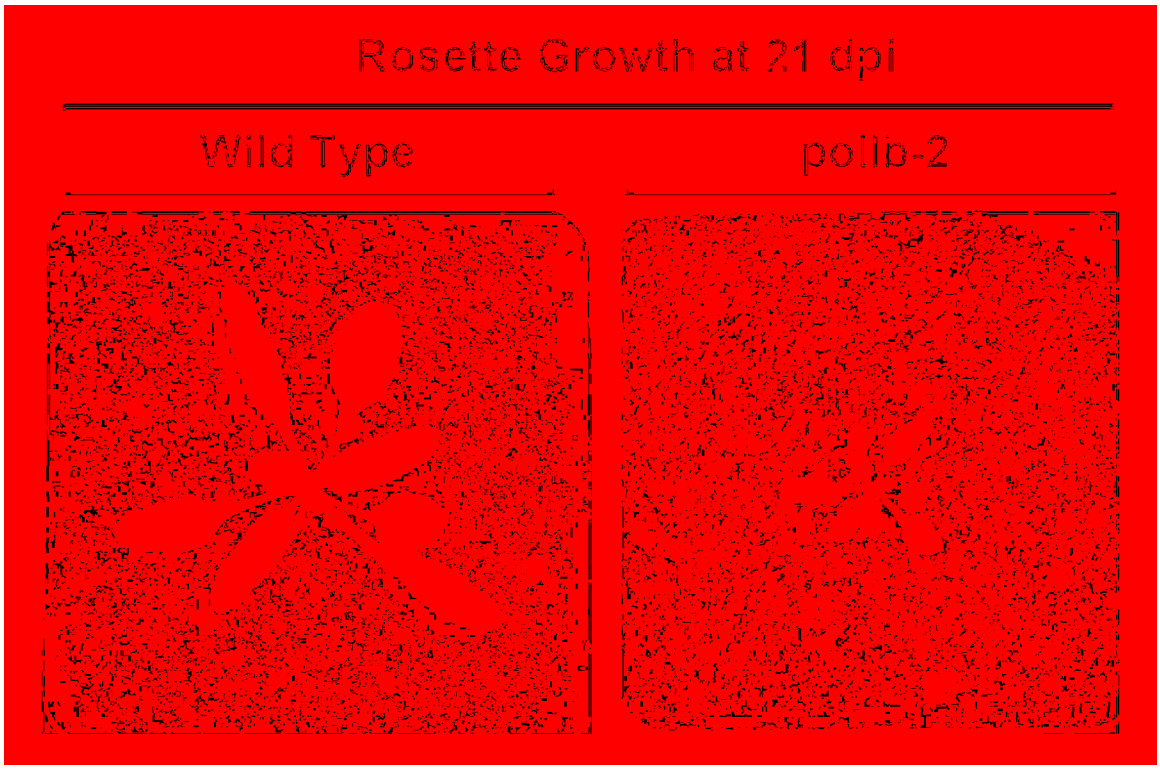

Figure 14. DNA Polymerase IB Rosette Growth Difference
The rosette area of the pollb-2 mutant is significantly smaller at 21 dpi.

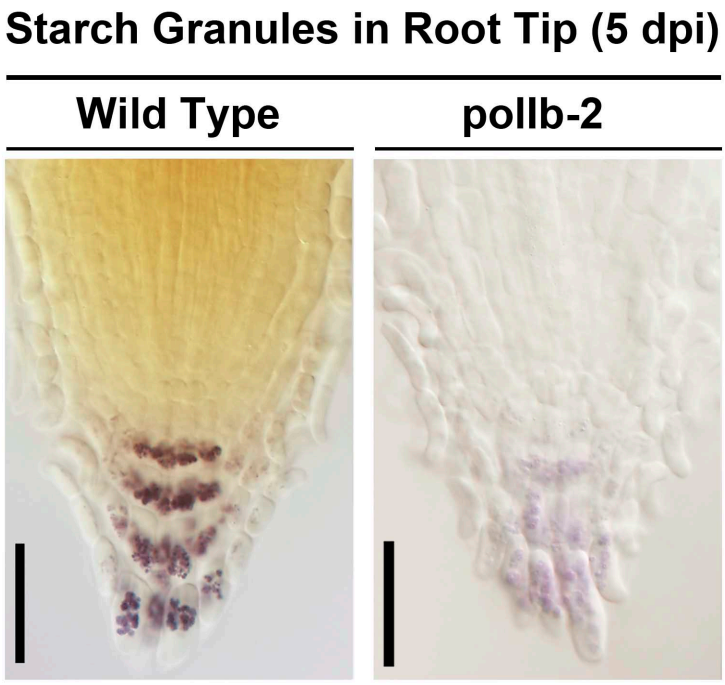

Figure 15. Starch Deposits in Root Tip at 5 DPI
Starch granule levels are lower in the polIb-2 mutant when compared to wild type at 5 dpi. Size Bars 100 μm.

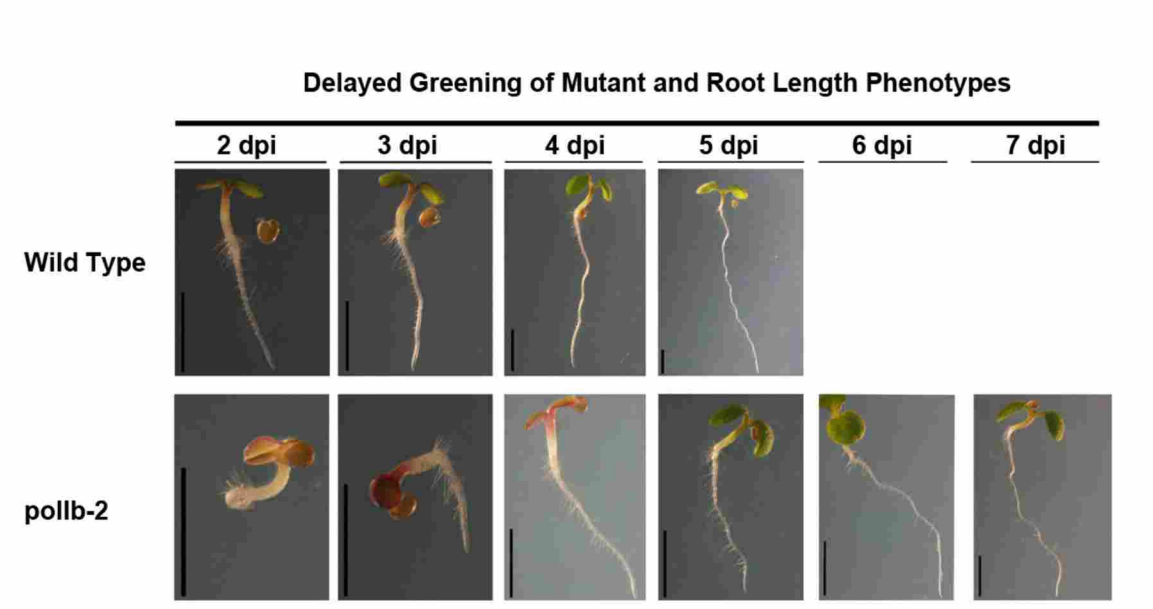

Figure 16. Mutant Delayed Greening, Reduced Root Length, and Partial Loss of Gravitropism
The pollb-2 mutant has a delay in greening up to 4 days post germination when compared to wild type. Also the polIb-2 mutants have a slower root growth phenotype with a partial loss of gravitropism. Size Bars 2mm.

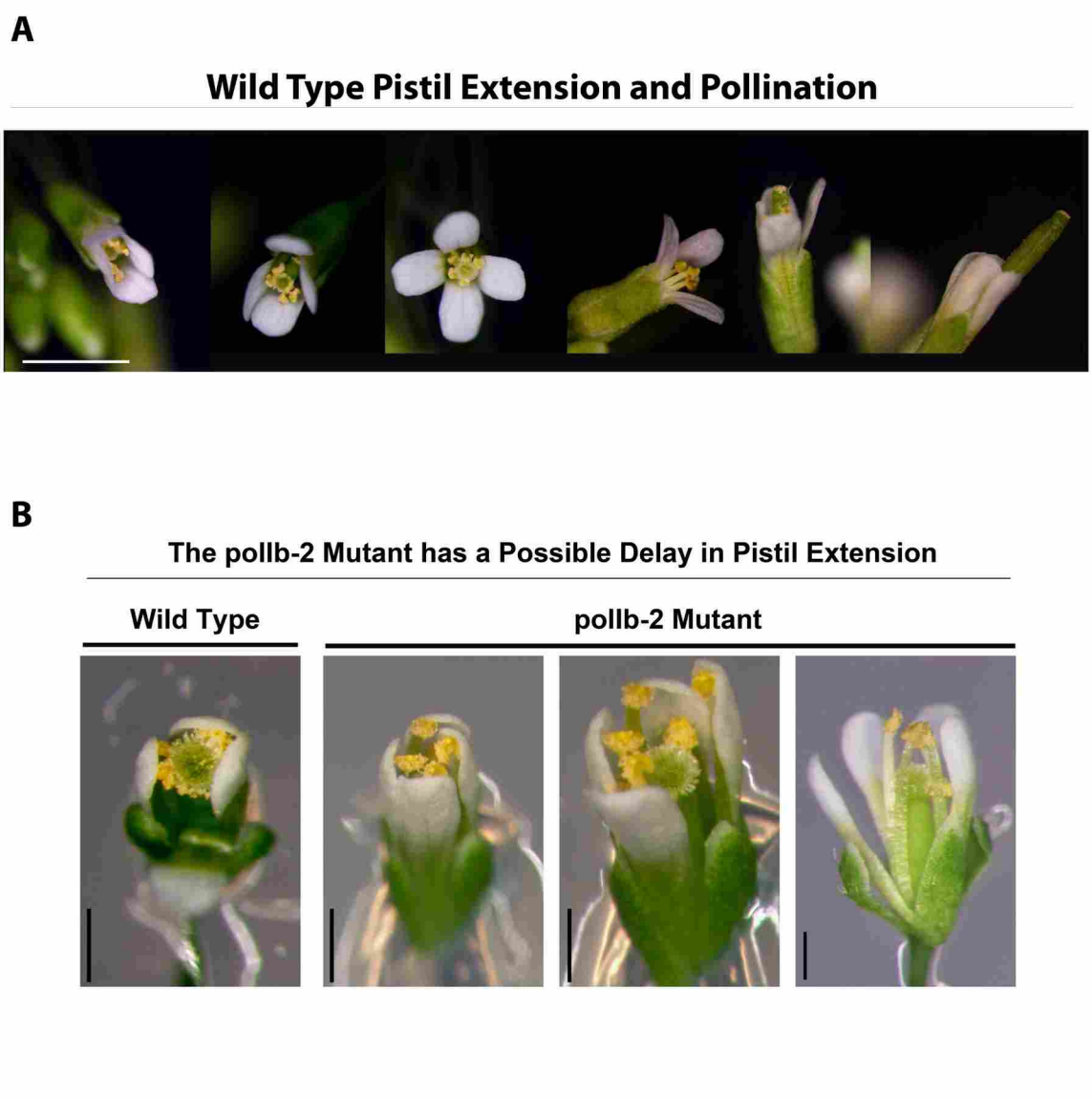

Figure 17. PolIB Mutant has a Decreased Rate of Pistil Extension
A) From left to right demonstrates the process of pistil extension and pollination in wild type flowers. B) On average polIb-2 mutants that have anthers releasing pollen are observed to have a shorter pistil within the 24 hour time frame prior to pollination. Size Bars 500 μm.

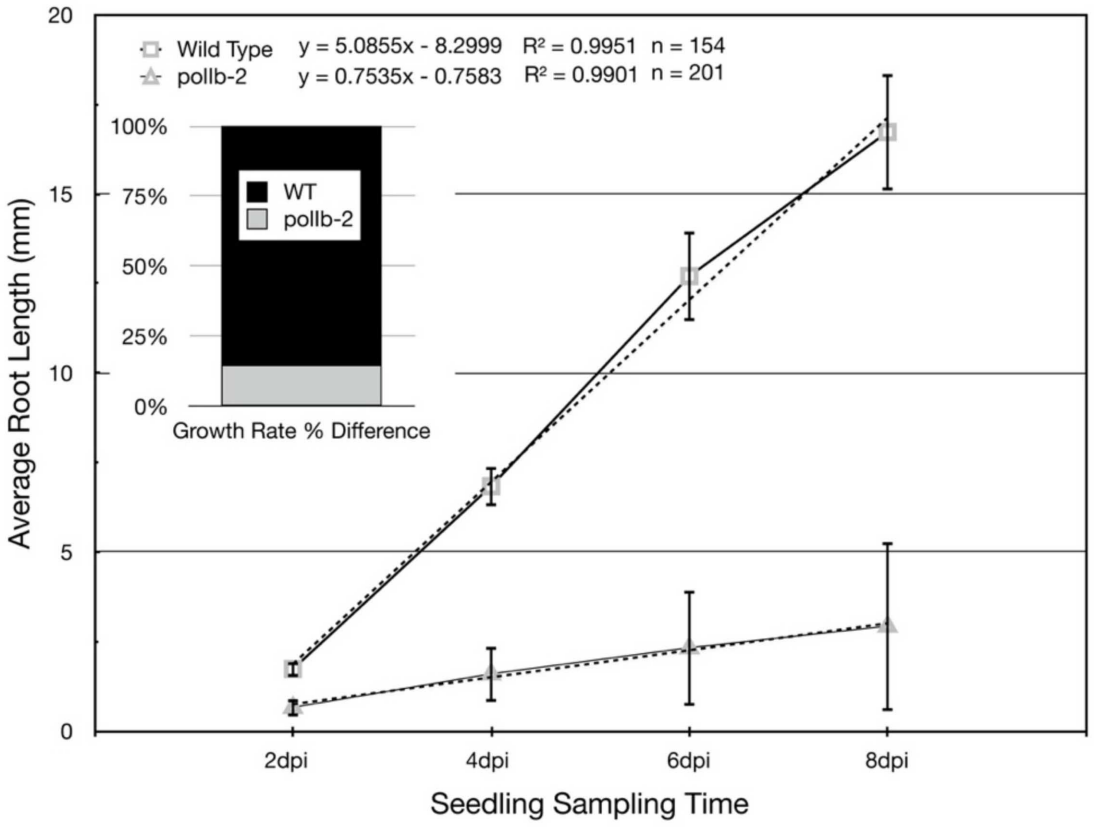

Figure 18. Root Growth Rate (Growth Media without 1% Sucrose)
The pollb-2 mutant has a root growth rate of only 14.5% of wild type when germinated on media that does not contain 1% sucrose. Error bars represent standard deviation.

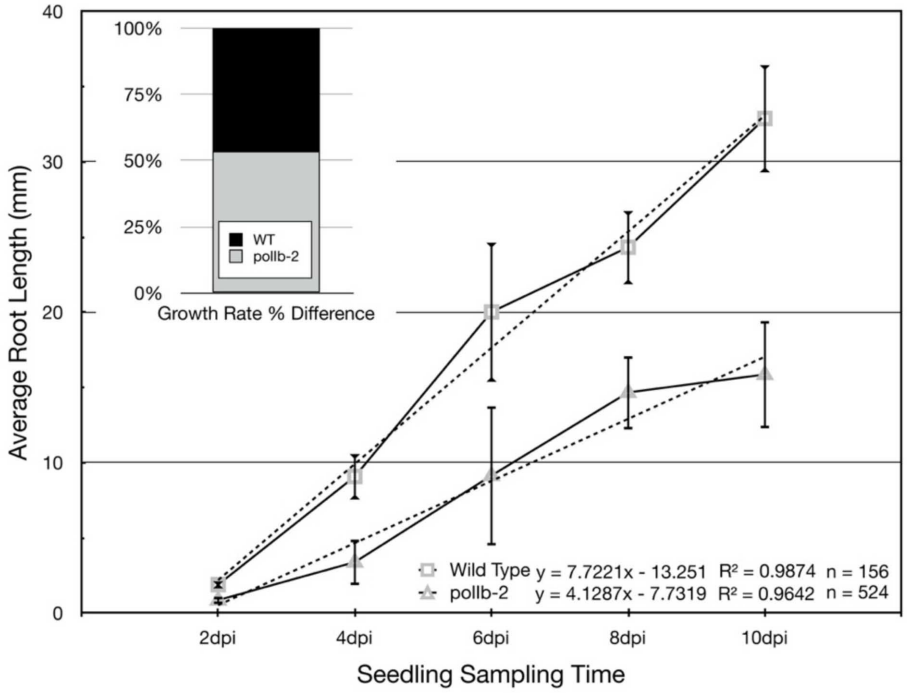

Figure 19. Root Growth Rate (Growth Media with 1% Sucrose)
When 1% sucrose is added to growth medium at germination, the polIb-2 mutant has a 52.7% root growth rate when compared to wild type plants at the same biological age and under the same growth conditions. Error bars represent standard deviation.

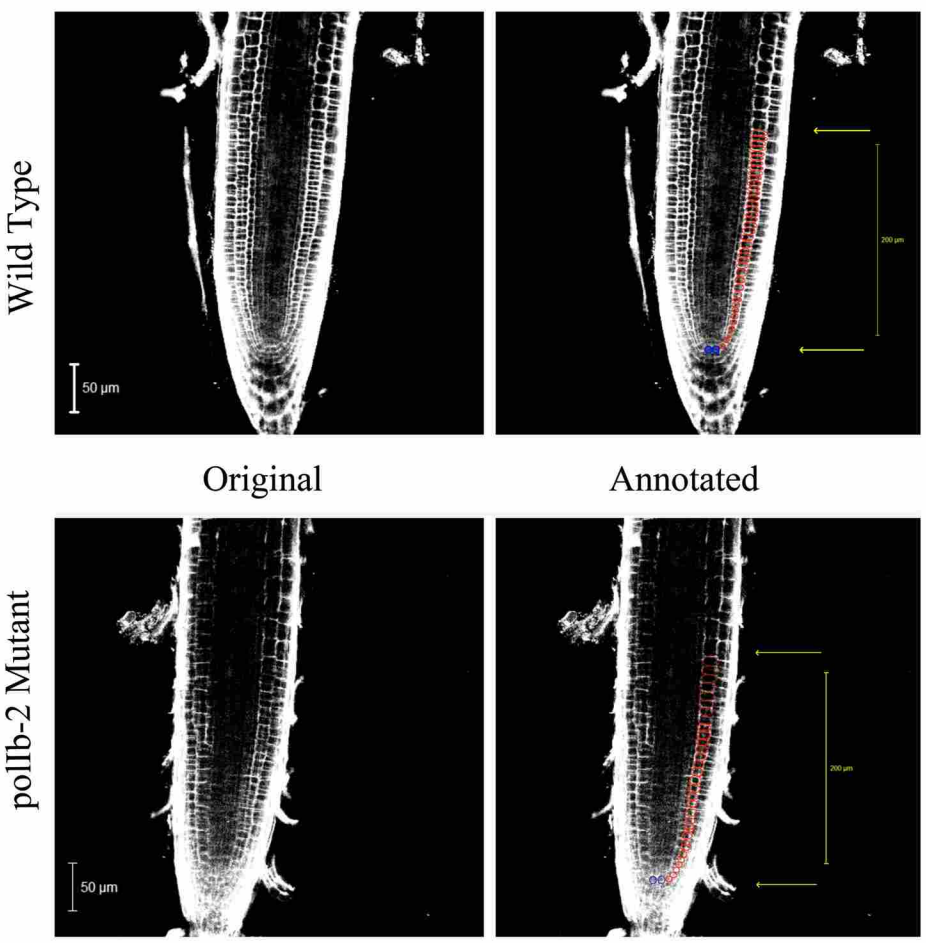

Figure 20. Root Tip Meristematic Region
Confocal analysis of root tip cortex cell numbers within the primary root meristematic region zone of cell division indicates no significant differences in the number of cortex cells extending up from the QC to the root zone of cell elongation. Size Bars: 200 µm.

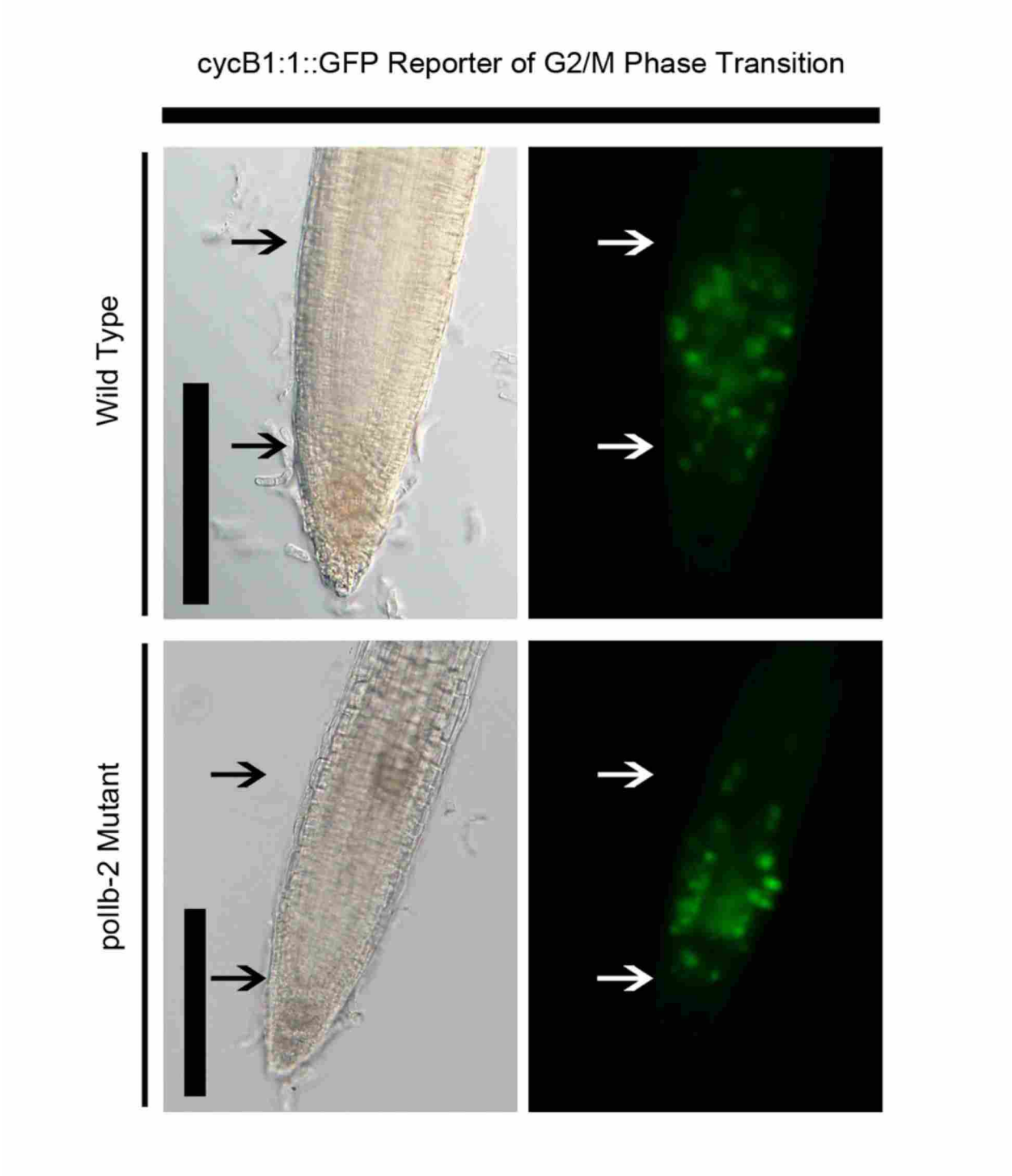

Figure 21. CycB1;1::GFP Transgenic Reporter of G2/M Phase Transition
Expression of the cycB1;1::GFP reporter of G2/M phase transition indicates no significant difference in Cyclin B signal between wild type and mutant. Region between arrows represents the zone of cell division. Size Bars:200 µm.

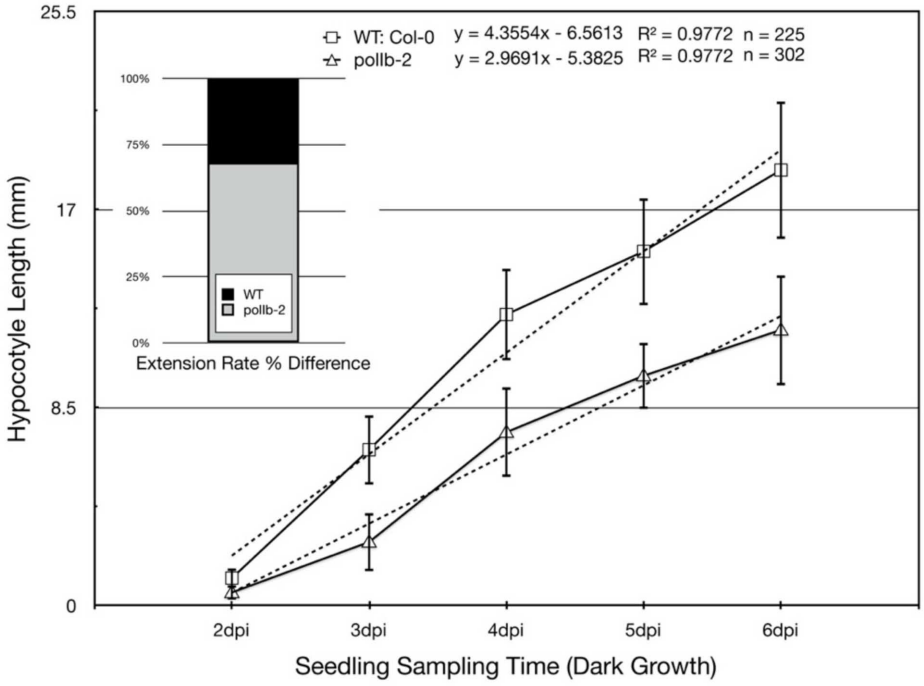

Figure 22. Hypocotyl Expansion Rate
The pollb-2 mutant has a slower hypocotyl extension rate that is only 68.2% of the wild type rate when germinated under dark growth conditions. Error bars indicate standard deviation.

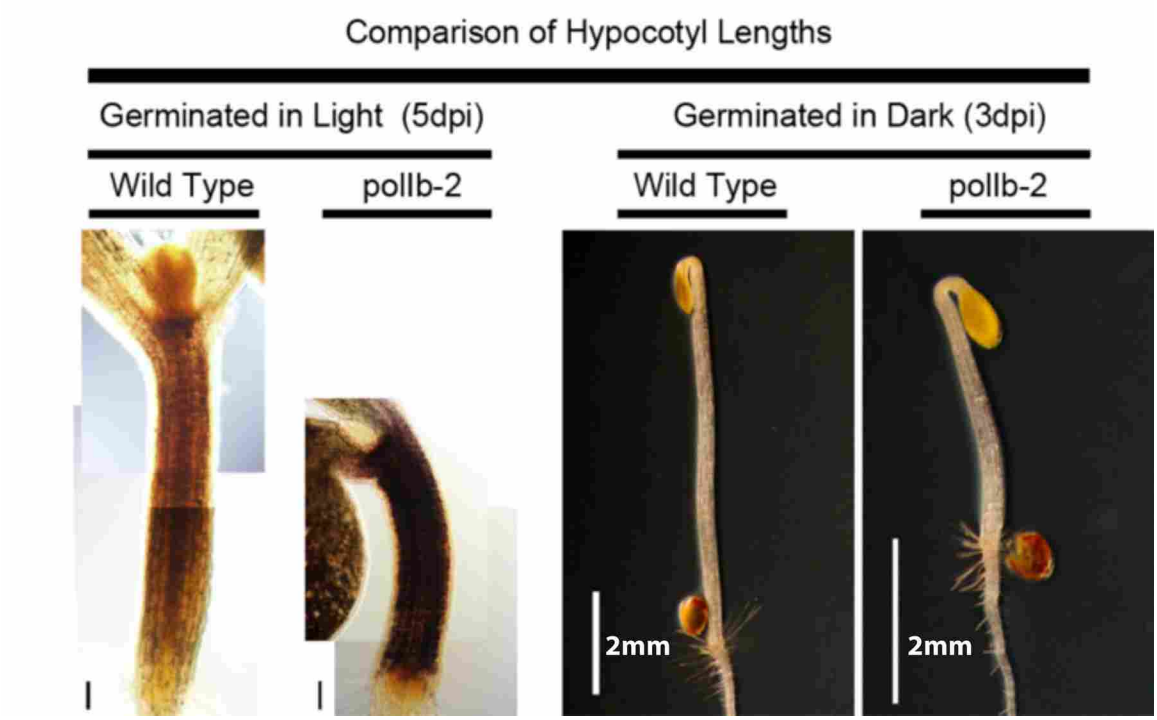

Figure 23. Hypocotyl Expansion Under Light and Dark Growth Conditions
Images of hypocotyls (iodine stained for contrast) germinated under light and dark growth conditions. The mutant has a shorter hypocotyl under both light and dark growth conditions. Size Bars: light, 100 μm; dark, 2 mm (samples are at different magnification but the size bars represent the same length).

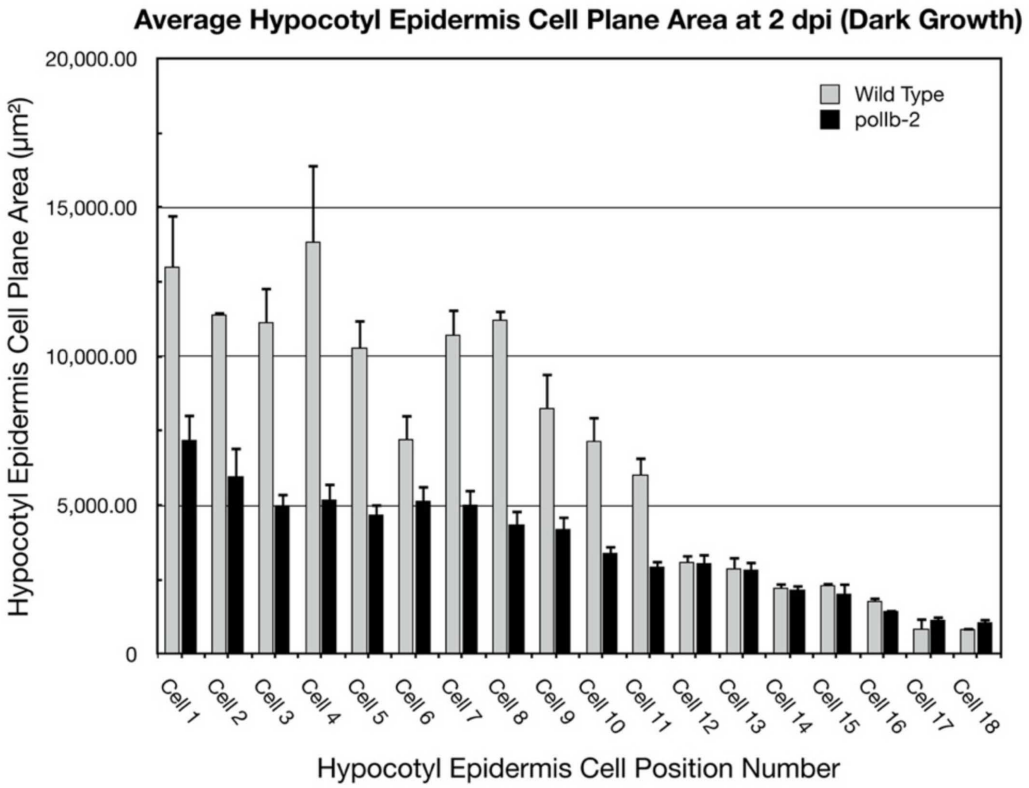

Figure 24. Hypocotyl Epidermis Cell Expansion
The hypocotyl epidermis extends temporally with wild type but at a slower rate when comparing the cell planer area of pollb-2 mutant to wild type seedlings. The cell at position 1 is near the root shoot junction and the cells at position 18 are nearer the cotyledons. Error bars are SEM.

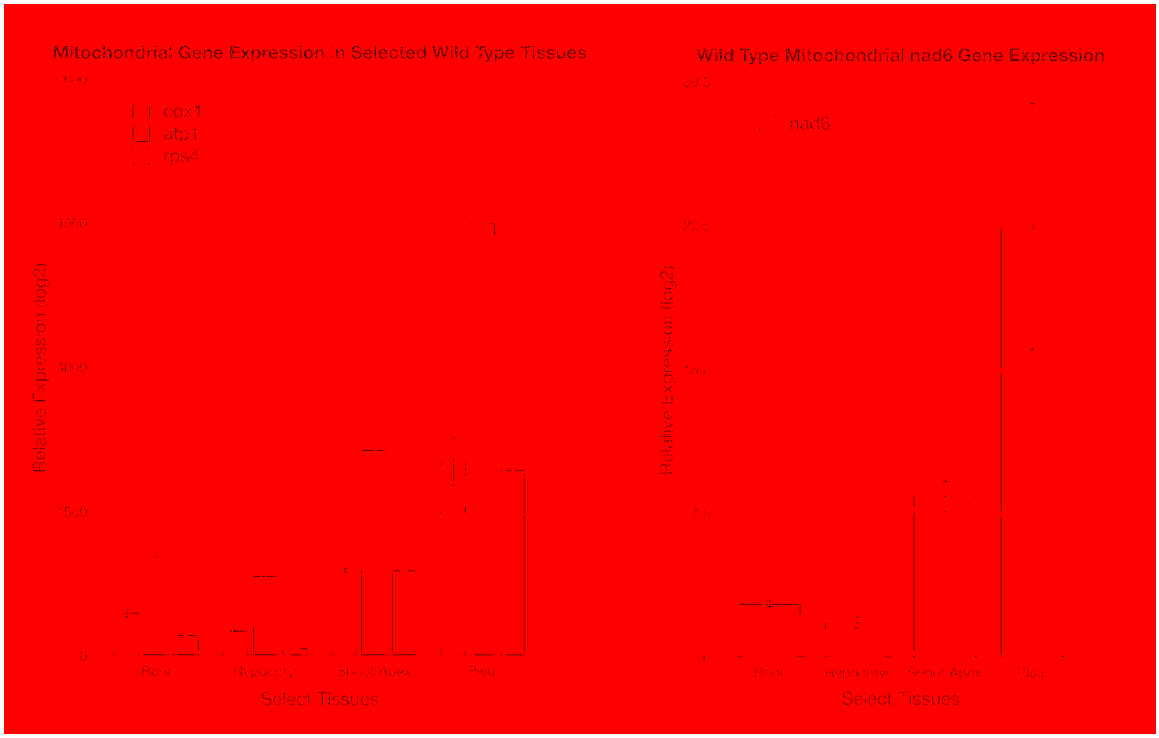

Figure 25. Mitochondrial Encoded Gene Expression in Tissues with Significant polIB Gene Expression
Gene expression profile of cox1, atp1, and rps4 (left graph) and nad6 (right graph) in wild type tissues. All gene expression experiments were normalized to Actin 2 gene expression (biological triplicates). Error bars represent positive SEM.

CHAPTER 4: Chloroplast and Mitochondria Effects

Summary

The purpose of this chapter is to address and to determine if the DNA polymerase 1B mutant has an organelle defect. PolIB mutant seedlings exhibit a delayed greening phenotype and a partial loss of gravitropism at germination (Chapter 3). Both of these phenotypes suggest a potential plastid dysfunction. In addition, reduced growth rates of the hypocotyl and the root may indicate either a plastid or a mitochondrial defect. No significant differences in hypocotyl extension rates are observed when mutants are germinated and prohibited to generate chloroplasts. This would suggest that the growth phenotype is indirectly related to mitochondria dysfunction and not chloroplast. It has been suggested by others (Gordon Research Conference 2010, unpublished) that mitochondria contribute to plastid development. Hence, the plastid-like phenotypes may be an indirect result of a mitochondrial functional defect. Therefore, both mitochondria and chloroplast numbers were characterized from the polIb-2 mutant. It was determined that the polIb-2 mutant has an increased incidence of mitochondrial fission, suggesting that mitochondrial function has been affected. In addition, chloroplast levels are not affected after plants have greened and gravitropism has been restored.

Methodology

Evidence of Organellar Genome Depletion

As previously discussed, the DNA polymerase IB has been shown to target both mitochondria and plastids. This enzyme has also been predicted to function as a plant organellar DNA polymerase because of its conserved protein domains that are homologous to other DNA polymerases that have been functionally characterized. Therefore, it is proposed that organellar

DNA levels could be potentially affected when this gene is mutated. That said, there remains another DNA polymerase IA which has also been shown to be targeted to both mitochondria and chloroplasts. In addition, when gene expression of polIB is knocked out the gene expression of polIA is increased. It has been proposed that polIA is attempting to compensate for the loss of polIB gene expression. Therefore, it is proposed that DNA levels would not deviate from wild type levels in the polIB mutant because of the potential compensation polIA provides to organellar DNA replication. Then again, why does the polIa mutant not have a phenotype while the polIB mutant has a slow growth phenotype? Potentially, polIB may either have additional functions or polIB may be preferentially targeted and required by one organelle.

To address these questions a quantitative PCR (QPCR) approach could be used to determine if the relative copy numbers of organellar chromosomes has been reduced (Preuten et al., 2010). A reduction in chromosomal numbers (not genome content) could potentially affect organellar function in addition to copy numbers of segregated chromosomes in organelles that have undergone fission. This could lead to a mitochondrial genome depletion effect that would also directly affect mitochondria movement, fusion, and fission rates (Okamoto and Shaw, 2005).

In this study QCPR was conducted to determine the relative copy numbers of the mitochondrial and plastid genomes. Efforts were made to generate specific primers that would target a single-copy DNA sequence within a single organellar genomic unit (or chromosome). This organellar group is considered the experimental group (as described in the methodology section of Chapter 2 (RTqPCR)). The reference control group consisted of primers that targeted a single copy gene in the nuclear genome. Comparison of relative copy number differences can

then be made between the single copy nuclear target to the single copy target of the organellar genome. This can be accomplished while keeping mindful of the three following caveats:

1) Not all tissues have the same mitochondrial density.
2) Not all cells have the same number of organelles.
3) Multiple chromosomal copies exist within organelles that contain a genome.
4) Not all organellar multi-copy genomes contain the same number of chromosomes.

Tissue sampling and DNA extraction techniques are the two essential factors that have to be tightly controlled in order to account for the four listed variables listed above and to receive consistent results. Best results are obtained when sampling young whole individual seedlings that are between 5 and 10 dpi in biological age. DNA must be extracted from seedlings of the same biological age. Commercial DNA extraction kits that use a column-based approach do not work well ("or at all" JC) with this experimental design. This is most likely because these commercial kits (like from Qiagen) require 10 fold more tissue that must be homogenized prior to DNA extraction. Often tissue can be lost or contaminated in the homogenization process. In addition, for unknown reasons the more plants that are sampled together result in a higher probability of inconsistency in organellar DNA content and concentrations[5]. DNA extractions from commercial kits have low yield of organellar DNA most likely because plant organelle genomes have shorter and more complex DNA fibers than the nuclear DNA. These shorter DNA fibers most likely pass through the column based chemistry more readily than longer DNA fiber of the nuclear DNA[6].

[5] Most likely due to sampling error

[6] There is no direct evidence to back these claims against the Qiagen plant DNA extraction kit other than DNA extracted using both the traditional CTAB method or Jiffy Prep methods (Sieburth Lab DNA extraction method) provided consistent results between biological replicated samples and between technical replicates.

One of the advantages to commercial DNA extraction kits is that they provide clean DNA as an end product. The advantages to the "Jiffy Prep" are that the DNA extractions are simple, have a low cost, can isolate high yield DNA from a single *Arabidopsis* seedling at 5 dpi, and the DNA used from this extraction for QPCR purposes provides consistent results between technical and biological replicates (See Appendix for "Jiffy Prep" protocol). In addition, results obtained with the "Jiffy Prep" are comparable to results reported by others that have conducted similar experiments on quantifying the relative copy numbers of organellar genomes (Preuten et al., 2010).

The major drawback that QPCR has when determining relative DNA copy numbers of organellar DNA is that QPCR results do not differentiate between changes in DNA levels or changes in the number of organelles present in the cell or sample. This is where organelle counts need to be conducted in conjunction with QPCR to validate a reduction in organellar DNA or to distinguish a reduction in organellar numbers.

Relative Numbers of Organelles

In this study there were four factors that were first considered prior to approaching the question of organelle numbers within the polIB mutants. First was to conduct QPCR experiments (as just discussed) on whole seedlings to determine if organellar DNA levels are different in mutants when compared to wild type. Second was to obtain a reporter system that would enable the visualization and dynamics of mitochondria (mtDNA transgenic crosses described in part in Chapter 1). A reporter could also be used for plastids, in addition to chloroplast auto-fluorescence. Third was to determine organelle density within tissues that normally express high levels of polIB (determined by RTqPCR in Chapter 3). Fourth was to

correlate organellar numbers to phenotypes observed (Chapter 3) that could indicate an organellar mutation.

Many reports have been published that used David Logan's mtDNA transgenic line to count mitochondria in cells and to visualize mitochondrial dynamics. The reporter line is a GFP fusion with a ATP synthase gene mitochondrial targeting sequence that is constitutively expressed from a 35S promoter (Logan and Leaver, 2000; Logan et al., 2004). This reporter has been shown to target specifically the mitochondria and not the plastid or the peroxisome. One caveat about this reporter line is that it works well with young plants (prior to bolting), but as has been reported by others this line has unpredictable silencing effects after the plants have begun to bolt a stem (unpublished results). Regardless, in young plants mtGFP has a strong signal in the root, root hairs, hypocotyl epidermis, leaf epidermis, leaf guard cells, and the leaf tricomb cells.

Chloroplasts do not require a reporter gene for visualization because of their far-red auto-fluorescence generated from chlorophyll (Zhang and Hu, 2010). Unfortunately, plastids are not visible in the root or in etiolated plants without some form of staining or transgenic reporter. In addition, mtGFP is difficult to distinguish in leaf tissue because of the organelle size and signal intensity generated from the chloroplasts. Alternatively, mitochondria can be visualized with the mtGFP reporter in the hypocotyl epidermis of etiolated plants without chloroplast interference. A disadvantage to this approach is that photomorphogenisis does not occur within these plants. Fortunately, it was determined in Chapter 3 that the polIB mutant has a reduced growth rate when grown in the light or the dark (Fig. 23). In addition, both polIA and polIB are normally expressed at the same levels in the hypocotyl (Fig. 12). It is predicted that mitochondrial numbers will be reduced in the hypocotyl epidermis cell, because of this organ's slow growth rate and reduced gene expression of mutant polIb-2.

Alternatively, a method to count mitochondria in leaf epidermal protoplasts has recently been published (Preuten et al., 2010). This report used QPCR in conjunction with mitochondrial counts in epidermis protoplast to determine mitochondrial genome depletion effects on an *Arabidopsis* mutant. The advantage to using epidermis tissue is that the epidermis contains very few or no chloroplasts (Preuten et al., 2010). To generate *Arabidopsis* epidermis leaf protoplasts, first epidermis leaf peals are conducted to remove the leaf epidermis from most of the mesophyll cells. Then the pealed epidermis tissue is placed in an enzymatic reaction that digests the cell wall (Yoo et al., 2007; Wu et al., 2009). Mitochondria in these protoplast cells can be visualized by confocal microscopy and counted using NIH image software (Image J).

The following are some of the disadvantages of this approach. Often there is a greater amount of mesophyll cell contamination. Sampling for this type of experiment is destructive and stressful to the cell. Mitochondrial dynamics are most likely to change in a single cell environment instead of in the intact plant environment. In addition, the process of screening cells and to acquire micrographs may damage the neighboring cells and is sample limiting. An experiment like this did not work for this study because the silencing effect of mtGFP expression had begun at the time the protoplasts needed to be generated.

Relative Mitochondrial Density in Apex Tissue

The relative density of mitochondria can be observed in tissue that does not contain auto-fluorescence from chlorophyll. Fluridone is an herbicide used to prevent the development of chloroplast by blocking carotenoid synthesis in the isoterpenoid pathway (Bartels and Watson, 1978; Van Norman et al., 2004; Atul Puri et al., 2006; Van Norman and Sieburth, 2007). Plants germinated on media containing 100 μM fluridone continue to undergo photomorphogenesis. More specifically this herbicide blocks the production of beta-carotene which results in the

photo-oxidation of the chloroplast and its photosystem. In addition, true leaves develop unlike etiolated plants under fluridone treatment. The amount of plant growth is limited without photosynthesis but wild type seedlings remain to have similar rosette area to untreated controls up until 14 dpi.

For this study fluridone treated wild type and mutants were examined by epifluorescent microscopy to determine the relative density of mitochondria within the shoot apex and the root apex regions. Portions of both of these apex regions contain meristematic cells. In addition, these two apex regions normally contain a high density of mitochondria. It was predicted that mitochondrial density within these two regions would be lower in the polIb-2 mutant than in the wild type. This prediction was made in part because of the elevated expression level of polIB in wild type shoot apex and root tissues.

Cellular Counts of Mitochondria

In this study mitochondria were counted in 2 dpi hypocotyl epidermis cells. Overlapping DIC images and fluorescence micrographs were taken in tandem of wild type and polIb-2 mutant hypocotyl epidermis cells from cell[7] position 1 up to cell[8] position 18. These overlapping DIC images were then merged together as a single layer with Adobe Photoshop to reconstruct a full-length hypocotyl RAW image. The DIC full-length hypocotyl image was used as a template to reconstruct matching overlapping fluorescence micrographs with GFP labeled mitochondria (at full HD resolution) into a single layer with Adobe Photoshop. Each layer was then saved at full resolution as an individual image.

Full length DIC and fluorescence micrograph hypocotyl composite images were imported into the program Image J (NIH Image Software). The DIC image was stacked on top of the GFP

[7] First hypocotyl epidermis cell at the root shoot junction
[8] Hypocotyl epidermis cell nearer to the hypocotyl cotyledon junction

image. Hypocotyl epidermis cells on the DIC image were then annotated by tracing cell border, numbering cell position, and numbering technical replicate of each cell at the same position. This was completed for three biological replicates.

The micrograph size bar was used to calibrate Image J prior to taking cell length and cell area measurements. The perimeter of each hypocotyl epidermis cell was traced and the cell area was measured from within the cell tracing. Annotations generated to measure cell area from the DIC image (top of image stack) were moved to the GFP image (on the bottom of the stack). The lower GFP image was calibrated and a threshold for GFP detection was determined. The threshold present "mean" was used with every GFP image. Image J particle counter function was used to count the number of particles (or mitochondria) within the predefined threshold and within the traced cell perimeter. In addition to counting particles the same particle counter function was also used to measure the sizes of the particles in which it counted. This analysis was completed for all technical replicates (4 to 8 cells) at each cell position (1 to 18) and for three biological replicates.

Chloroplast Counts

The plant leaf is the most photosynthetic organ of the plant. This organ is composed of mostly internal mesophyll cells with an epidermis skin. The primary role of the mesophyll cells is to conduct photosynthesis (Osteryoung et al., 1998). Therefore these cells are the most rich in chloroplast content. Not all mesophyll cells are the same size depending on which stage of development and on the location where these cells are on the leaf blade. In addition not all chloroplasts are the same size or at the same stage of plastid development. When experimenting with mesophyll cells and chloroplasts both of these factors need to be taken into account. The best approach to controlling cell size and variability in chloroplasts is by sampling cells from the

leaves that developed at the same time in addition to sampling tissue from the same location within the leaf blade. This can be accomplished easily as described previously with mid-leaf epidermis peels. Once the epidermis is removed then the mesophyll cell walls are readily digested with an enzyme mixture.

In this study the ratio of chloroplast numbers per given cellular area was determined from mesophyllic protoplasts generated from 5 week old biological triplicates of rosette leaf number four and five. Protoplasts were generated as previously discussed except mesophyll cells were isolated instead of epidermis cells. The confocal microscope was used to obtain micrographs where equal numbers of virtual sections with proportional distances between the cell midline[9] and the cell apex were generated. Of the eight virtual sections the fourth virtual section of each protoplast was measured for area and for chloroplast numbers. Individual protoplasts were examined in this way to compensate for potential differences in cell sizes between mutants and wild type samples.

It was proposed that all mesophyll cells would have a proportional number of chloroplasts per given cell area. Therefore, the area measured[10] from each protoplast cell would be plotted against the number of chloroplasts within that given area. If there is no proportional difference of chloroplasts per cellular area between the mutant and the wild type samples then there will be little difference observed in the slopes of regression lines generated with a scatter plot. In addition the average area of the proportional virtual sections is assumed to directly reflect the relative size differences between the two cells. Therefore, the inverse average area of the cell is determined by setting the Y-intercept[11] to zero and solving for the X-intercept[12]. The

[9] The location of a spherical cell with the greatest diameter.
[10] Using Image J (NIH Image Software)
[11] Y-axis equals chloroplast per cell

percentage difference of average cell size is derived from taking the reciprocal of the inverse area proportion of the mutant divided by the wild type.

Results

Organellar DNA Relative Levels

With the increase of polIA expression levels in the polIb-2 mutant and knowing that polIA can target both organelles (Christensen et al., 2005), it was predicted that if the DNA polymerases are redundant little to no change in either mtDNA or ptDNA levels would be observed in the polIb-2 mutants. To determine if the observed increase in polIA expression had the ability to fully compensate for the loss of expression of the polIB gene palm domain, a QPCR experiment was used to quantify the relative mtDNA and ptDNA levels in 7 dpi wild type and polIb-2 mutants (Fig. 26). Primers generated for these analyses targeted different regions of the organelle genomes, including four mitochondrial genes (Preuten et al., 2010), three noncoding regions within the mitochondrial genome, and three genes of the plastid genome (Kumar and Bendich, 2011).

Upon examination of the relative DNA levels of biological triplicates, we observed a statistically significant 30% decrease for all mtDNA targets (Fig. 26). No significant differences in ptDNA levels were observed when comparing polIb-2 mutants to wild type plants at 7 or 14 dpi (Fig. 26).

With the observed delays in chloroplast development at germination and accumulation of starch from statoliths (amyloplasts) (Fukaki et al., 1997) in the root cap it was questioned whether the polIb-2 mutants had an observable difference in the numbers of chloroplasts per cell. Based on no difference in ptDNA abundance at 7 dpi it was predicted that there would be no

[12] X-axis equals area per cell

differences in chloroplast numbers per cell when counted from 4-week mesophyllic protoplasts (leaf numbers 4 and 5).

Chloroplast Counts

By counting chloroplasts within a given cell area we attempted to compensate for inconsistencies based on plastid or cell developmental stages. A scatter plot was generated that compared the number of chloroplasts to the cell plane area (Fig. 27). No significant differences correlating the number of chloroplasts per cell area was found when generating a best fitting regression line for both wild type and mutants. Alternatively, a significant difference was observed in the average plane area of mesophyll cells when comparing wild type to polIb-2 mutants. Mesophyll cells from the mutants had significantly less planar area than wild type cells. These results are consistent with the observed decreased rosette leaf size and area (Fig. 28, 29) and support the predicted decreased rate of cell expansion of the polIb-2 mutant.

Mitochondrial Density in Apex Tissues

Next it was determined if the polIb-2 mutant had a greater difference in mitochondria numbers within tissue regions prominent for cell expansion. The root tip and shoot apex relative mitochondrial density was examined using a transgenic mtGFP reporter (homozygous) crossed into the polIb-2 mutant. With this same construct mitochondrial counts within 2 dpi hypocotyl epidermis cells were also made. A lower density of mitochondria was observed in the shoot apical meristematic zones when using epifluorescence microscopy at low magnification (n = 10, at 5 & 7 dpi) (Fig. 30). The meristematic zone of root tips also exhibited a significant reduction in mitochondrial density when observed by confocal microscopy (focused to the PI stained QC (not shown)) (n = 10, at 5 & 7 dpi and 24 hour light growth conditions) (Fig. 31). In addition, the mitochondria density was severely reduced (at 14 dpi) within the polIb-2 mutant root tips

when germinated on media without sucrose.

Mitochondria Numbers in Epidermis Cells

In addition to observing mitochondria in the root tip and shoot apex tissue, the average number of mitochondria per hypocotyl epidermis cell was also determined (at 2 dpi under continuous dark growth conditions) (Fig. 32). Epidermis cells showed similar reduced size or density of mitochondria in the mutant. The purpose for germinating these seedlings in the dark was to prevent the development of autofluorescent chlorophyll, which could confound our mitochondrial observations in the epidermis by epifluorescence microscopy.

Interestingly, an increased number of mitochondria was observed in the polIb-2 mutants (Fig. 33). However, the labeled mitochondria within the mutant emitted a GFP signal with similar intensity but which extended over a smaller area than observed in wild type GFP labeled mitochondria (Fig. 34), resulting in an observable difference in mitochondrial size. Hence, on average the mitochondrial network in wild type cells had greater area than that in the mutant cells. As an experimental control, the ratio of wild type mitochondrial counts to a given cell planer area (epidermis cell) remained consistent regardless of cell position (Fig. 35). It is proposed that the mitochondria in the polIb-2 mutant are not fusing together correctly resulting in smaller sized but greater numbers of mitochondria (and potentially with less total mitochondrial mass). It appears that the polIb-2 mutant potentially has an overall reduction of the total mitochondrial network size per cell.

Discussion

The polIb-2 mutant mitochondrial network contains a 30% reduction in mtDNA. Interestingly, the polIb-2 mutants have a greater number of mitochondria per hypocotyl

epidermis cell[13] than the wild type. In contrast the relative size of mitochondria in the polIb-2 mutants is significantly smaller than in wild type cells. Mitochondrial fractionation occurs when a large number of mitochondrial fission events generate a cascading accumulation of smaller mitochondria (Galloway and Yoon, 2012). Occasional mitochondria fusion and fission events are part of normal mitochondrial dynamics. Most often mitochondrial diseases are associated with excessive fission events that occur to fractionate the mitochondria network. The majority of the time these fractionated organelles continue to respire. In addition, the more organellar fission that occurs the greater the chance that daughter organelles will be void of a genome until fusing back into a mitochondrial network where genomic mixing is occurring.

As previously discussed the shoot apex contains the meristematic region. Within this region are the stem cells and associated with the stem cell is a cage-like mitochondrion that surrounds the nucleus (Segui-Simarro et al., 2008). Mitochondria with larger volume have a greater capacity to conduct additional cellular functions other than just cellular respiration. Many of these functions involve maintaining cellular homeostasis. Some of these functions which were previously discussed in the literature review are heme biosynthesis, free Ca^{2+} accumulation, lipid metabolism, and sterol metabolism. Generally, fractionated mitochondrial organellar networks are proposed to be incapable of maintaining or performing required biological function to control aspects of cellular homeostasis.

[13] The following were the justifications for using epifluorescence over confocal microscopy to determine mitochondrial numbers within the hypocotyl epidermis: 1) Epifluorescence imaging time was more rapid for acquiring images over a confocal scan where mitochondria were more likely to move, 2) Greater depth of field could work to receive a greater representation of average mitochondria numbers per plane view area, and 3) Light images could be taken with the epifluorescence (light) microscope that could be combined with the GFP images in the same orientation and used as a template to determine cell borders (see methodology section above).

When mitochondria fractionate into smaller organelles they often move slower than when fused as a larger mass. Mitochondrial fission events are possibly a way to compartmentalize damaged DNA or protein complexes that have been damaged by ROS and need to undergo mitophagy. The mitochondrial structures counted within the epidermis indicate a fractionated network of mitochondria that are not fusing together. Hence the number of different observable phenotypes.

From a decreased density of mitochondria observed in the shoot apex to the degradation of mitochondria in the root cap, the mitochondrial morphology has been affected in the polIb-2 mutant. It remains unclear whether a mitochondrial phenotype is observed in a polIa homozygous mutant. It also remains unclear if the mitochondria phenotype is directly caused by the reduction in mtDNA or if it is a result of the reduction in polIb-2 gene expression. The latter statement is more likely the case.

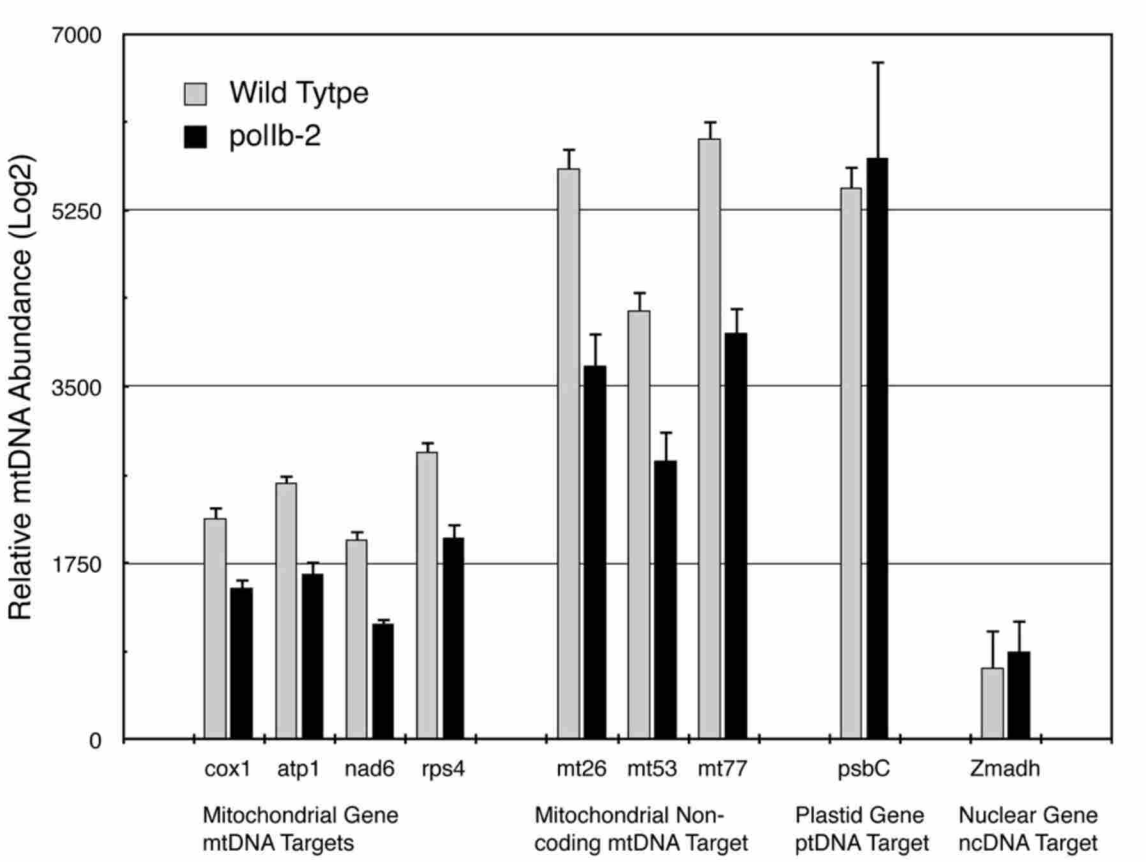

Figure 26. Measurement of Organellar DNA Relative Abundance
Four gene specific and 3 non- coding regions of the mitochondrial genome each showed a 30% reduction of mtDNA when sampled at 7 dpi. No differences in the relative DNA abundance were detected in either the plastid genome (psbC) or the nuclear genome (Zmadh) at 7 dpi. Biological triplicates were tested and normalized to the nuclear encoded plastid RNA polymerase gene DNA levels (AtRpo). Error bars represent positive SEM.

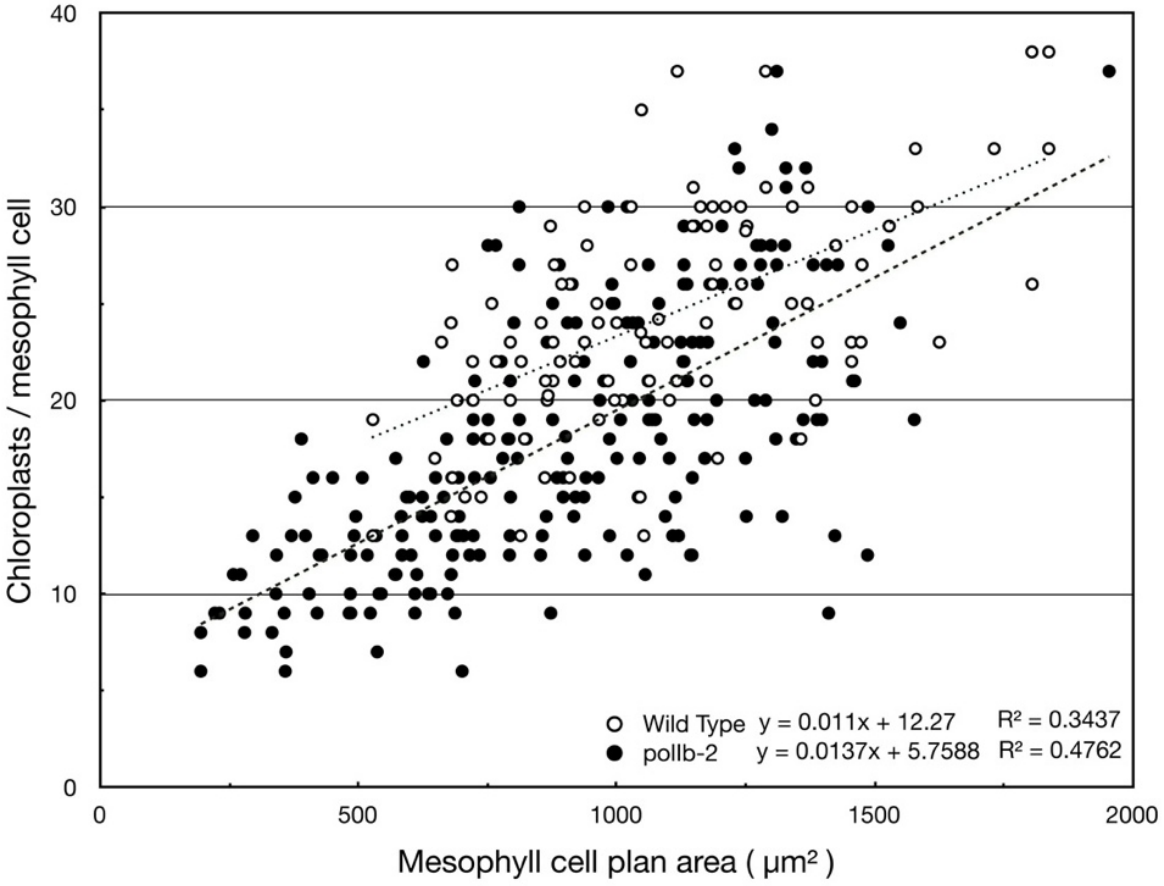

Figure 27. Determination of Chloroplast Counts
Scatter plot relating chloroplast numbers to cell planer area regression lines indicate there is no significant differences in chloroplast numbers between mutant and wild type mesophyllic protoplasts but there is a significant difference in the size of the polIb-2 cells.

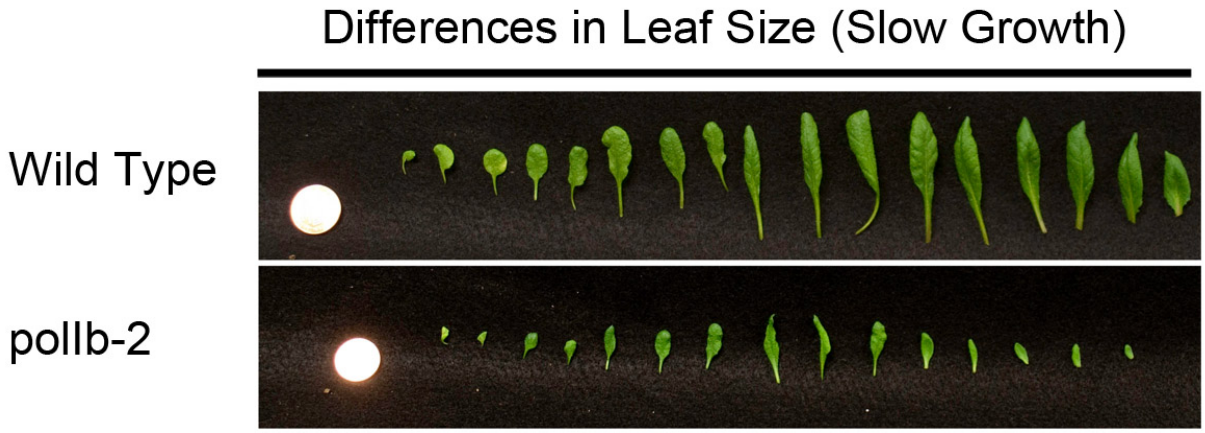

Figure 28. Leaf Profile
Leaf profile (5 weeks) of wild type and pollb-2 mutant.

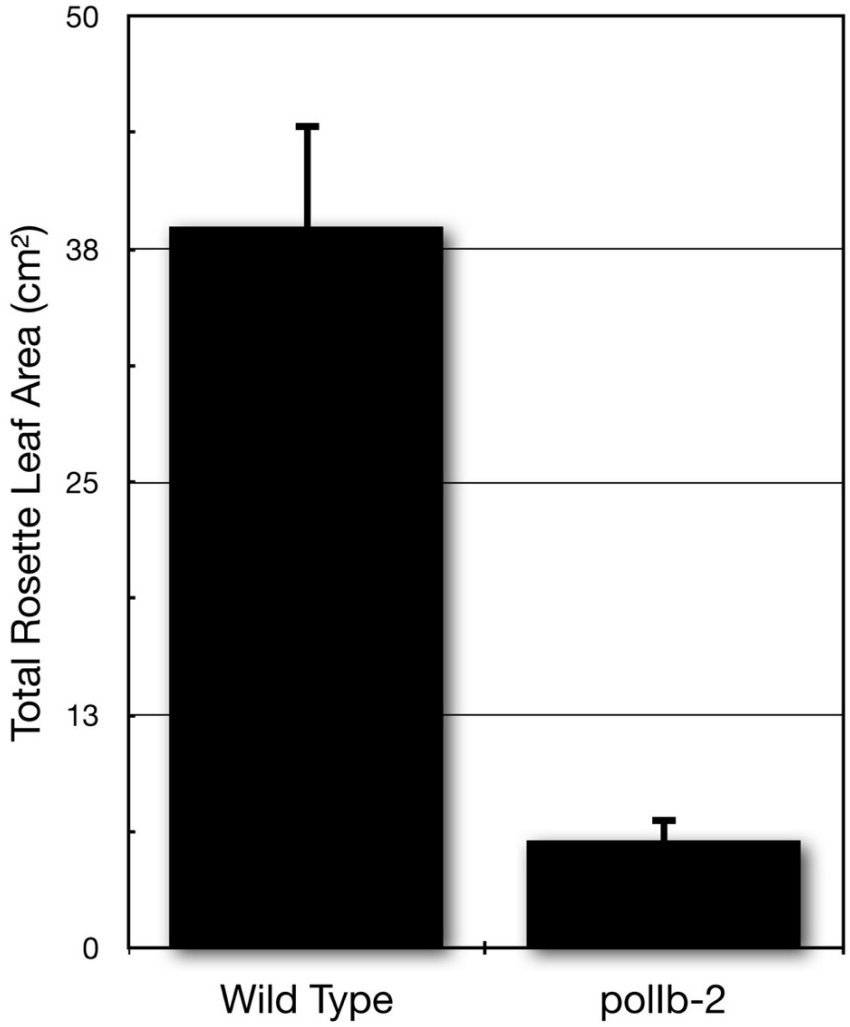

Figure 29. Average Leaf Area
Leaf profile (5 weeks) of wild type and polIb-2 mutant indicates that mutant and wild type produce the same number of rosette leaves but the mutant leaves have a significantly lower total leaf area.

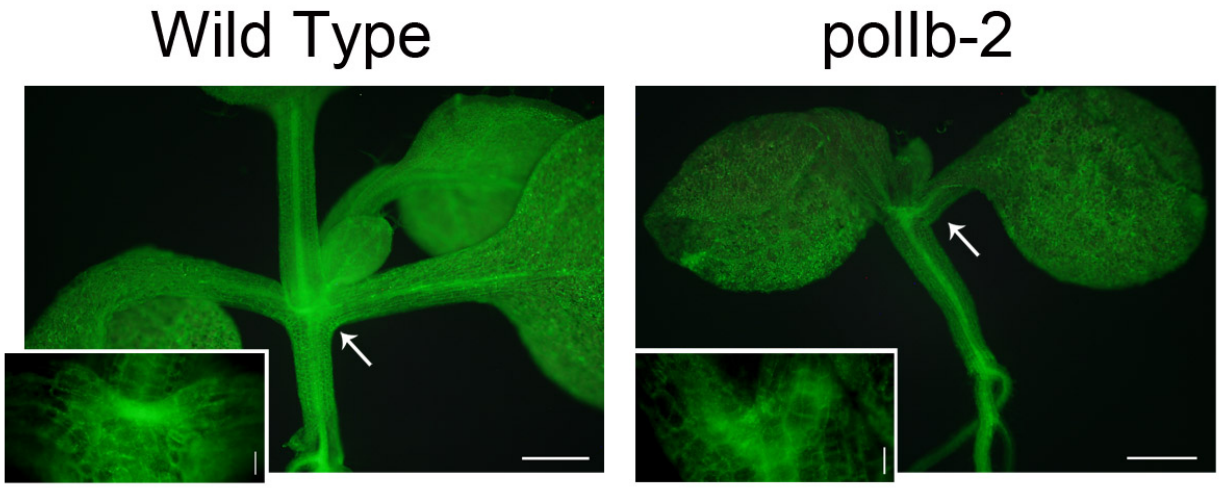

Figure 30. Analysis of GFP Labeled Mitochondria in the Shoot Apex
Epifluorescence of shoot apex mitochondrial density. Arrows point to the shoot apex region, which is magnified in the lower left corner of each image. The shoot apex of the pollb-2 mutant has a lower density of GFP labeled mitochondria. Size bars: 200 μm.

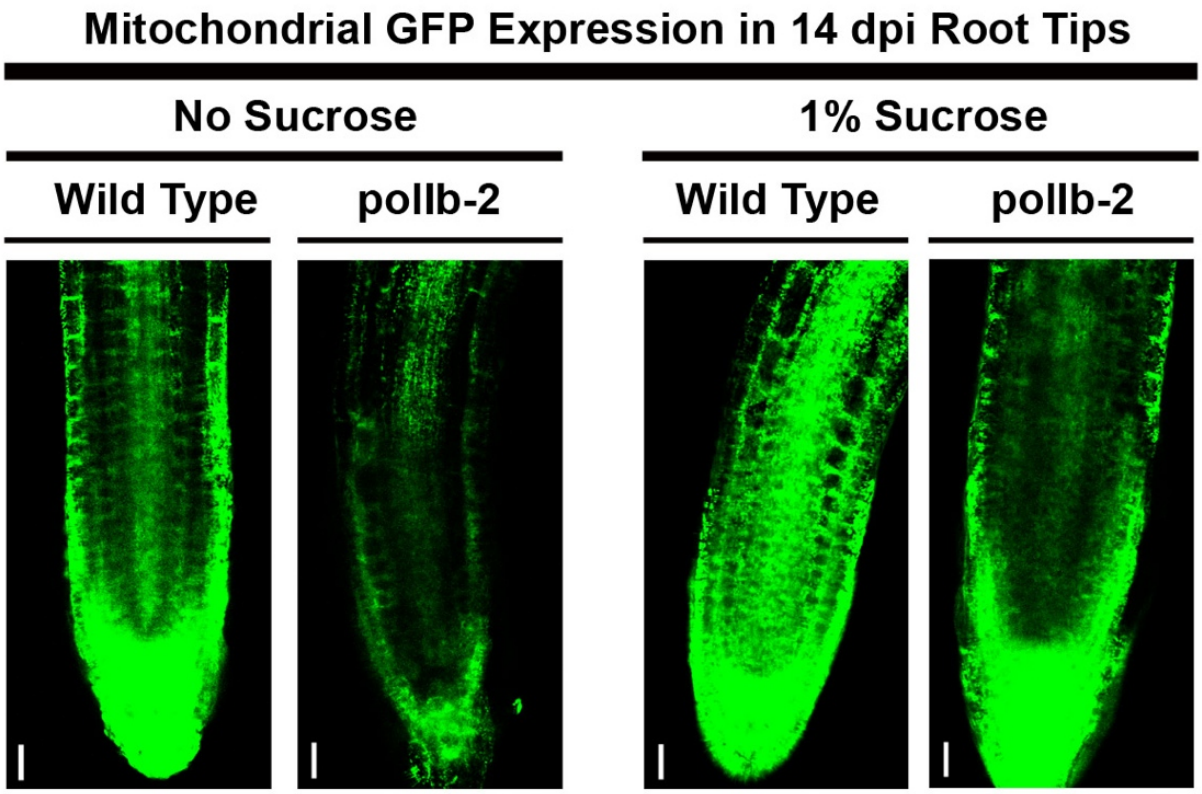

Figure 31. Analysis of GFP Labeled Mitochondria in the Root Tip
Confocal analysis of GFP-labeled mitochondria in the root tip. Without sucrose mitochondria are not maintained in the root cap of pollb-2 mutants at 14 dpi. With sucrose added to growth media there remains a reduction in mitochondrial density within the root meristematic zone. Size bars: 20 μm.

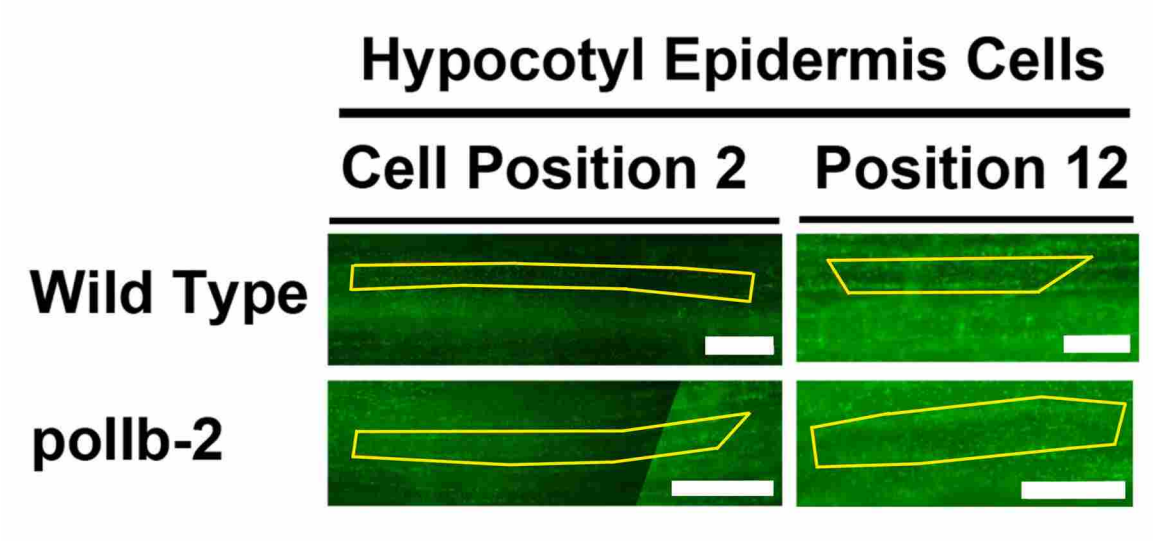

Figure 32. Analysis of GFP Labeled Mitochondria Hypocotyl Epidermis
Mitochondria in hypocotyl epidermis in the 12th cell up from the root shoot junction. There are more observed mitochondria per cell plane area in the polIb-2 mutant at the 12th hypocotyl epidermis cell. Size bars: 50 μm.

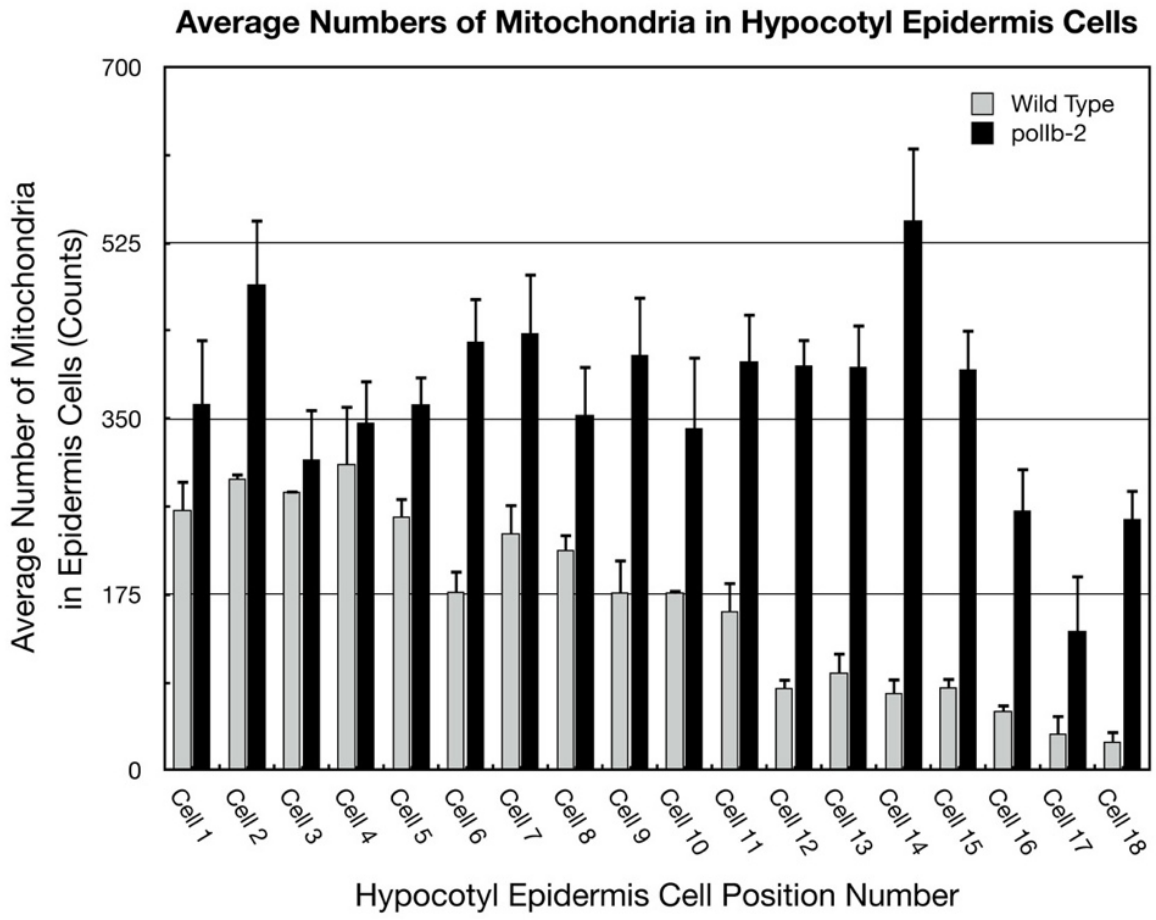

Figure 33. Mitochondria Counts
Measurements and analysis in hypocotyl epidermis cells from position 1 (near the root shoot junction) to position 18 (near the cotyledons). Counts of mitochondria per cell. The poIb-2 mutant has on average more mitochondria per epidermis cell than wild type. Error bars represent positive SEM.

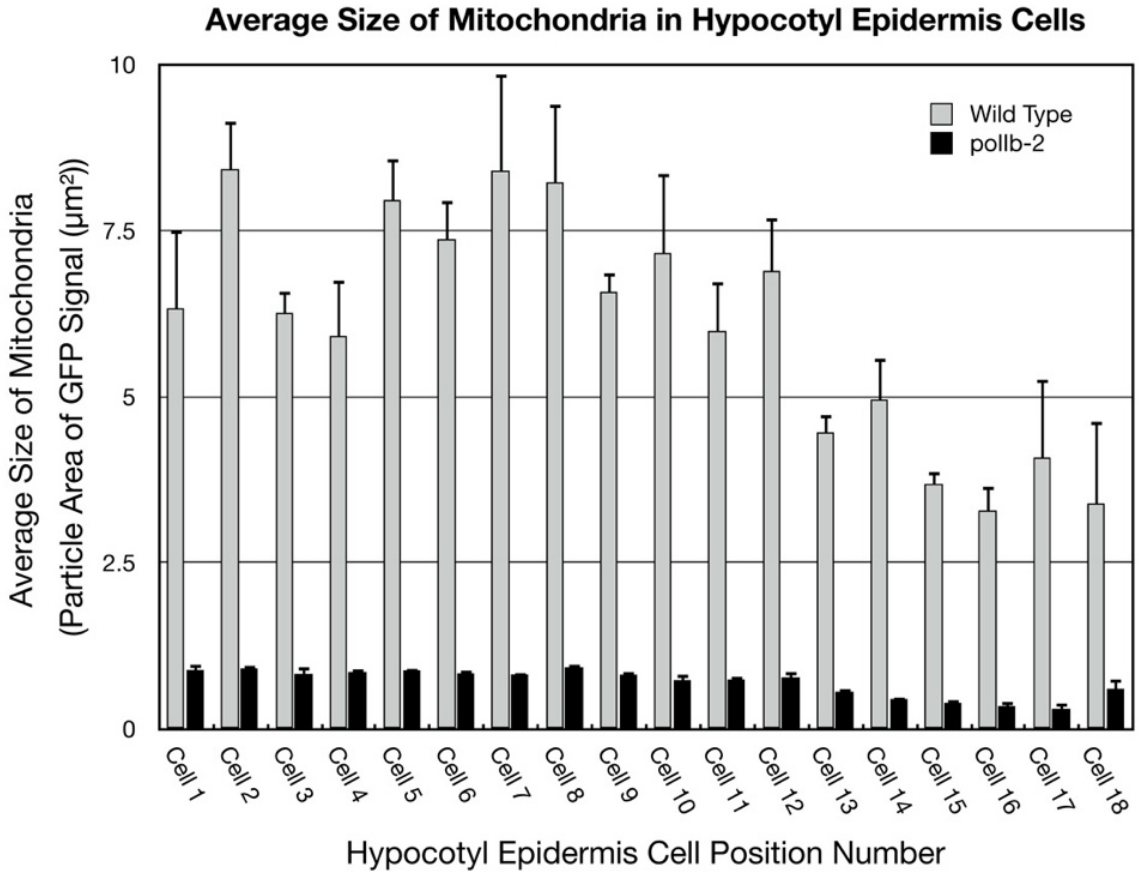

Figure 34. Mitochondria Size
Relative size of mitochondria in the pollb-2 mutant is smaller than wild type. Error bars represent positive SEM.

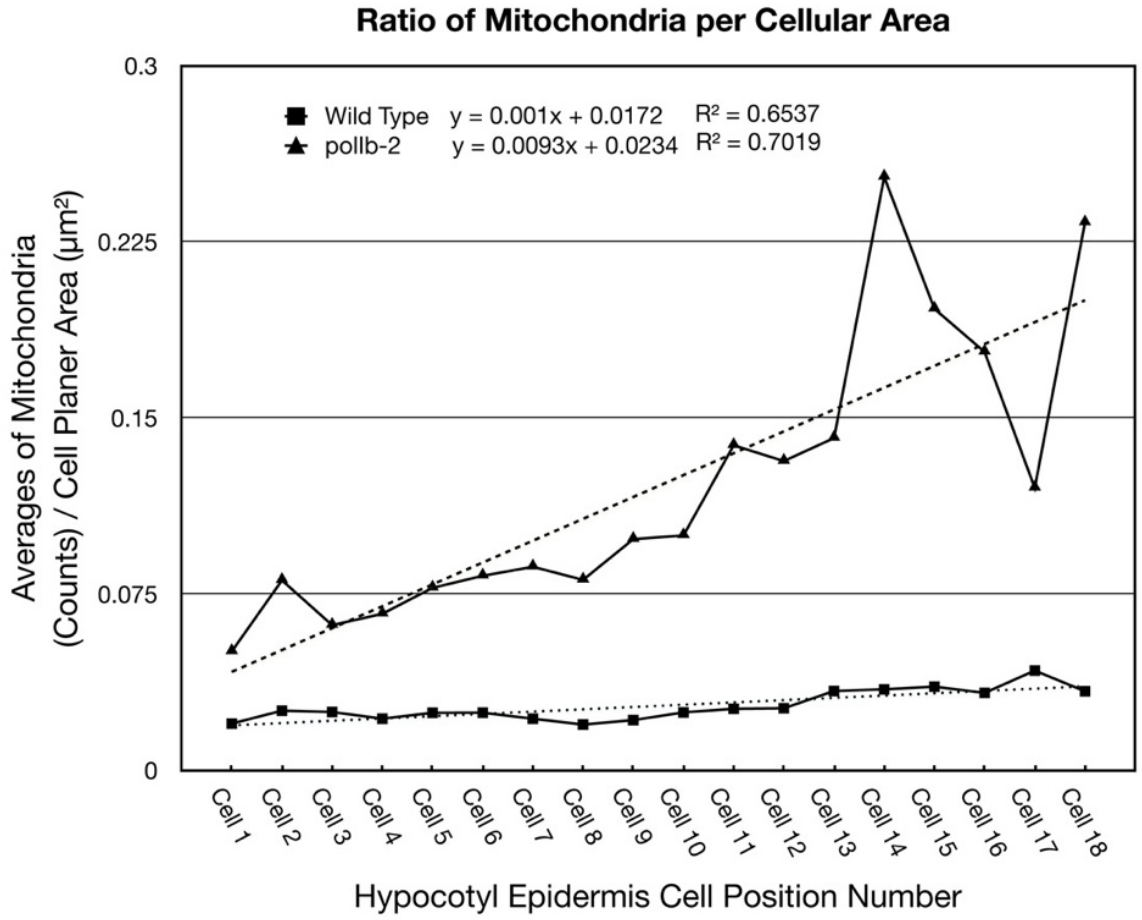

Figure 35. Mitochondria Ratio
The ratio of mitochondrial numbers to cell area does not change in the wild type but does change in the mutant. Error bars represent positive SEM. Error bars represent positive SEM.

CHAPTER 5: Plant Response to a Reduction in mtDNA

Summary

The purpose of the studies conducted within this chapter was to determine if mitochondrial and plastid functions were affected by the 30% reduction in mtDNA in addition to a 70% induction in polIA and a 90% reduction of polIB expression. Gas exchange experiments were conducted to determine carbon assimilation capacity, photosynthesis capacity, Rubisco activity, Rubisco-limited photosynthesis, cellular respiration levels in the light, and cellular respiration levels in the dark. In addition gene expression was determined for 4 mitochondria encoded genes in addition to 3 plastid encoded genes. These gene expression experiments correlated closely with gas exchange experiments. Finally, simple metabolic experiments were conducted to help determine potential organelle dysfunction. Overall, the results from these experiments indicate that cell homeostasis has adjusted to compensate for dysfunction within the mitochondrial network.

Methodology

Gas Exchange Experiments

Gas exchange experiments can be used to directly measure the rate of net photosynthesis in a plant leaf (Long and Bernacchi, 2003). These experiments can also generate results for cellular respiration levels, carbon assimilation capacity, photosynthesis capacity, respiration under "light" growth conditions, respiration under "dark" growth conditions, Rubisco activity, and RUBP limited photosynthesis (Farazdaghi, 2011). All of these analyses can be generated using a LiCor 6400XT portable photosynthesis system. This instrument has the ability to control multiple variables while measuring the flux of carbon dioxide and water of the system. In

addition, this instrument can be used to generate a light response curve and a carbon assimilation curve.

To conduct these gas exchange experiments on *Arabidopsis* using the LiCor 6400XT portable photosynthesis system the plants need to be grown in scintillation vials. These plants are germinated on 5 ml of general growth medium. It is good to prepare 4 to 8 biological replicates per experimental group. After 4 weeks growth, gas exchange measurements can be taken in a LicCor conifer chamber. After measurements are obtained the plants are destructively sampled and leaf area is measured. Leaves can be placed between lab tape and magic tape, digitally photographed, and measured with Image J. The area measured with Image J is then inserted back into the data as a correction factor to account for total leaf area. When conducting these experiments it is important to be mindful to avoid canopy effect that is generated from overlapping leaves (Knohl, 2008). If not corrected shadows will lower net photosynthesis reading and introduce error between biological replicates.

Carbon Dioxide Exchange in Plants

Carbon is directly assimilated from ambient carbon dioxide into *Arabidopsis* via the C3 metabolic pathway (Monson et al., 1984). This is accomplished by carbon dioxide passing through open stomata and diffusing into the intracellular leaf space and eventually into the cell (Barragan et al., 2012). In addition, water transpiration occurs through the stomata (Jones, 1998). The opening and closing of stomata is tightly regulated by the chloroplast within the guard cell (Hetherington, 2001). The stomata opening is a result of increased osmotic pressure within the guard cells as potassium ion concentration increases (Bassil et al., 2011). As carbon dioxide levels increase the stomata will close. Also, when the plant is under drought stress conditions the stomata will stay closed to preserve water. The closing of the stomata is affected

by increased pH levels and increased calcium ion levels within the cytosol which in effect cause the loss of potassium and other anions (Hills et al., 2012). This exchange lowers the osmotic pressure within the guard cell and the stomata are then closed. In summary, the balance between water transpiration, carbon dioxide assimilation and exchange, and oxygen exchange is controlled by the stomata or guard cell chloroplasts.

Light Response Curve

A light response curve is generated to determine the maximum photosynthesis capacity of the plant (Ögren and Evans 1993). These curves are generally parabolic. Just as low levels of light prevent effective photosynthesis, too much light also has detrimental effects on photosynthesis (Franco et al., 2007). In addition, a light response curve can determine the respiration levels of plant growth in the light and the dark. Generally, photosynthesis continues until a compensation point is reached where light levels are too low to maintain photosynthesis. At this point, the slope of the light curve increases significantly. Solving for the Y-intercept[14] from a curve generated from data points generated below the compensation point will determine the rate of cellular respiration in the dark. Respiration level under lighted growth conditions can also be determined by taking at least four points after[15] the light compensation point[16], generating a best fit regression curve and then solving for the Y-intercept. Typically, respiration levels when plants are growing in the light are low. Positive values generated from a light curve represent photosynthesis and negative values represent respiration. Therefore, the more negative the value the greater the respiration capacity, and the more positive the value the greater the photosynthetic capacity.

[14] Y-axis is the rate of photosynthesis.
[15] Four point on the X-axis that are to the right of the light compensation or when the plant is actively undergoing photosynthesis.
[16] Determined graphically. This is the point where photosynthesis and respiration are balanced.

Carbon Assimilation Curve

When a C3 pathway plant is exposed to low levels of carbon dioxide photosynthesis is limited by the rate limiting activity of ribulose-1,5-bisphosphate carboxylase oxygenase (Rubisco) (Gutteridge and Gatenby, 1995). Rubisco will bind to oxygen instead of carbon dioxide at low carbon dioxide levels. In addition the rate of transfer of carbon dioxide to ribulose-1,5-bisphosphate (RuBP) is a relatively slow process. At high carbon dioxide concentration photosynthesis is rate limited by the substrate RuBP. When carbon dioxide is bound to RuBP by Rubisco the intermediate 3-keto-2-carboxyarabinitol 1,5-bisphosphate is formed. This intermediate is highly unstable and breaks down almost immediately after being synthesized. Rubisco can also transfer an oxygen to RuBP (Kim and Portis, 2004). This combination leads to the process of photorespiration (Leegood et al., 1995). The process of photorespiration does not generate ATP but instead consumes carbon. Photorespiration does initiate the formation of glycine in the peroxisome in addition to the conversion of glycine to serine in the mitochondria. Serine is also converted to pyruvate in the peroxisome.

A carbon assimilation curve is generated by plotting net photosynthesis against the intercellular concentration of carbon dioxide (Wullshleger, 1993; Manter and Kerrigan, 2004). Rubisco activity can be determined at lower carbon dioxide levels by solving for y-max of a logarithmic regression line. At higher carbon dioxide level the RuBP effects on limiting photosynthesis is determined by generating a best fitting curve.

Gene Expression

Gene expression experiments using the previously described RTqPCR approach can serve as a follow up to gas exchange experiments. These experiments can be used to correlate

the gene expression of components of the cellular respiration complexes found within the mitochondria in addition to components required for photosynthesis found within the chloroplast.

Growth Analysis on Metabolite Supplements

Plant roots have the capacity to take in nutrients from the environment. Nutrients can include but are not limited to the uptake of amino acids, monosaccharides, and disaccharides. Disaccharides like sucrose travel throughout the plant. Generally sucrose is a temporary storage molecule for glucose. Glucose generated from mesophyll chloroplasts within the leaf tissue is combined with fructose to generate sucrose. Sucrose is transported from the leaf to the root where sucrose enters the cells and is metabolized back to glucose and fructose. These two monomers have multiple uses, but glucose is generally metabolized to pyruvate and fructose is needed as a precursor for plant cell wall components.

If the plant requires a substrate in which it is limited, often these substrates can be introduced through the root. In the experiments to follow it is predicted that supplementing polIb-2 plants with sucrose will help improve plant growth and may provide the chemical fuel required by the mitochondria prior to plastid and chloroplast development. Alternatively, sucrose concentrations can also influence the plants cells osmolality (Sokol et al., 2007). In addition serine and glycine in which normally drive photorespiration, can also be added to the root media. Pyruvate, which is used as a metabolic intermediate in numerous cellular pathways (Timm et al., 2008), can also be directly applied for root absorption.

In this study serine, glycine, and pyruvate were supplemented into growth media to help determine mitochondrial and chloroplast respiration and photorespiration functions. These metabolic growth experiments can be interpreted along with gas exchange experiments and gene expression experiments to gain a better understanding of organellar function.

It is predicted if photorespiration levels are elevated then plant growth will be low. If intracellular sucrose levels are high then plant growth will be slow. Elevated sucrose levels will also indirectly lead to elevated mitorespiration. Lower CO_2 levels will lead to stomata opening and increased transpiration of water. Stomata opening also leads to greater CO_2 and O_2 gas exchange and therefore greater photosynthesis and less photorespiration. The more photorespiration in a cell that contains a functional mitochondrial network the more serine will be generated.

Results

It was determined if the mitochondrial physiology of the polIb-2 mutant had been altered by testing for differences in gene expression levels within the mitochondrial genome and for differences in cellular respiration levels (through gas exchange experiments). Using an RTqPCR approach the relative gene expression levels of four mitochondrial genes were measured that encoded subunits for complex I (nad6), complex IV (cox1), and complex V (atp1) from mitorespiration and rps4, which encodes a subunit of the mitochondrial ribosome (Giege et al., 2005). A significant increase was observed in the relative gene expression levels of all four of the listed mitochondrial genes at 5 dpi (biological triplicates) (Fig. 36). The polIb-2 mutants were observed to have a 23.8% increase in dark respiration level when compared to wild type plants (at 5 weeks) by using a light response curve to measure whole plants (with non-shaded rosette leaves; n=3) (Fig. 37A). The polIb-2 mutants had a 6% greater respiration level under light growth conditions (Fig. 37B). These results indicate that the mutants have greater respiration levels and greater expression of genes required for respiration.

It was determined that these mutants have a greater net photosynthesis saturation point (Fig. 38). When conducting a carbon assimilation curve it was observed that these mutants had a

greater capacity to assimilate carbon and had potentially greater Rubisco activity at lower internal carbon dioxide concentrations (Fig. 39). It was also observed with RTqPCR a greater relative gene expression of both rubisco and psaI in the polIb-2 mutants when compared to wild type plants of the same biological age (Fig. 40). With a greater observed photosynthesis capacity, an increased abundance of starch accumulation was observed the polIb-2 mutants hypocotyls (n=16, at 7 dpi) (Fig. 23B). Overall an increase of cellular metabolic function was observed in both the mitochondria and the plastids in the polIb-2 mutant.

Discussion

Gas Exchange Experiments

A carbon assimilation curve generated from polIb-2 mutants indicated that these plants have a greater capacity to assimilate carbon from low atmospheric concentrations of carbon dioxide than wild type plants. Rubisco also has greater enzymatic activity at lower intracellular carbon dioxide levels to transfer CO_2 instead of oxygen to RuBP. Normally the enzymatic reaction of transferring CO_2 to RuBP is rate limiting. Therefore, relative gene expression levels were determined for a plastid encoded gene, the large Rubisco subunit. RTqPCR indicated that relative gene expression levels were significantly increased for the large Rubisco subunit. Therefore, we propose increased Rubisco activity is correlated to increased gene expression.

Increased Rubisco activity can also be an indicator of elevated levels of reactive oxidative species, that the plant is under drought stress, or that the plant has the potential to undergo additional photorespiration events. Under drought response the stomata of the plants are normally closed to prevent the additional loss of water by transpiration. Therefore, when the stomata are closed CO_2 and O_2 exchange is limited as well. When CO_2 is limited Rubisco will bind and transfer oxygen to RuBP. A 2-phospho-glycolate intermediate is generated prior to the

formation of glycolate. Glycolate is transfered out of the chloroplast and into the peroxisome. In the peroxisome glycolate is converted through multiple steps to glycine. Glycine moves out of the peroxisome into the cytosol where it may remain or glycine is transferred through the mitochondrial inner membrane amino acid translocator. Inside the mitochondrion the glycine molecule is converted into serine. Serine departs from the mitochondria through an amino acid translocator and either remains inside the cytosol or is localized into the peroxisome. Serine is then converted to pyruvate and pyruvate is converted to glycerate. Glycerate is transferred out of the peroxisome and into the chloroplast and back into the Calvin Cycle. This process does not generate ATP but consumes two ATP molecules in the chloroplast, one NADH in the peroxisome, and one $NADH_2$ in the mitochondrion. The byproducts of photorespiration reactions are ammonia and carbon dioxide that are released from the mitochondria in addition to hydrogen peroxide accumulation in the peroxisome.

Two of the potential advantages that photorespiration provides for the cell are increased pools of serine and glycine. Seedlings were germinated on media supplemented with either glycine or serine to determine if the polIb-2 mutant was deficient in either serine or glycine. Growth curves that measured root length over time indicated that sucrose was a primary requirement for plant growth and that serine in combination with sucrose helped to rescue the mutant phenotype even more (Fig. 41). Serine had no effect when sucrose was not added to the growth media (Fig. 42). Glycine had no effect with (Fig. 44) or without sucrose (Fig. 43). Increasing glycine levels should also increase photorespiration levels if mitochondria are functional and convert the glycine to serine. Alternatively, if serine levels are normal then additional serine will feed into the photorespiration system and cause an inhibition of growth.

Interestingly, serine supplements resulted in an increased growth rate phenotype instead of a decreased growth rate phenotype observed in photorespiration.

Pyruvate is another byproduct of photorespiration that is generated in the peroxisome through the metabolism of serine. In addition, cytosolic metabolism of glucose by the process of glycolysis produces pyruvate for the cell and for the mitochondria. Seedlings were germinated on growth medium containing 1% sucrose or equivalent molar value of pyruvate. Interestingly, a pyruvate level equivalent to the pyruvate that is generated from sucrose showed poor to detrimental effects on mutant seedling growth rate but showed an enhanced growth rate for wild type seedlings. In fact, wild type growth on pyruvate outperformed wild type growth on sucrose (Fig. 45). Therefore pyruvate levels were not toxic to the plant and it is speculated that the mutant was using pyruvate in photorespiration instead of oxidative phosphorylation.

These results indicated that greater respiration levels are generated from the polIb-2 mutant when compared to the wild type. RTqPCR was conducted to determine the relative gene expression levels of 3 mitochondrial genes that encode protein subunits for three separate complexes of the mitochondrial electron transport chain. As predicted, relative gene expression for these components was elevated in the polIb-2 mutant when compared to wild type gene expression levels.

As discussed in the last chapter, mitochondrial fission is often detrimental to the cell. In addition to many fractionated organelles, there is an increased probability that many of the organelles do not contain a functional genome. In addition, if the organelle did contain a genome then it would be in danger from reactive oxidative species generated from the abundance of respiration that is taking place. Most of the proteins for electron transport are synthesized in and incorporated into the mitochondrial membrane prior to fission. It is known that fused

mitochondrial structures are essential for the additional functions within the mitochondria that control cellular homeostasis.

Saturated net photosynthesis (A_{sat}) is achieved at relatively the same light intensity for both the polIb-2 mutant and the wild type. In contrast, the polIb-2 mutant had a greater capacity for net photosynthesis than the wild type plants. In conjunction with photosynthesis is chlororespiration. Chlororespiration, unlike photorespiration, generates ATP. This process is not as effective in generating ATP as oxidative phosphorylation generated by the mitochondrial electron transport chain. Gene expression generated by RTqPCR also indicated that plastid encoded genes for photosystem I and the cytochrome F complex are expressed at higher levels in the polIb-2 mutant. In addition to photosynthesis both photosystem I and the cytochrome f complexes are used by chlororespiration.

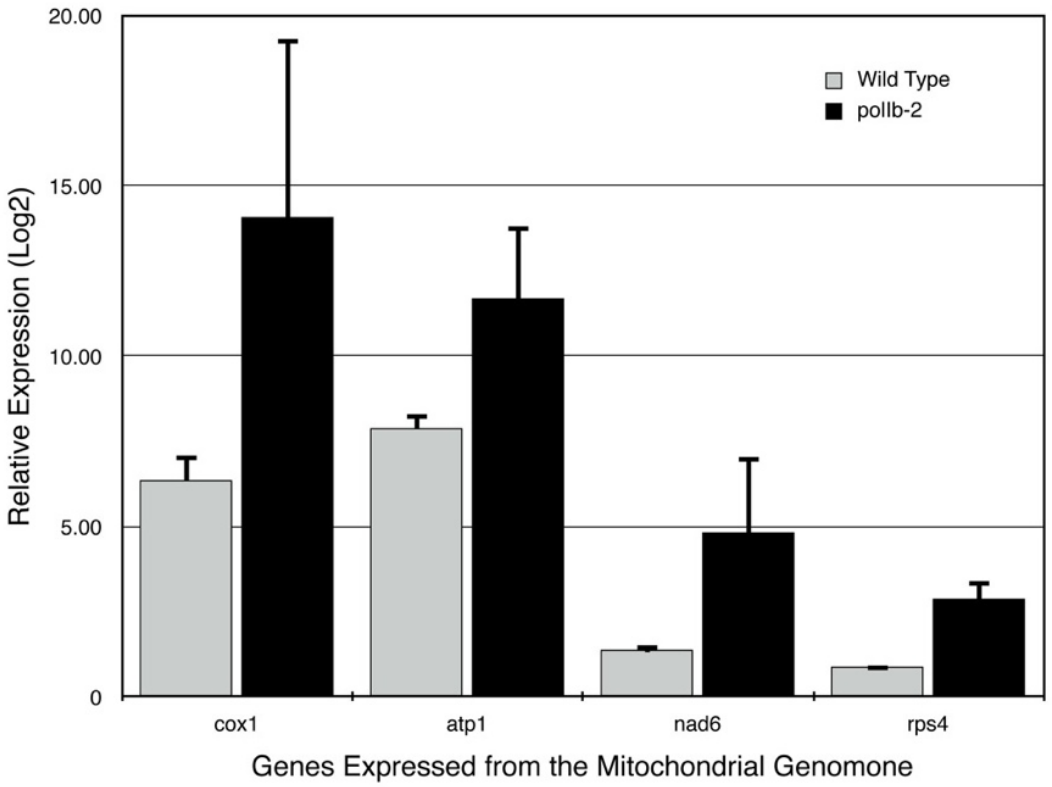

Figure 36. Mitochondrial Gene Expression
Expression of selected mitochondrial encoded genes. There is a significant increase in gene expression of 3 genes from the mitochondrial genome, which are required for electron transport. Also the expression of the mitochondrial encoded ribosomal subunit gene (rps4) has greater expression in the mutant. Error bars represent positive SEM.

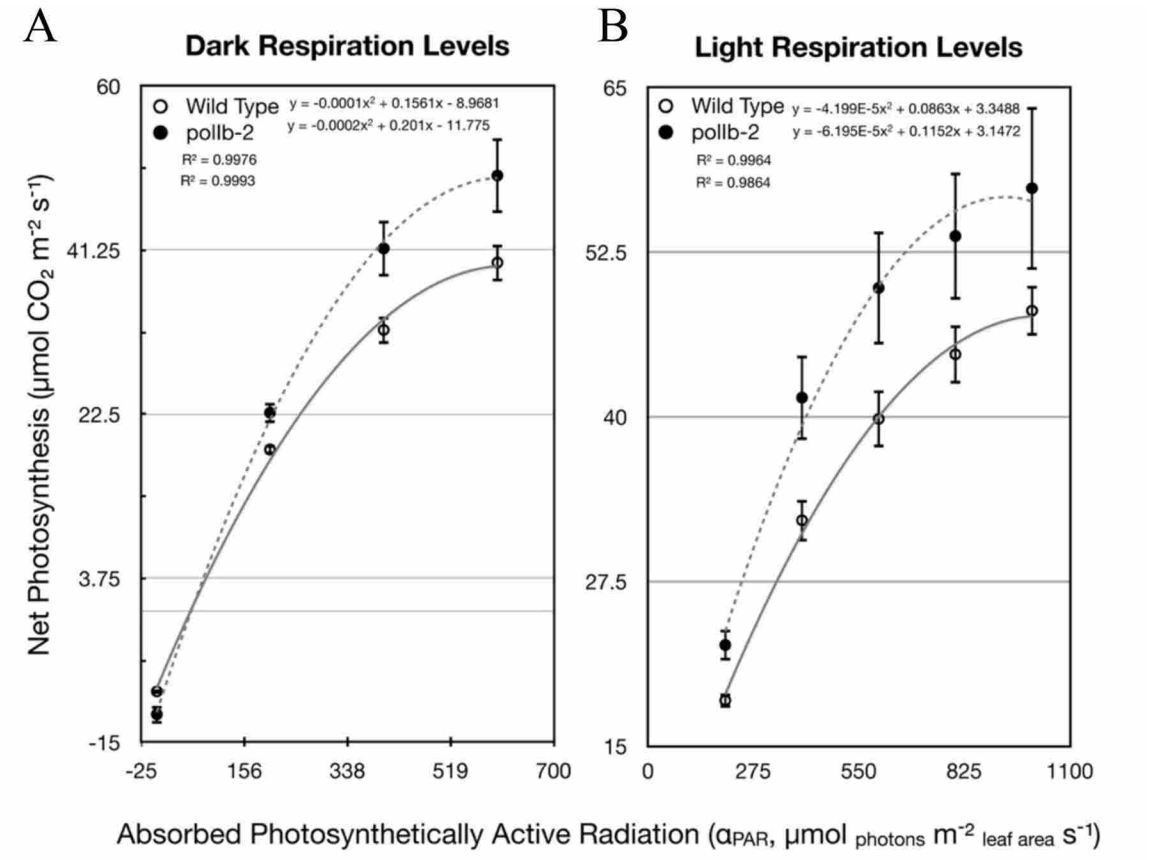

Figure 37. Respiration Levels Generated from Light Curves
A) Respiration levels in the dark. The mutant has a 6% greater respiration level under light growth conditions when compared to wild type. Error bars represent SEM; n=5. B) Respiration levels in the light. The mutant has 23.8% greater dark respiration levels than wild type (determined at the y-intercept) Error bars represent SEM; n=5.

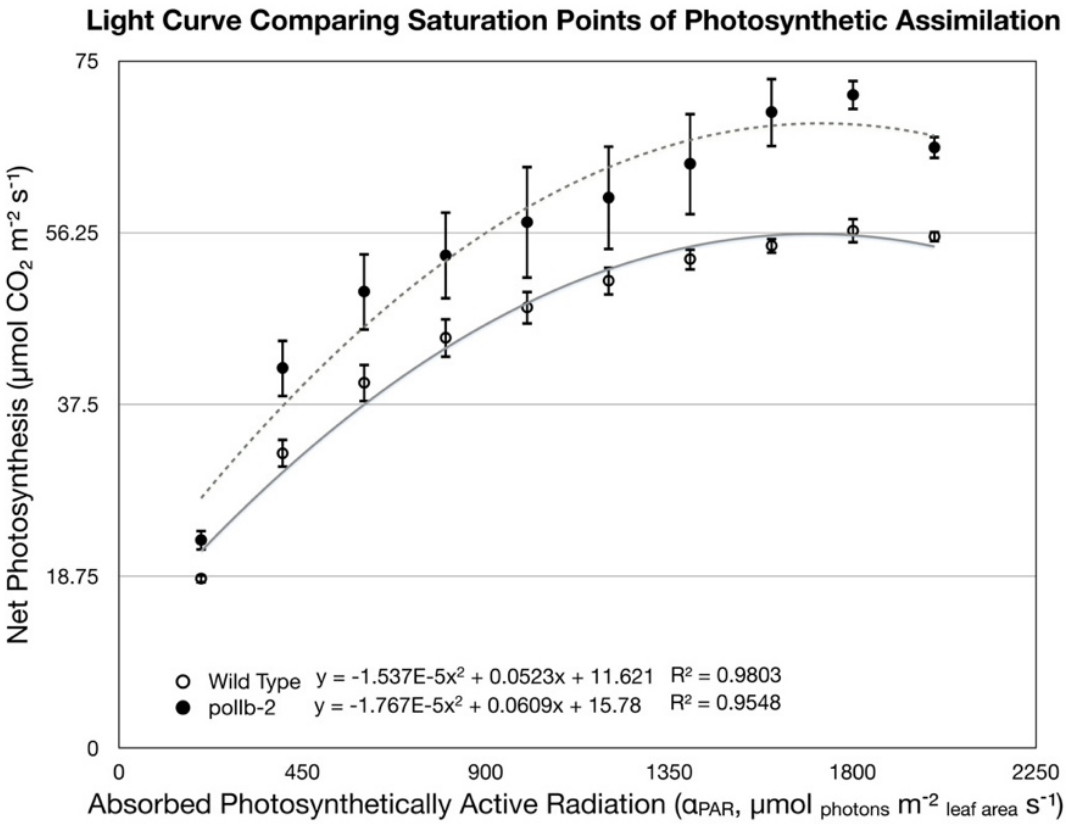

Figure 38. Photosynthesis Saturation Point Generated from Light Curves
The mutant has a greater photosynthesis capacity and greater net photosynthesis saturation (A_{sat} determined at Y_{max}) point than wild type.

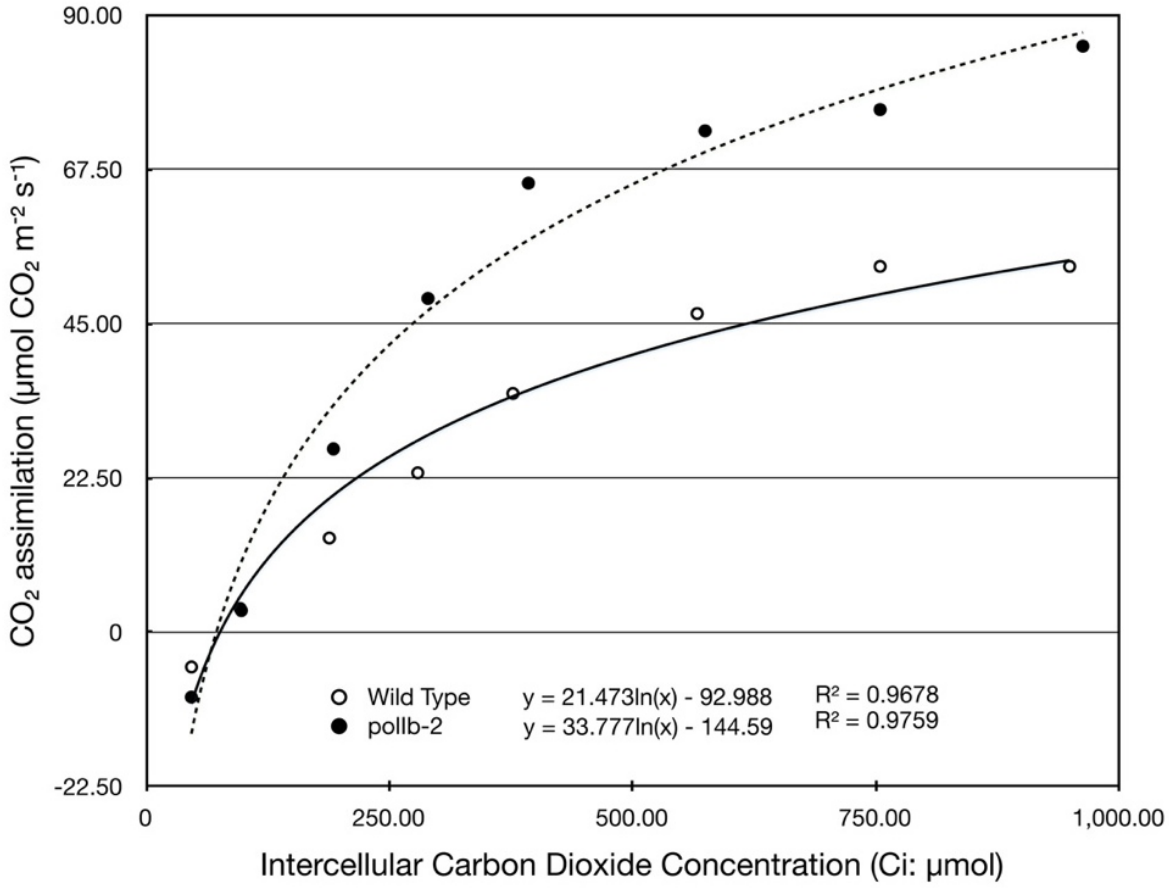

Figure 39. Carbon Assimilation Curve
Carbon assimilation curve indicates that the polIb-2 mutant has a greater capacity to assimilate carbon at lower carbon dioxide levels. The mutant also has greater Rubisco activity than the wild type (n=5).

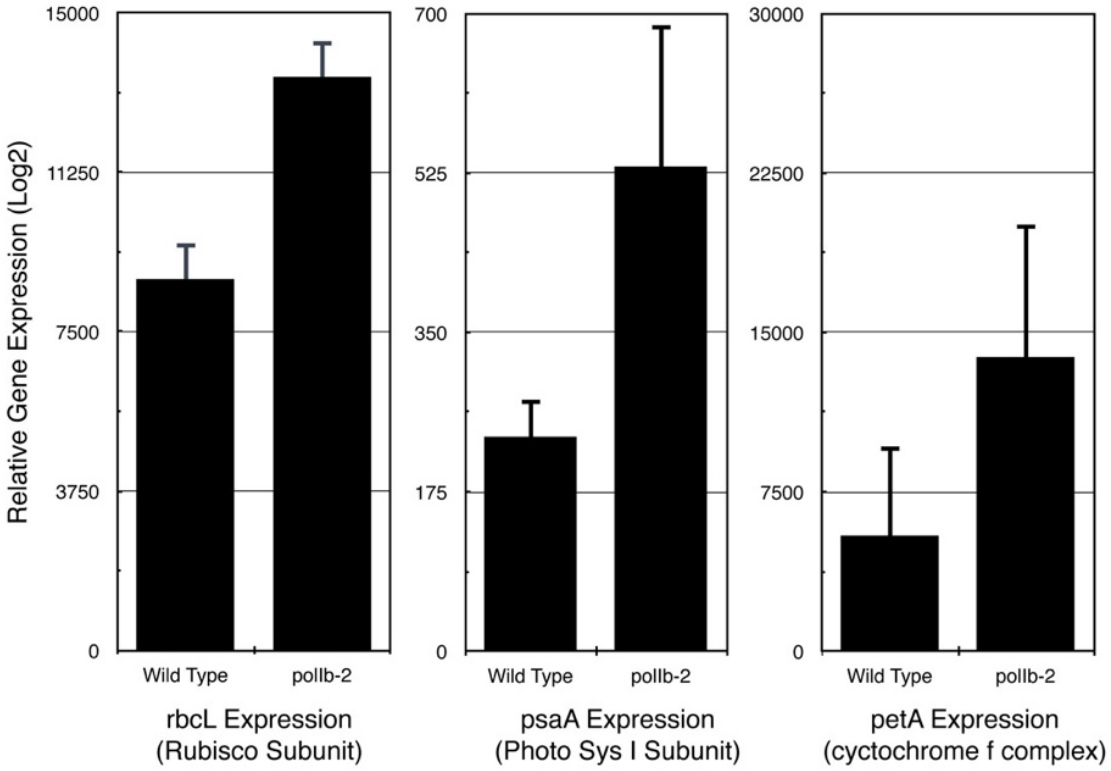

Figure 40. Chloroplast Gene Expression
Expression of chloroplast genes required for photosynthesis. The expression of plastid encoded genes required for rubisco, photosystem I, and the cytochrome f complex have greater expression in the mutant. Error bars represent positive SEM.

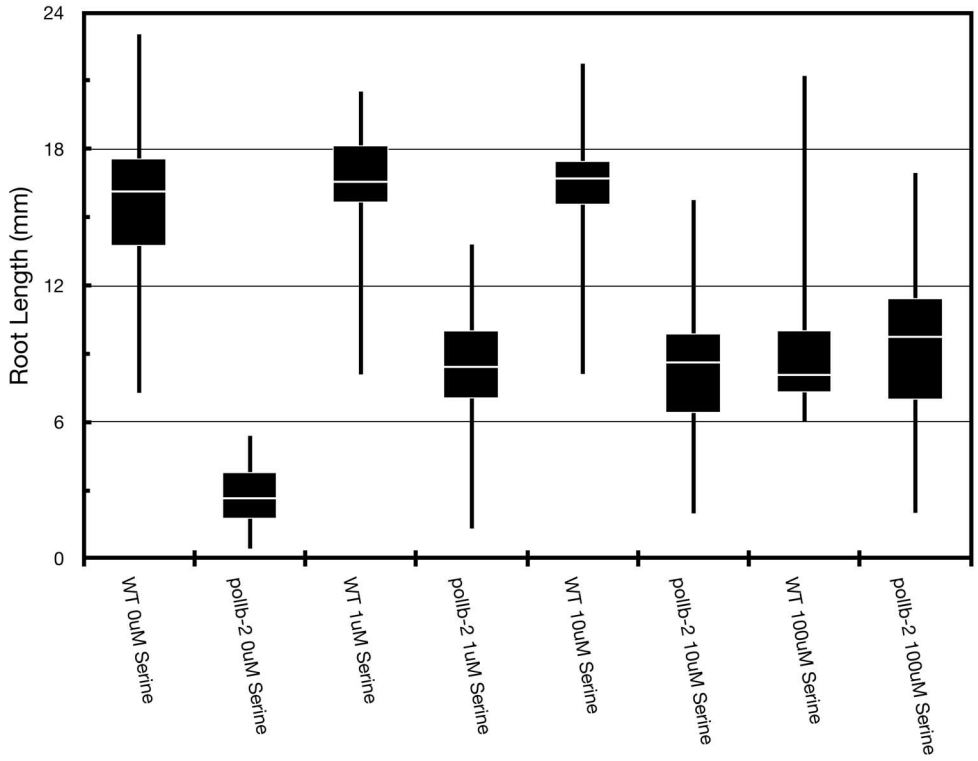

Figure 41. Root Growth on Growth Medium Supplemented with Serine and Sucrose
Root growth of wild type and polIb-2 mutants after 7 dpi growth on 0.5 x MS growth medium supplemented with different concentrations of serine. Mutants supplemented with both serine and sucrose exhibit a significant increase in growth. P-value < 0.001 between wild type and polib-2 measured roots at individual treatments. P-value < 0.05 between wild type treated with 10 μM and 100 μM serine.

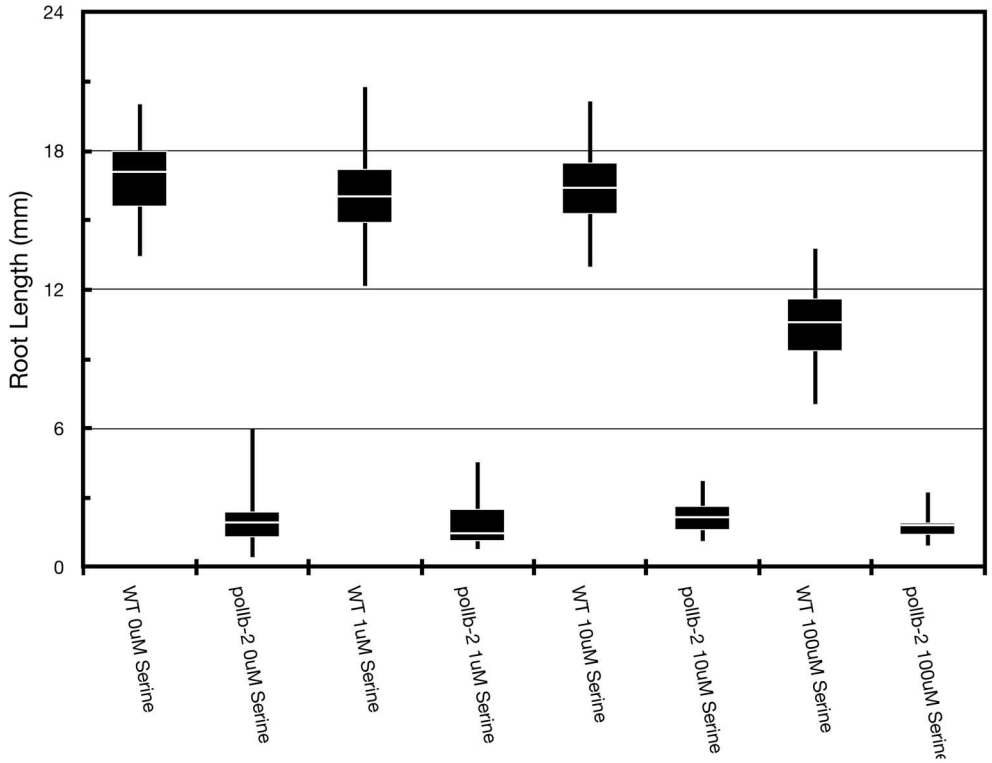

Figure 42. Root Growth on Growth Medium Supplemented with Serine
Root growth by serine supplemented to 0.5 x MS media (no sucrose). Root lengths observed at 7dpi. No significant differences between control and serine treated mutants. P value <0.001 between wild type and polIb-2 mutants root lengths at individual treatments. P value < 0.05 between wild type treated with 10 µM and 100 µM serine.

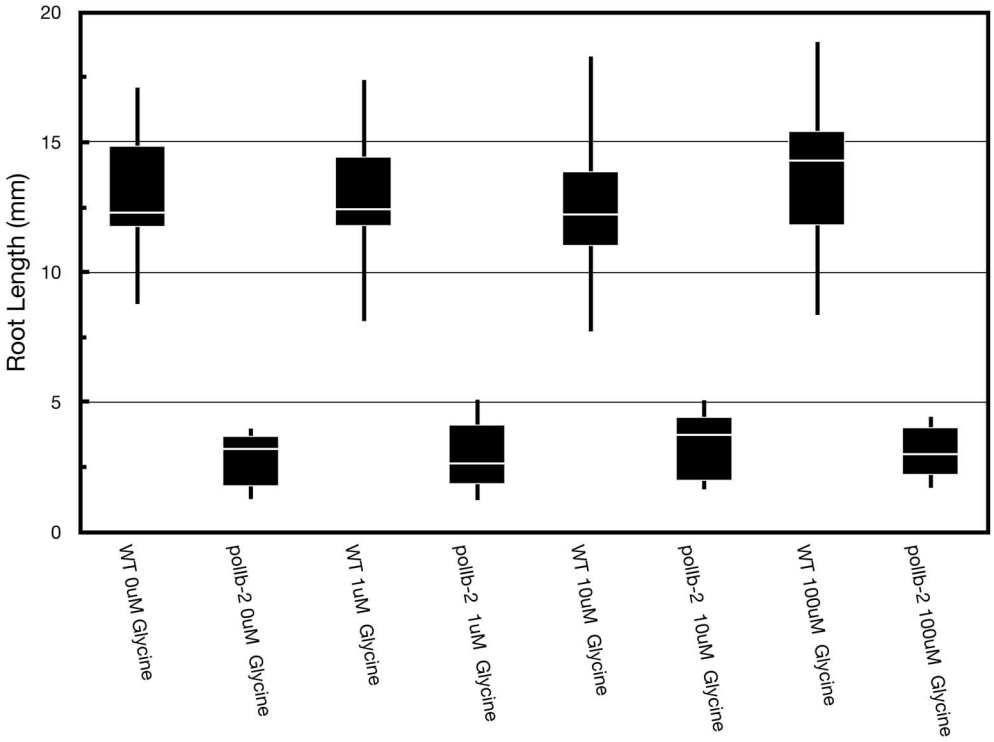

Figure 43. Root Growth on Growth Medium Supplemented with Glycine and Sucrose
Root growth of wild type and polIb-2 mutants after 7 dpi growth on 0.5 x MS growth medium supplemented with different concentrations of glycine. No significant differences between control and glycine treated mutants.

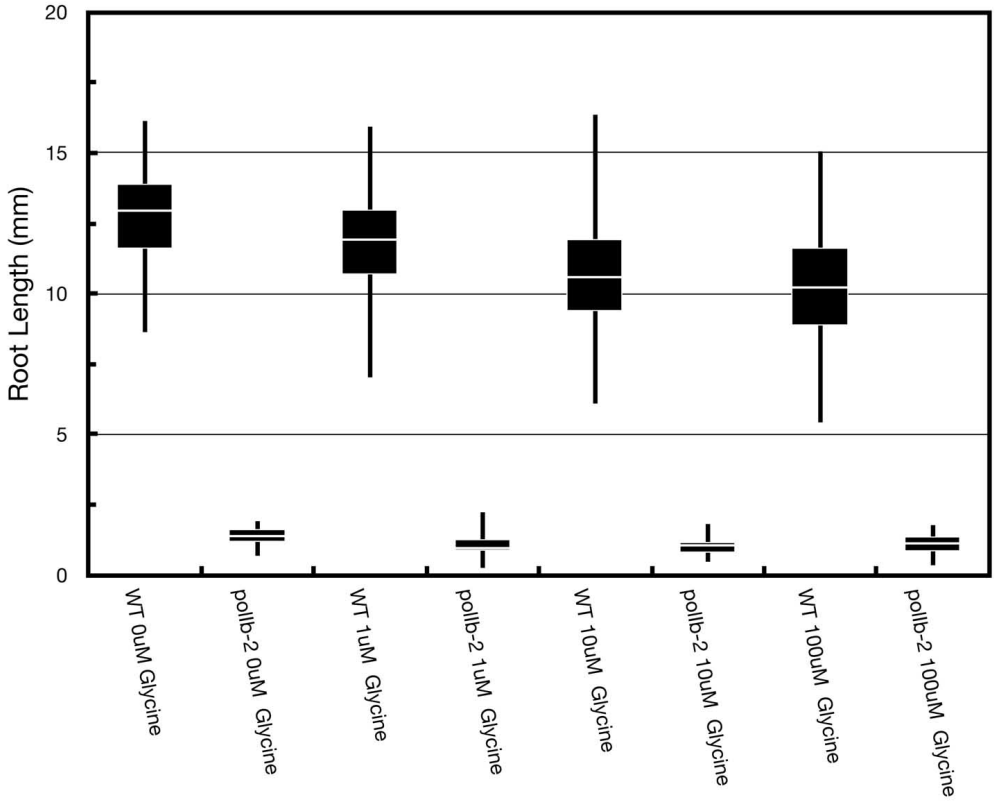

Figure 44. Root Growth on Growth Medium Supplemented with Glycine
Root growth of wild type and pollb-2 mutants after 7 dpi growth on 0.5 x MS medium (no sucrose) supplemented with different concentrations of glycine. No significant differences between control and glycine treated mutants.

Figure 45. Root Growth on Growth Medium Supplemented with Either Pyruvate or Sucrose
This analysis exhibits root growth of both wild type and polIb-2 mutants when germinated on 0.5x MS media with or without 1% sucrose. Ramps represent increasing concentrations of pyruvate ranging from 0, 7.3, 14.5, and 21.8 μM. Within each box there are two sample type; wild type samples are found above the left ramp and polIb-2 mutant samples are found above the right ramp. In general, wild type plants germinate and exhibit better plant growth on pyruvate than growth on sucrose. Pyruvate does not enhance mutant root growth over time. Media containing sucrose and increasing concentrations of pyruvate show a decreased rate of mutant root growth. Pyruvate does not assist in the rescues of the polIb-2 mutants root growth phenotype. Figure is on next page.

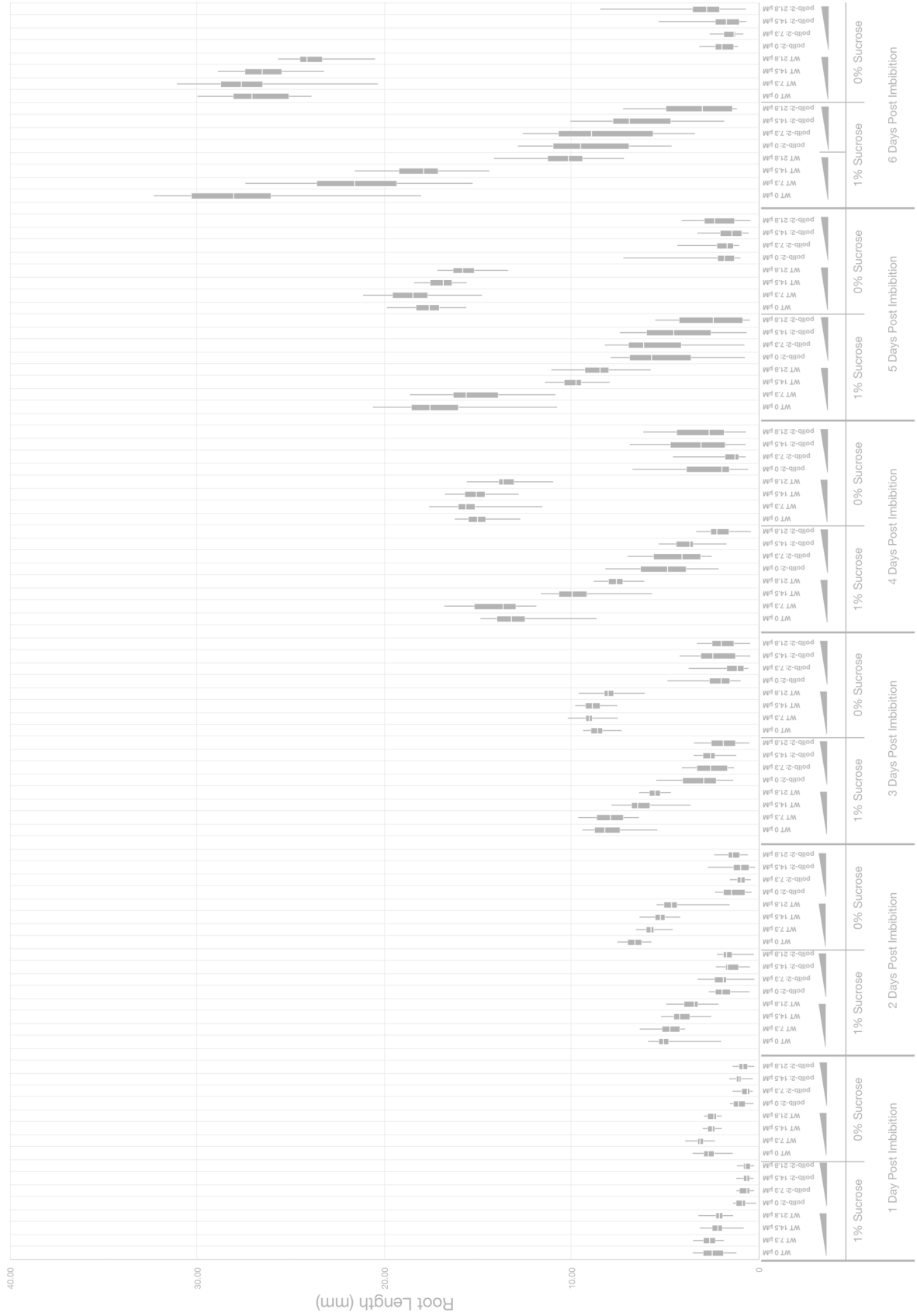
Root Length (mm)
40.00
30.00
20.00
10.00
0
1 Day Post Imbibition
2 Days Post Imbibition
3 Days Post Imbibition
4 Days Post Imbibition
5 Days Post Imbibition
6 Days Post Imbibition
0% Sucrose
1% Sucrose
WT 0 µM
WT 7.3 µM
WT 14.5 µM
WT 21.8 µM
polib-2- 0 µM
polib-2- 7.3 µM
polib-2- 14.5 µM
polib-2- 21.8 µM

CHAPTER 6: Summary of Unfinished Work

Discussion of polIa Mutants

As reported by Parent et al. (2011) two homozygous allelic T-DNA mutants in the polIA gene exhibited no phenotype. These experiments were conducted under standard *Arabidopsis* growth conditions with long day intervals. In addition this group reported an overall 30% decrease in mtDNA when the polIA gene is knocked out. Similar preliminary results to the Parent et al (2011) report were obtained by this study of polIA (Fig. 46).

As discussed in Chapter 2 the polIA mutant took at least 5 backcrossed generations into wild type to segregate out additional T-DNA mutations. Prior to backcrossing, one of these exon lines exhibited a promising bushy plant phenotype. The short root phenotype of this mutant described in Chapter 2 has been determined to be linked to the bushy phenotype observed in the older plants (Fig. 5, 6, 47). After the 5th backcross, 100% of the F2 homozygous generation did not contain a bushy phenotype. Therefore, both the short root and bushy phenotype have been determined to be artifacts generated from additional T-DNA insertions. Those two phenotypes proved to be intriguing but not significant to this study.

Interestingly, the polIA "clean" mutant exhibit a significantly greater increase in cellular respiration levels than the polIB mutant (Fig. 48). Crosses between polIA and polIB were generated and genetically and phenotypically screened through the F2 generation. No crosses were generated between polIA and mtGFP or cycB1;1::GFP.

Similar experiments that were originally conducted with polIB can now be conducted with polIA. Preliminary evidence indicated that the polIa mutant was sensitive to minor heat stress when germinated and grown at 30°C. In addition the "clean" mutant exhibited the following phenotypes as a mature plant. On average, when grown under optimal growth

conditions the polIA mutant bolted or generated stems one week before the wild type plants. This mutant also had a low seed set. When examining the anthers and pistils there was a consistent dusting of pollen deposited at relatively the same location on the style of the pistil. It was observed that the anthers extend at a slower rate than the pistil and pollen was released at a later time in the polIA mutant when compared to wild type. Reciprocal-crosses and manual self-crosses that were generated remain inconclusive in the determination of whether the polIA mutation affects either the embryo or gametes.

Discussion of polIa x polIb Double Mutants

An attempt was made to generate a double homozygous polIa x polIb mutant. Crosses were generated and F3 generation progeny plants were phenotypically and genotypically screened. Three plants in a population of 180 plants had a dwarfed phenotype. The rest of the plants had a range of phenotypes. Two of the three dwarf plants were destructively sampled and confirmed to have a homozygous T-DNA insertion in both organellar DNA polymerase genes. The third plant, which had the similar phenotype as the two plants that were genotyped, died within 7 dpi. The organellar DNA polymerase double mutant that had died was proposed to be seedling lethal. Additional genotypic screens need to be conducted in order to determine if the organellar DNA polymerase double mutant was genuine and reproducible.

Prior to the experiment described above an F2 generation crossed plant with the genotype polIa-$2^{(+/-)}$ x polIb-$2^{(+/-)}$ was self crossed. Seedlings from the F3 generation were genetically screened to isolate an organelle DNA polymerase double mutant. The following combinations of genotypes were observed from the remaining 177 plants that germinated: polIa-$2^{(+/+)}$ x polIb-$2^{(+/+)}$, polIa-$2^{(+/-)}$ x polIb-$2^{(+/-)}$, polIa-$2^{(+/+)}$ x polIb-$2^{(+/-)}$, polIa-$2^{(+/-)}$ x polIb-$2^{(+/+)}$, and polIa-$2^{(-/+)}$ x polIb-$2^{(-/-)}$ (Fig. 49).

Plants with the following genotype, polIa-2$^{(-/-)}$ x polIb-2$^{(+/-)}$, were not confirmed within either the F2 or F3 populations of plants. It is proposed that this genotype was not observed because the polIb-2 heterozygous mutant is haplo-insufficient whereas the polIa-2 heterozygote mutant is haplo-sufficient. The single allelic gene expression of the polIb-2 heterozygous mutant may not be enough to compensate. This mutant is proposed to be either germination or seedling lethal.

As discussed in Chapter 3, both DNA polymerases exhibit relatively different gene expression profiles. As discussed in Chapter 2 the relative gene expression levels of polIA are increased when the gene expression levels of polIB are decreased. In addition the relative gene expression levels of polIB show a minor but significant increase when the gene expression levels of polIA are decreased (Fig. 46). There is a 30 % reduction in mtDNA regardless of the observed compensation response of increased expression from either gene (Fig. 7,3). With these differences it is predicted that both organellar DNA polymerases are redundant isoforms that target and function in both organelles but also that cells express these two organellar polymerases in a dosage dependent response. Alternatively, it is proposed that the maximum depletion of mtDNA that the *Arabidopsis* mitochondrial genome can manage without experiencing a deleterious genotypic and phenotypic effect is 35%.

Discussion of polIb-2 x AtTWINKLE-helicase Double Mutants

As discussed in Chapter 2, the *Arabidopsis* TWINKLE-helicase homozygous T-DNA mutant does not exhibit a plant phenotype when germinated under optimal growth conditions (Fig. 11). In addition no plant phenotype is observed when gene expression is confirmed to be knocked down from a homozygous T-DNA insertion mutation within three independent alleles. In contrast, the homozygous T-DNA insertion within the TWINKLE-helicase gene exhibited a

significant increase in relative mtDNA copy numbers when the mutant was confirmed to have reduced protein abundance (Western Blot) and a reduced gene expression level (RTqPCR). These experiments were conducted in biological triplicates. Even though this mutant[17] did not exhibit a plant phenotype it did exhibit a molecular phenotype.

Wild type gene expression levels of *Arabidopsis* TWINKLE-helicase are not evenly expressed in selected tissues (Fig. 50). Interestingly the relative expression levels of TWINKLE-helicase are similar to polIB relative gene expression within the same tissues. In addition, when polIA gene expression levels are increased due to a reduction in polIB expression the relative gene expression of TWIKLE is also significantly increased above wild type TWINKLE expression levels. Therefore it is proposed that TWINKLE-helicase has a potential organellar function that is not directly linked to DNA replication but is responsive to changes in either mtDNA levels or changes in organelle DNA polymerase expression levels. This protein may function in DNA repair or DNA recombination.

Primary crosses were generated for TWINKLE-helicase and polIb-2. There is no phenotypic or genotypic data at this time for these samples. F2 seeds have been collected from over 100 individual plants. Heterozygous F1 plants exhibited a haplo-insufficient polIb-2 heterozygous phenotype. Pollen from the polIb-2 mutant was successfully received by the TWINKLE-helicase mutant.

[17] This TWINKE-helicase T-DNA insertion line has not been backcrossed to wild type to eliminate potential T-DNA genomic contaminants.

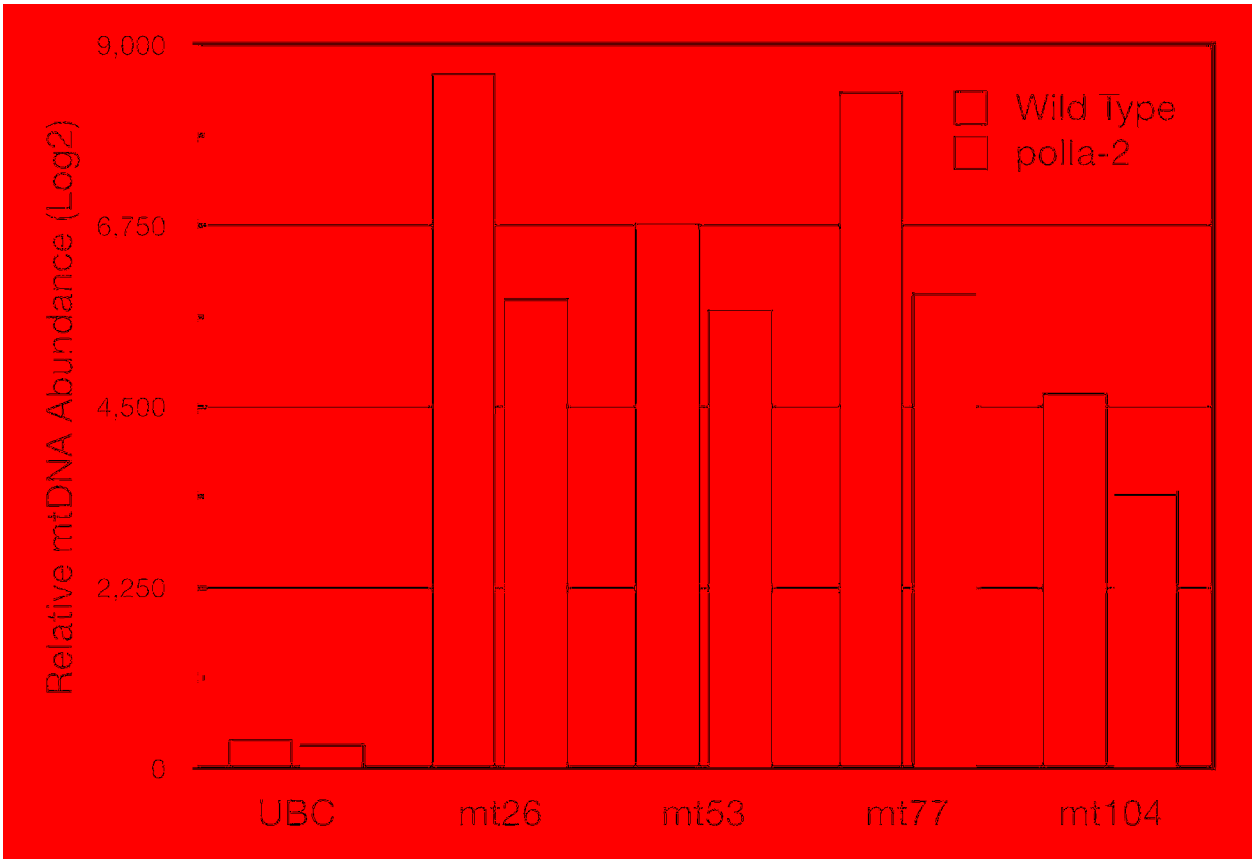

Figure 46. polIa-2 Mutant Mitochondrial DNA Levels (Preliminary Results)
Mitochondrial DNA levels are reduced in the polIa-2 homozygous mutant. These results were generated with unclean polIa-2 homozygous T-DNA mutant line prior to backcrossing. Results generated from three biological replicates.

Figure 47. polIa-2 Plant Growth Phenotype (Preliminary Results)
Analysis of growth from mature polIa-2 mutant plants. Segregated by plant size and growth rates. These are preliminary results prior to conducting backcrosses in an attempt to challenge the bushy intermediate phenotype observed. Plants are of the same biological age and this photograph was taken 7 weeks after germination.

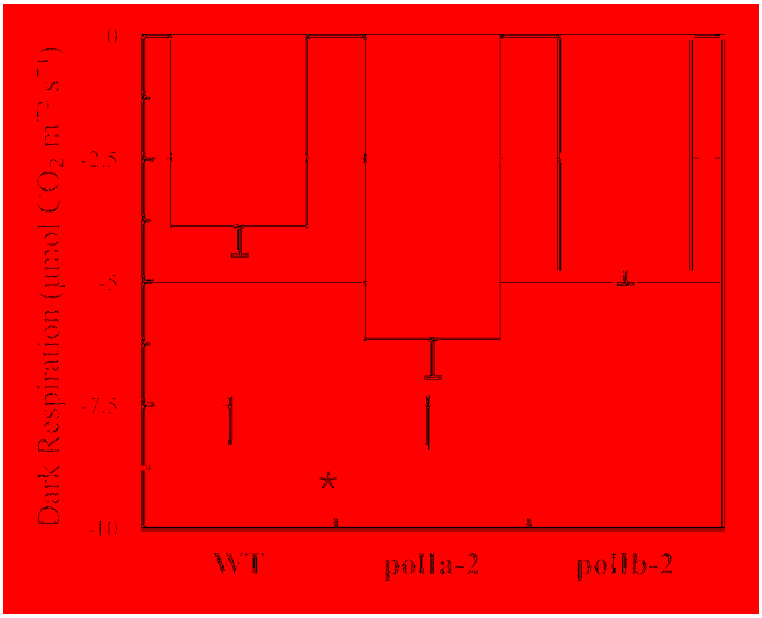

Figure 48. Total Cellular (Dark) Respiration Levels for polIa-2 and polIb-2 Mutants
Total respiration levels taken from dark adjusted (> 20 minutes dark incubation) plants. The more negative the value the greater the respiration levels. There is a significant difference in mitorespiration in the polIa-2 "clean" homozygous mutant, p-value < 0.05. There is not a significant difference in polIb-2 mitorespiration. Error bars indicate SEM of n = 8 samples.

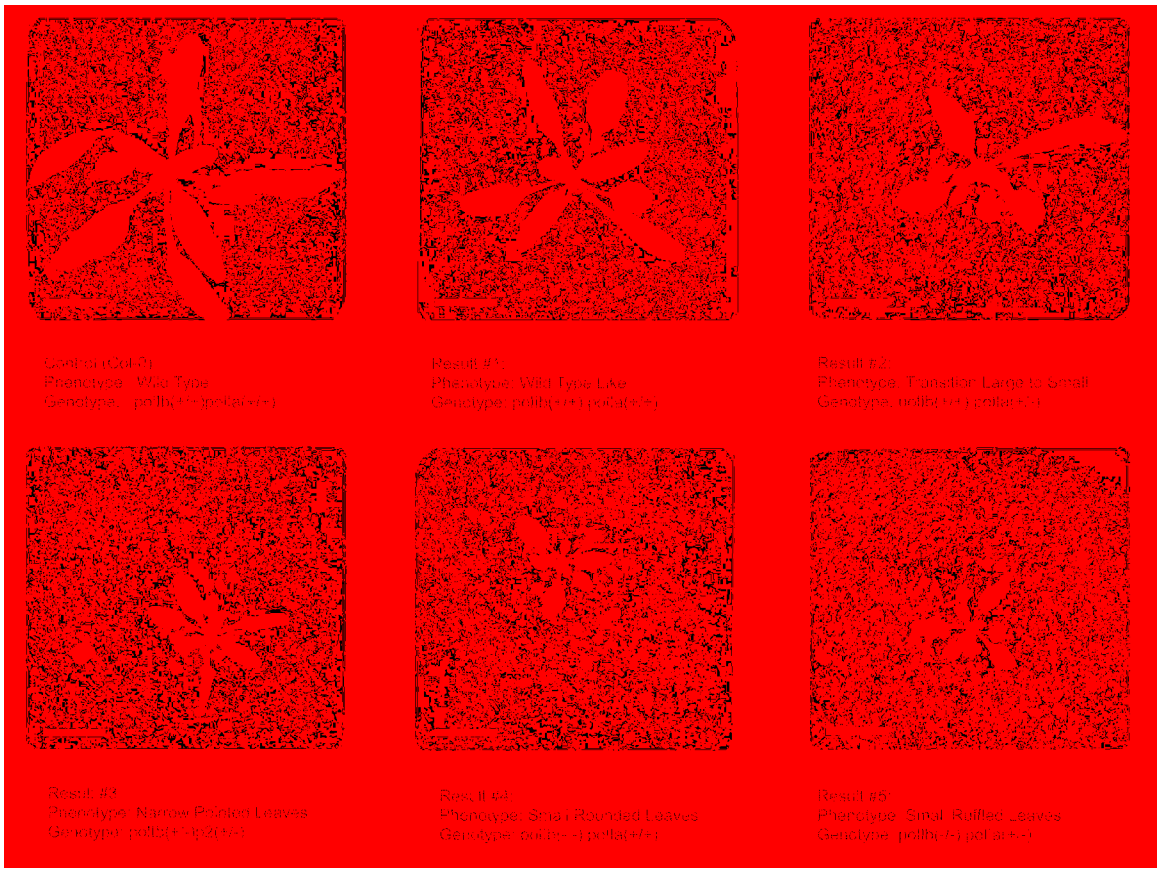

Figure 49. polIa-2 x polIb-2 Double Mutant Screen (F2 Generation)
Rosette growth with the corresponding genotype to confirm allelic T-DNA insertions. The true double mutant is proposed to be seedling lethal and was not observed in this preliminary screening of segregated phenotypes and genotypic analysis.

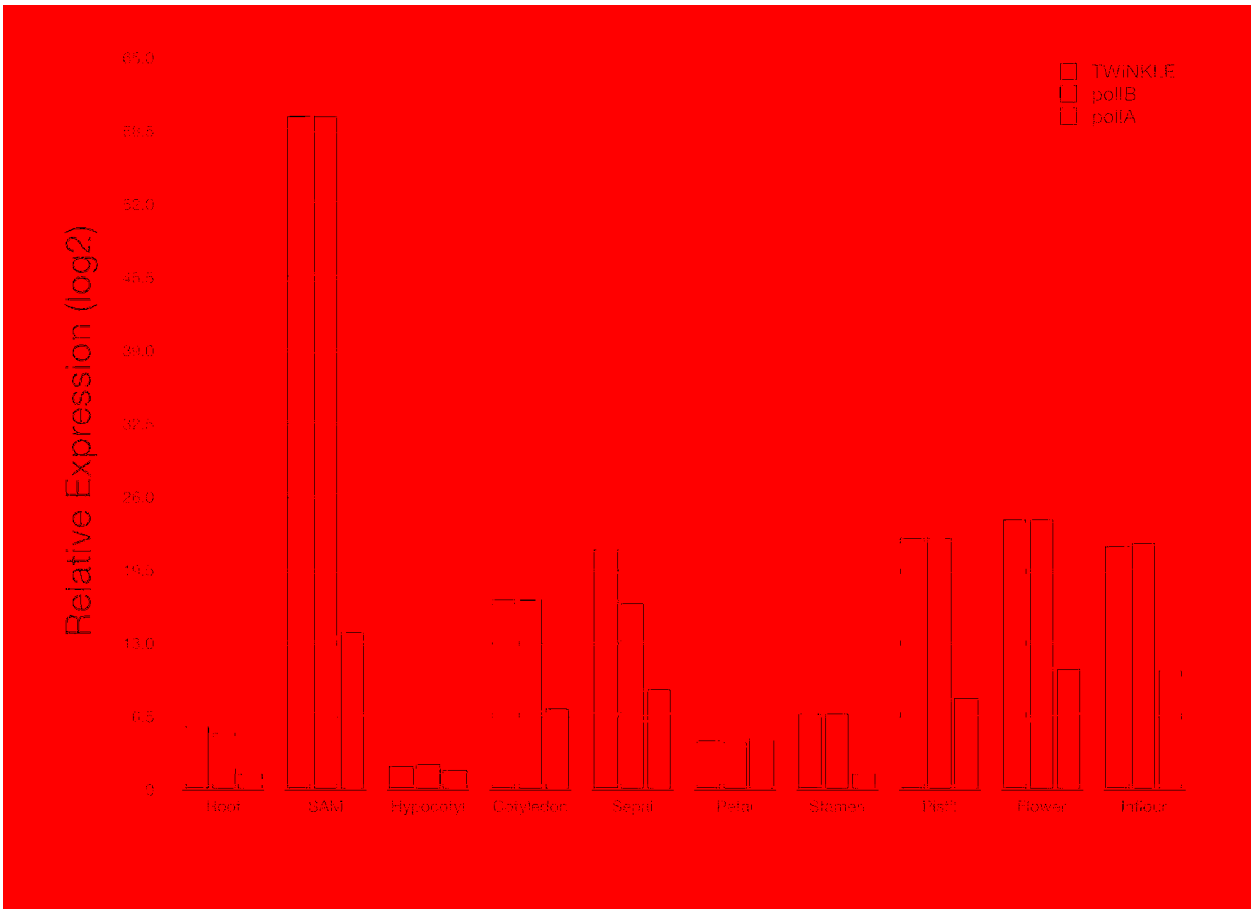

Figure 50. TWINKLE and polIB Gene Expression in Wild Type Tissues (Preliminary Results)
Gene expression profile of TWINKLE, polIB, and polIA in wild type tissues. PolIa and PolIB results are the same as in figure 12. TWINKLE expression follows polIB gene expression in wild type tissue. All gene expression experiments were normalized to Actin 2 gene expression (biological triplicates).

CONCLUDING REMARKS

The polIB mutant has a decreased rate of cell expansion. It was found that polIA, without the function of polIB in the mutant, is incapable of maintaining wild type levels of mitochondrial genome copy numbers. Provided evidence exhibited that this mutant had changes in gene expression in nuclear polIA; plastid petA, psaA, and rbcL; and mitochondrial nad6, cox1, atp1, and rps4 in response to a reduction of polIB expression and a 30% reduction in mtDNA levels. Data was provided on additional phenotypic, mitochondrial morphological, and physiological effects that suggest a feedback response is generated from the reduction of polIB expression and mtDNA levels within the polIB mutant.

It appears that the two *Arabidopsis* organelle-targeted DNA polymerase genes are dynamically expressed based on tissue type and function. The polIB gene is expressed at higher levels in tissues with a primary function other than photosynthesis. In contrast, polIA is expressed at greater levels than the polIB gene in photosynthetically active leaf tissue. The ratio between wild type expression levels between these two genes also differs greatly based on tissue type. For example, the differences in expression at the shoot apex are greater than the expression differences within the hypocotyl. Regardless of the tissue-specific gene expression level differences, both genes are expressed at the same time in all tissues. When polIB expression is knocked down, the expression level of polIA is increased by 70% of normal levels, possibly in an attempt to compensate for the loss of polIB expression. Even with this compensation in expression, polIA is only capable of maintaining 70% of the wild type mtDNA levels.

It has been observed when polIA expression is knocked down there is a significant reduction in mtDNA levels with little or no plant phenotype (Parent et al., 2011). This suggests

that polIB alone is not capable of maintaining wild type mtDNA levels. In contrast, it was shown that when polIB expression is knocked down there is a similar 30% reduction in mtDNA levels and a significant cell expansion defect. At this time there is not a definitive explanation regarding how a decrease in polIB expression leads to an overall decreased rate of cell expansion, but with hypocotyl growth curves, mesophyll cell size differences, hypocotyl epidermis expansion differences, and potential pistil expansion differences, direct phenotypic evidence is provided for a cell expansion defect in these mutants. It is proposed that the mutant growth phenotype is an indirect result of shifts in cellular dynamics to compensate for either the loss of polIB gene expression or the increase in polIA expression. Regardless of either scenario, there appears to be some feedback mechanism that is triggered when mitochondrial DNA polymerase expression is altered, which causes an adjustment in cellular dynamics to reach a new cellular homeostasis point.

This cellular dynamic shift is evident in nuclear expression of polIA, mitochondrial genome expression and function, and plastid genome expression and function. Within the mitochondrial genome there is an increase in the expression of genes required for mitorespiration. Also there is an increase in mitochondrial respiration levels. Increased mitochondrial fission events occur resulting in smaller fragmented mitochondria structures, some of which might not contain mtDNA (Collins et al., 2002; Chen and Butow, 2005). Similar mutations are found in yeast petite mitochondria (Chen and Butow, 2005). The rate of cellular mitochondrial movement is also reduced (data not shown), which is consistent with studies that demonstrate increased mitochondrial fission and slower movement in mutants of human cells (Chen and Chan, 2009).

Excessive mitochondrial fission is detrimental to the cell, where mitochondrial fusion is

required for mtDNA mixing and for energy dispersion to different parts of the cell (Skulachev, 2001; Collins et al., 2002; Westermann, 2010). The expression levels of genes required for photosynthesis within the plastid genome are also increased. Rubisco activity and photosynthesis capacity are also increased in the mutant. There is no evidence to support a reduction in ATP generation or sugar production. These mutants exhibit a significant reduction in plastid temporal development shortly after germination. As observed by Parent et al. (2011) ptDNA levels are reduced at 3, 4, and 5 dpi. There is an observable difference in chloroplast greening and statolith generation of starch granules within this time frame. There are no significant differences in ptDNA levels or chloroplast numbers per mesophyll cell after greening has occurred and gravitropism is restored. Overall, the plastid remains unaffected except during early development of the seedling. These results collectively suggest that polIB may not be needed for sustainable maintenance of the plastid genome but is required for the sustainable maintenance of the mitochondrial genome.

In conclusion, many factors remain unknown regarding how the plant mitochondrial genome is maintained. This work provides evidence that plant mitochondrial genome levels are monitored for maintenance. Both polIA and polIB appear to be redundantly expressed and required to maintain wild type mtDNA levels. A reduced cell expansion phenotype and a dynamic adjustment in cellular homeostasis occur when polIB gene expression is reduced relative to wild type levels. Even though both DNA polymerases have the ability to target the chloroplast and the mitochondria, it is evident PolIB is essential for the maintenance of the mitochondrial genome (Fig. 51).

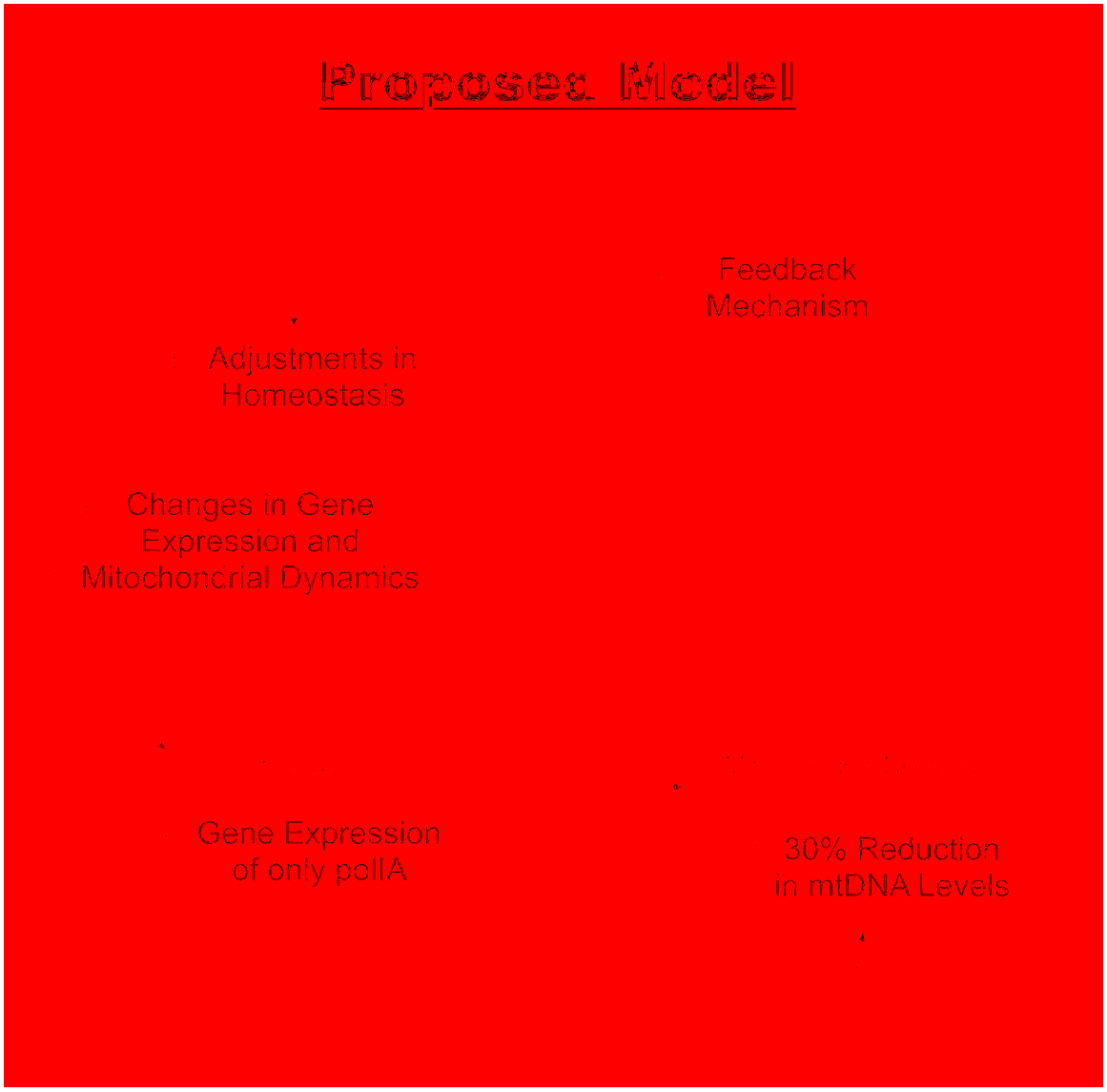

Figure 51. Final Proposed Research Model
Mitochondrial dynamics and gene expression are adjusted when the polIB gene is mutated. It is proposed that by some unknown mechanism mtDNA levels are monitored and cellular homeostasis is adjusted to compensate for either a reduction in mtDNA levels or the reduced expression of polIB.

REFERENCES

Agarwal S, Loar S, Steber C, Zale J (2009) Floral transformation of wheat. Methods in Molecular Biology 478: 105-113

Aharoni A, Giri AP, Deuerlein S, Griepink F, de Kogel WJ, Verstappen FW, Verhoeven HA, Jongsma MA, Schwab W, Bouwmeester HJ (2003) Terpenoid metabolism in wild type and transgenic *Arabidopsis* plants. Plant Cell 15: 2866-2884

Aksyonova E, Sinyavskaya M, Danilenko N, Pershina L, Nakamura C, Davydenko O (2005) Heteroplasmy and paternally oriented shift of the organellar DNA composition in barley-wheat hybrids during backcrosses with wheat parents. Genome / National Research Council Canada 48: 761-769

Alabadi D, Gil J, Blazquez MA, Garcia-Martinez JL (2004) Gibberellins repress photomorphogenesis in darkness. Plant Physiology 134: 1050-1057

Alonso JM, Stepanova AN, Leisse TJ, Kim CJ, Chen H, Shinn P, Stevenson DK, Zimmerman J, Barajas P, Cheuk R, Gadrinab C, Heller C, Jeske A, Koesema E, Meyers CC, Parker H, Prednis L, Ansari Y, Choy N, Deen H, Geralt M, Hazari N, Hom E, Karnes M, Mulholland C, Ndubaku R, Schmidt I, Guzman P, Aguilar-Henonin L, Schmid M, Weigel D, Carter DE, Marchand T, Risseeuw E, Brogden D, Zeko A, Crosby WL, Berry CC, Ecker JR (2003) Genome-wide insertional mutagenesis of *Arabidopsis* thaliana. Science 301: 653-657

Aluru MR, Rodermel SR (2004) Control of chloroplast redox by the IMMUTANS terminal oxidase. Physiologia Plantarum 120: 4-11

Andersen JR, Lubberstedt T (2003) Functional markers in plants. Trends in Plant Science 8: 554-560

Antico Arciuch VG, Elguero ME, Poderoso JJ, Carreras MC (2012) Mitochondrial regulation of cell cycle and proliferation. Antioxidants & Redox Signaling 16: 1150-1180

Armisen D, Lecharny A, Aubourg S (2008) Unique genes in plants: specificities and conserved features throughout evolution. BMC Evolutionary Biology 8: 280

Arrieta-Montiel MP, Shedge V, Davila J, Christensen AC, Mackenzie SA (2009) Diversity of the *Arabidopsis* mitochondrial genome occurs via nuclear-controlled recombination activity. Genetics 183: 1261-1268

Assmann SM (1999) The cellular basis of guard cell sensing of rising CO 2. Plant, Cell & Environment 22: 629–637

Atul Puri, G. E. MacDonald, W. T. Haller, Singh M (2006) Phytoene and β-Carotene Response of Fluridone-Susceptible and -Resistant Hydrilla (Hydrilla verticillata) Biotypes to Fluridone. Weed Science 54: 995-999

Autran D, Jonak C, Belcram K, Beemster GT, Kronenberger J, Grandjean O, Inze D, Traas J (2002) Cell numbers and leaf development in *Arabidopsis*: a functional analysis of the STRUWWELPETER gene. EMBO Journal 21: 6036-6049

Azpiroz-Leehan R, Feldmann KA (1997) T-DNA insertion mutagenesis in *Arabidopsis*: going back and forth. Trends in Genetics 13: 152-156

Backert S, Borner T (2000) Phage T4-like intermediates of DNA replication and recombination in the mitochondria of the higher plant Chenopodium album (L.). Current Genetics 37: 304-314

Backert S, Dorfel P, Lurz R, Borner T (1996) Rolling-circle replication of mitochondrial DNA in the higher plant Chenopodium album (L.). Molecular and Cellular Biology 16: 6285-6294

Baldauf SL (2003) The deep roots of eukaryotes. Science 300: 1703-1706

Barr CM, Neiman M, Taylor DR (2005) Inheritance and recombination of mitochondrial genomes in plants, fungi and animals. New Phytologist 168: 39-50

Barragan V, Leidi EO, Andres Z, Rubio L, De Luca A, Fernandez JA, Cubero B, Pardo JM (2012) Ion exchangers NHX1 and NHX2 mediate active potassium uptake into vacuoles to regulate cell turgor and stomatal function in *Arabidopsis*. Plant Cell 24: 1127-1142

Barratt DH, Derbyshire P, Findlay K, Pike M, Wellner N, Lunn J, Feil R, Simpson C, Maule AJ, Smith AM (2009) Normal growth of *Arabidopsis* requires cytosolic invertase but not sucrose synthase. Proceedings of the National Academy of Sciences of the United States of America 106: 13124-13129

Barry CS, Aldridge GM, Herzog G, Ma Q, McQuinn RP, Hirschberg J, Giovannoni JJ (2012) Altered Chloroplast Development and Delayed Fruit Ripening Caused by Mutations in a Zinc Metalloprotease at the lutescent2 Locus of Tomato. Plant Physiology 159: 1086-1098

Bartels PG, Watson CW (1978) Inhibition of Carotenoid Synthesis by Fluridone and Norflurazon. Weed Science 26: 198-203

Bassil E, Tajima H, Liang YC, Ohto MA, Ushijima K, Nakano R, Esumi T, Coku A, Belmonte M, Blumwald E (2011) The *Arabidopsis* Na+/H+ antiporters NHX1 and NHX2 control vacuolar pH and K+ homeostasis to regulate growth, flower development, and reproduction. Plant Cell 23: 3482-3497

Bedford E, Tabor S, Richardson CC (1997) The thioredoxin binding domain of bacteriophage T7 DNA polymerase confers processivity on Escherichia coli DNA polymerase I.

Proceedings of the National Academy of Sciences of the United States of America 94: 479-484

Beemster GT, Baskin TI (1998) Analysis of cell division and elongation underlying the developmental acceleration of root growth in *Arabidopsis* thaliana. Plant Physiology 116: 1515-1526

Bendich AJ (1996) Structural analysis of mitochondrial DNA molecules from fungi and plants using moving pictures and pulsed-field gel electrophoresis. Journal of Molecular Biology 255: 564-588

Bendich AJ (2004) Circular chloroplast chromosomes: the grand illusion. Plant Cell 16: 1661-1666

Bent A (2006) *Arabidopsis* thaliana floral dip transformation method. Methods in Molecular Biology 343: 87-103

Bertrand H, Collins RA, Stohl LL, Goewert RR, Lambowitz AM (1980) Deletion mutants of Neurospora crassa mitochondrial DNA and their relationship to the "stop-start" growth phenotype. Proceedings of the National Academy of Sciences of the United States of America 77: 6032-6036

Bieniawska Z, Paul Barratt DH, Garlick AP, Thole V, Kruger NJ, Martin C, Zrenner R, Smith AM (2007) Analysis of the sucrose synthase gene family in *Arabidopsis*. Plant Journal 49: 810-828

Birky CW, Jr. (2001) The inheritance of genes in mitochondria and chloroplasts: laws, mechanisms, and models. Annual Review of Genetics 35: 125-148

Blancaflor EB, Fasano JM, Gilroy S (1998) Mapping the functional roles of cap cells in the response of *Arabidopsis* primary roots to gravity. Plant Physiology 116: 213-222

Bogenhagen DF (2010) Does mtDNA nucleoid organization impact aging? Experimental Gerontology 45: 473-477

Bohmdorfer G, Schleiffer A, Brunmeir R, Ferscha S, Nizhynska V, Kozak J, Angelis KJ, Kreil DP, Schweizer D (2011) GMI1, a structural-maintenance-of-chromosomes-hinge domain-containing protein, is involved in somatic homologous recombination in *Arabidopsis*. Plant Journal 67: 420-433

Bowmaker M, Yang MY, Yasukawa T, Reyes A, Jacobs HT, Huberman JA, Holt IJ (2003) Mammalian mitochondrial DNA replicates bidirectionally from an initiation zone. Journal of Biological Chemistry 278: 50961-50969

Breton S, Beaupre HD, Stewart DT, Hoeh WR, Blier PU (2007) The unusual system of doubly uniparental inheritance of mtDNA: isn't one enough? Trends in Genetics 23: 465-474

Brookes PS, Yoon Y, Robotham JL, Anders MW, Sheu SS (2004) Calcium, ATP, and ROS: a mitochondrial love-hate triangle. American Journal of Physiology. Cell {hysiology 287: C817-833

Bullerwell CE, Gray MW (2004) Evolution of the mitochondrial genome: protist connections to animals, fungi and plants. Current Opinion in Microbiology 7: 528-534

Burger G, Gray MW, Lang BF (2003) Mitochondrial genomes: anything goes. Trends in Genetics 19: 709-716

Butow RA, Avadhani NG (2004) Mitochondrial signaling: the retrograde response. Molecular Cell 14: 1-15

Carrie C, Kuhn K, Murcha MW, Duncan O, Small ID, O'Toole N, Whelan J (2009) Approaches to defining dual-targeted proteins in *Arabidopsis*. The Plant journal : for cell and molecular biology 57: 1128-1139

Carrie C, Kuhn K, Murcha MW, Duncan O, Small ID, O'Toole N, Whelan J (2009) Approaches to defining dual-targeted proteins in *Arabidopsis*. Plant Journal 57: 1128-1139

Chalfun-Junior A, Mes JJ, Mlynarova L, Aarts MG, Angenent GC (2003) Low frequency of T-DNA based activation tagging in *Arabidopsis* is correlated with methylation of CaMV 35S enhancer sequences. FEBS Letters 555: 459-463

Chan CS, Gertler TS, Surmeier DJ (2009) Calcium homeostasis, selective vulnerability and Parkinson's disease. Trends in Neurosciences 32: 249-256

Charuvi D, Kiss V, Nevo R, Shimoni E, Adam Z, Reich Z (2012) Gain and loss of photosynthetic membranes during plastid differentiation in the shoot apex of *Arabidopsis*. Plant Cell 24: 1143-1157

Chen G, Law K, Ho P, Zhang X, Li N (2012) EGY2, a chloroplast membrane metalloprotease, plays a role in hypocotyl elongation in *Arabidopsis*. Molecular Biology Reports 39: 2147-2155

Chen XJ, Butow RA (2005) The organization and inheritance of the mitochondrial genome. Nature Reviews Genetics 6: 815-825

Christensen AC, Lyznik A, Mohammed S, Elowsky CG, Elo A, Yule R, Mackenzie SA (2005) Dual-domain, dual-targeting organellar protein presequences in *Arabidopsis* can use non-AUG start codons. The Plant cell 17: 2805-2816

Christensen AC, Lyznik A, Mohammed S, Elowsky CG, Elo A, Yule R, Mackenzie SA (2005) Dual-domain, dual-targeting organellar protein presequences in *Arabidopsis* can use non-AUG start codons. Plant Cell 17: 2805-2816

Christensen CA, Gorsich SW, Brown RH, Jones LG, Brown J, Shaw JM, Drews GN (2002) Mitochondrial GFA2 is required for synergid cell death in *Arabidopsis*. Plant Cell 14: 2215-2232

Christensen CA, King, E. J., Jordan, J. R., and Drews, G. N. (1997) Megagametogenesis in *Arabidopsis* wild type and the Gf mutant. Sex. Plant Reprod. 10: 49–64

Christensen CA, Subramanian S, Drews GN (1998) Identification of gametophytic mutations affecting female gametophyte development in *Arabidopsis*. Developmental biology 202: 136-151

Clay Montier LL, Deng JJ, Bai Y (2009) Number matters: control of mammalian mitochondrial DNA copy number. Journal of Genetics and Genomics 36: 125-131

Clayton DA (1982) Replication of animal mitochondrial DNA. Cell 28: 693-705

Clough SJ, Bent AF (1998) Floral dip: a simplified method for Agrobacterium-mediated transformation of *Arabidopsis* thaliana. The Plant Journal 16: 735-743

Collings DA, Gebbie LK, Howles PA, Hurley UA, Birch RJ, Cork AH, Hocart CH, Arioli T, Williamson RE (2008) *Arabidopsis* dynamin-like protein DRP1A: a null mutant with widespread defects in endocytosis, cellulose synthesis, cytokinesis, and cell expansion. Journal of Experimental Botany 59: 361-376

Collins TJ, Berridge MJ, Lipp P, Bootman MD (2002) Mitochondria are morphologically and functionally heterogeneous within cells. EMBO Journal 21: 1616-1627

Colon-Carmona A, You R, Haimovitch-Gal T, Doerner P (1999) Technical advance: spatio-temporal analysis of mitotic activity with a labile cyclin-GUS fusion protein. Plant Journal 20: 503-508

Conley CA, Hanson MR (1995) How do alterations in plant mitochondrial genomes disrupt pollen development? Journal of Bioenergetics and Biomembranes 27: 447-457

Copeland WC, Longley MJ (2008) DNA2 resolves expanding flap in mitochondrial base excision repair. Molecular Cell 32: 457-458

Correia RL, Oba-Shinjo SM, Uno M, Huang N, Marie SK (2011) Mitochondrial DNA depletion and its correlation with TFAM, TFB1M, TFB2M and POLG in human diffusely infiltrating astrocytomas. Mitochondrion 11: 48-53

Curtis IS (2005) Production of transgenic crops by the floral-dip method. Methods in Molecular Biology 286: 103-110

Curtis MD, Grossniklaus U (2003) A gateway cloning vector set for high-throughput functional analysis of genes in planta. Plant Physiology 133: 462-469

Das A, Ghosh J, Bhattacharya A, Samanta D, Das D, Das Gupta C (2011) Involvement of mitochondrial ribosomal proteins in ribosomal RNA-mediated protein folding. Journal of Biological Chemistry 286: 43771-43781

Davila JI, Arrieta-Montiel MP, Wamboldt Y, Cao J, Hagmann J, Shedge V, Xu YZ, Weigel D, Mackenzie SA (2011) Double-strand break repair processes drive evolution of the mitochondrial genome in *Arabidopsis*. BMC Biology 9: 64

Davis AF, Clayton DA (1996) In situ localization of mitochondrial DNA replication in intact mammalian cells. Journal of Cell Biology 135: 883-893

De Grauwe L, Vandenbussche F, Tietz O, Palme K, Van Der Straeten D (2005) Auxin, ethylene and brassinosteroids: tripartite control of growth in the *Arabidopsis* hypocotyl. Plant & Cell Physiology 46: 827-836

de Grey AD (2005) Forces maintaining organellar genomes: is any as strong as genetic code disparity or hydrophobicity? BioEssays : News and Reviews in Molecular, Cellular and Developmental Biology 27: 436-446

Dimmock D, Tang LY, Schmitt ES, Wong LJ (2010) Quantitative evaluation of the mitochondrial DNA depletion syndrome. Clinical Chemistry 56: 1119-1127

Dlaskova A, Hlavata L, Jezek J, Jezek P (2008) Mitochondrial Complex I superoxide production is attenuated by uncoupling. International Journal of Biochemistry & Cell Biology 40: 2098-2109

Dolan L, Janmaat K, Willemsen V, Linstead P, Poethig S, Roberts K, Scheres B (1993) Cellular organisation of the *Arabidopsis* thaliana root. Development 119: 71-84

Donahue RAMEP, Gerald E. Edwards (1997) A method for measuring whole plant photosynthesis in *Arabidopsis* thaliana. Photosynthesis Research 52: 263–269

Dowton M, Campbell NJ (2001) Intramitochondrial recombination - is it why some mitochondrial genes sleep around? Trends in Ecology & Evolution 16: 269-271

Driss-Ecole D, Lefranc A, Perbal G (2003) A polarized cell: the root statocyte. Physiologia Plantarum 118: 305-312

Dubessay P, Garreau-Balandier I, Jarrousse AS, Fleuriet A, Sion B, Debise R, Alziari S (2007) Aging impact on biochemical activities and gene expression of Drosophila melanogaster mitochondria. Biochimie 89: 988-1001

Echaniz-Laguna A, Chanson JB, Wilhelm JM, Sellal F, Mayencon M, Mohr M, Tranchant C, Mousson de Camaret B (2010) A novel variation in the Twinkle linker region causing late-onset dementia. Neurogenetics 11: 21-25

Edmondson AC, Song D, Alvarez LA, Wall MK, Almond D, McClellan DA, Maxwell A, Nielsen BL (2005) Characterization of a mitochondrially targeted single-stranded DNA-binding protein in *Arabidopsis* thaliana. Molecular Genetics and Genomics 273: 115-122

Elo A, Lyznik A, Gonzalez DO, Kachman SD, Mackenzie SA (2003) Nuclear genes that encode mitochondrial proteins for DNA and RNA metabolism are clustered in the *Arabidopsis* genome. Plant Cell 15: 1619-1631

Elo A, Lyznik A, Gonzalez DO, Kachman SD, Mackenzie SA (2003) Nuclear genes that encode mitochondrial proteins for DNA and RNA metabolism are clustered in the *Arabidopsis* genome. The Plant cell 15: 1619-1631

Elpeleg O, Mandel H, Saada A (2002) Depletion of the other genome-mitochondrial DNA depletion syndromes in humans. Journal of Molecular Medicine 80: 389-396

Fan L, Sanschagrin PC, Kaguni LS, Kuhn LA (1999) The accessory subunit of mtDNA polymerase shares structural homology with aminoacyl-tRNA synthetases: implications for a dual role as a primer recognition factor and processivity clamp. Proceedings of the National Academy of Sciences of the United States of America 96: 9527-9532

Farazdaghi H (2011) The single-process biochemical reaction of Rubisco: a unified theory and model with the effects of irradiance, CO(2) and rate-limiting step on the kinetics of C(3) and C(4) photosynthesis from gas exchange. Bio Systems 103: 265-284

Farge G, Holmlund T, Khvorostova J, Rofougaran R, Hofer A, Falkenberg M (2008) The N-terminal domain of TWINKLE contributes to single-stranded DNA binding and DNA helicase activities. Nucleic Acids Research 36: 393-403

Farquhar GvC, S; Berry, JA (1980) Abiochemical model of photosynthetic CO2 assimilation in leaves of C3 species. Planta 149: 78-90

Feng S, Martinez C, Gusmaroli G, Wang Y, Zhou J, Wang F, Chen L, Yu L, Iglesias-Pedraz JM, Kircher S, Schafer E, Fu X, Fan LM, Deng XW (2008) Coordinated regulation of *Arabidopsis* thaliana development by light and gibberellins. Nature 451: 475-479

Feng X, Kaur AP, Mackenzie SA, Dweikat IM (2009) Substoichiometric shifting in the fertility reversion of cytoplasmic male sterile pearl millet. Theoretical and Applied Genetics 118: 1361-1370

Fernie AR, Willmitzer L, Trethewey RN (2002) Sucrose to starch: a transition in molecular plant physiology. Trends in Plant Science 7: 35-41

Finer JJ, Finer KR, Ponappa T (1999) Particle bombardment mediated transformation. Current Topics in Microbiology and Immunology 240: 59-80

Fischer P, Klein U (1988) Localization of Nitrogen-Assimilating Enzymes in the Chloroplast of Chlamydomonas reinhardtii. Plant Physiology 88: 947-952

Foyer CH, Noctor G (2005) Redox homeostasis and antioxidant signaling: a metabolic interface between stress perception and physiological responses. Plant Cell 17: 1866-1875

Francis D (2011) A commentary on the G(2)/M transition of the plant cell cycle. Annals of Botany 107: 1065-1070

Franco AC, Matsubara S, Orthen B (2007) Photoinhibition, carotenoid composition and the co-regulation of photochemical and non-photochemical quenching in neotropical savanna trees. Tree Physiology 27: 717-725

Francs-Small CC, Kroeger T, Zmudjak M, Ostersetzer-Biran O, Rahimi N, Small I, Barkan A (2012) A PORR domain protein required for rpl2 and ccmF(C) intron splicing and for the biogenesis of c-type cytochromes in *Arabidopsis* mitochondria. Plant Journal 69: 996-1005

Fry AC (1992) The effects of acute training status on reliability of integrated electromyographic activity and "efficiency of electrical activity" during isometric contractions: a case study. Electromyography and Clinical Neurophysiology 32: 565-570

Fukaki H, Fujisawa H, Tasaka M (1997) The RHG gene is involved in root and hypocotyl gravitropism in *Arabidopsis* thaliana. Plant & Cell Physiology 38: 804-810

Futami K, Shimamoto A, Furuichi Y (2007) Mitochondrial and nuclear localization of human Pif1 helicase. Biological & Pharmaceutical Bulletin 30: 1685-1692

Galloway CA, Yoon Y (2012) Mitochondrial Morphology in Metabolic Diseases. Antioxidants & Redox Signaling

Galtier N (2011) The intriguing evolutionary dynamics of plant mitochondrial DNA. BMC Biology 9: 61

Garcia-Diaz M, Bebenek K (2007) Multiple Functions of DNA Polymerases. Critical reviews in plant sciences 26: 105-122

Gelvin SB (2003) Agrobacterium-mediated plant transformation: the biology behind the "gene-jockeying" tool. Microbiology and Molecular Biology Reviews 67: 16-37, table of contents

Gendreau E, Traas J, Desnos T, Grandjean O, Caboche M, Hofte H (1997) Cellular basis of hypocotyl growth in *Arabidopsis* thaliana. Plant Physiology 114: 295-305

Giege P, Sweetlove LJ, Cognat V, Leaver CJ (2005) Coordination of nuclear and mitochondrial genome expression during mitochondrial biogenesis in *Arabidopsis*. Plant Cell 17: 1497-1512

Glick D, Zhang W, Beaton M, Marsboom G, Gruber M, Simon MC, Hart J, Dorn GW, 2nd, Brady MJ, Macleod KF (2012) BNip3 regulates mitochondrial function and lipid metabolism in the liver. Molecular and Cellular Biology 32: 2570-2584

Grbic V, Bleecker AB (2000) Axillary meristem development in *Arabidopsis* thaliana. Plant Journal 21: 215-223

Griffiths AJ (1992) Fungal senescence. Annual Review of Genetics 26: 351-372

Gutteridge S, Gatenby AA (1995) Rubisco Synthesis, Assembly, Mechanism, and Regulation. Plant Cell 7: 809-819

Hagopian JC, Reis M, Kitajima JP, Bhattacharya D, de Oliveira MC (2004) Comparative analysis of the complete plastid genome sequence of the red alga Gracilaria tenuistipitata var. liui provides insights into the evolution of rhodoplasts and their relationship to other plastids. Journal of Molecular Evolution 59: 464-477

Hamel P, Corvest V, Giege P, Bonnard G (2009) Biochemical requirements for the maturation of mitochondrial c-type cytochromes. Biochimica et Biophysica Acta 1793: 125-138

Hammond JP, White PJ (2008) Sucrose transport in the phloem: integrating root responses to phosphorus starvation. Journal of Experimental Botany 59: 93-109

Hance N, Ekstrand MI, Trifunovic A (2005) Mitochondrial DNA polymerase gamma is essential for mammalian embryogenesis. Human Molecular Genetics 14: 1775-1783

Hatefi Y (1985) The mitochondrial electron transport and oxidative phosphorylation system. Annual Review of Biochemistry 54: 1015-1069

Hattori N, Kitagawa K, Takumi S, Nakamura C (2002) Mitochondrial DNA heteroplasmy in wheat, Aegilops and their nucleus-cytoplasm hybrids. Genetics 160: 1619-1630

Hausler RE, Geimer S, Kunz HH, Schmitz J, Dormann P, Bell K, Hetfeld S, Guballa A, Flugge UI (2009) Chlororespiration and grana hyperstacking: how an *Arabidopsis* double mutant can survive despite defects in starch biosynthesis and daily carbon export from chloroplasts. Plant Physiology 149: 515-533

He ZG, Richardson CC (2004) Effect of single-stranded DNA-binding proteins on the helicase and primase activities of the bacteriophage T7 gene 4 protein. Journal of Biological Chemistry 279: 22190-22197

Hederstedt L (2012) Heme A biosynthesis. Biochimica et Biophysica Acta 1817: 920-927

Hedrick LA, Heinhorst S, White MA, Cannon GC (1993) Analysis of soybean chloroplast DNA replication by two-dimensional gel electrophoresis. Plant molecular biology 23: 779-792

Hetherington AM (2001) Guard cell signaling. Cell 107: 711-714

Hills A, Chen ZH, Amtmann A, Blatt MR, Lew VL (2012) OnGuard, a Computational Platform for Quantitative Kinetic Modeling of Guard Cell Physiology. Plant Physiology 159: 1026-1042

Holec S, Lange H, Kuhn K, Alioua M, Borner T, Gagliardi D (2006) Relaxed transcription in *Arabidopsis* mitochondria is counterbalanced by RNA stability control mediated by polyadenylation and polynucleotide phosphorylase. Molecular and Cellular Biology 26: 2869-2876

Holt IJ (2009) Mitochondrial DNA replication and repair: all a flap. Trends in Biochemical Sciences 34: 358-365

Holt IJ, Lorimer HE, Jacobs HT (2000) Coupled leading- and lagging-strand synthesis of mammalian mitochondrial DNA. Cell 100: 515-524

Hwang DS, Kornberg A (1992) Opposed actions of regulatory proteins, DnaA and IciA, in opening the replication origin of Escherichia coli. Journal of Biological Chemistry 267: 23087-23091

Ishiguro S, Nishimori Y, Yamada M, Saito H, Suzuki T, Nakagawa T, Miyake H, Okada K, Nakamura K (2010) The *Arabidopsis* FLAKY POLLEN1 gene encodes a 3-hydroxy-3-methylglutaryl-coenzyme A synthase required for development of tapetum-specific organelles and fertility of pollen grains. Plant & Cell Physiology 51: 896-911

Jandova J, Janda J, Sligh JE (2012) Changes in mitochondrial DNA alter expression of nuclear encoded genes associated with tumorigenesis. Experimental cell research

Jansen RP (2000) Germline passage of mitochondria: quantitative considerations and possible embryological sequelae. Human Reproduction 15 Suppl 2: 112-128

Janska H, Sarria R, Woloszynska M, Arrieta-Montiel M, Mackenzie SA (1998) Stoichiometric shifts in the common bean mitochondrial genome leading to male sterility and spontaneous reversion to fertility. Plant cell 10: 1163-1180

Jazayeri M, Andreyev A, Will Y, Ward M, Anderson CM, Clevenger W (2003) Inducible expression of a dominant negative DNA polymerase-gamma depletes mitochondrial DNA and produces a rho0 phenotype. Journal of Biological Chemistry 278: 9823-9830

Jin JB, Bae H, Kim SJ, Jin YH, Goh CH, Kim DH, Lee YJ, Tse YC, Jiang L, Hwang I (2003) The *Arabidopsis* dynamin-like proteins ADL1C and ADL1E play a critical role in mitochondrial morphogenesis. Plant cell 15: 2357-2369

Jones HG (1998) Stomatal control of photosynthesis and transpiration. Journal of Experimental Botany 49: 387–398

Josse EM, Halliday KJ (2008) Skotomorphogenesis: the dark side of light signalling. Current Biology 18: R1144-1146

Joyard J, Ferro M, Masselon C, Seigneurin-Berny D, Salvi D, Garin J, Rolland N (2010) Chloroplast proteomics highlights the subcellular compartmentation of lipid metabolism. Progress in Lipid Research 49: 128-158

Juszczuk IM, Szal B, Rychter AM (2012) Oxidation-reduction and reactive oxygen species homeostasis in mutant plants with respiratory chain complex I dysfunction. Plant, Cell & Environment 35: 296-307

Kaguni LS (2004) DNA polymerase gamma, the mitochondrial replicase. Annual Review of Biochemistry 73: 293-320

Kang BH, Busse JS, Bednarek SY (2003) Members of the *Arabidopsis* dynamin-like gene family, ADL1, are essential for plant cytokinesis and polarized cell growth. Plant Cell 15: 899-913

Kang BH, Plescia J, Dohi T, Rosa J, Doxsey SJ, Altieri DC (2007) Regulation of tumor cell mitochondrial homeostasis by an organelle-specific Hsp90 chaperone network. Cell 131: 257-270

Kessler F, Schnell D (2009) Chloroplast biogenesis: diversity and regulation of the protein import apparatus. Current Opinion in Cell Biology 21: 494-500

Kim K, Portis AR, Jr. (2004) Oxygen-dependent H2O2 production by Rubisco. FEBS Letters 571: 124-128

Klee HJ (2010) Improving the flavor of fresh fruits: genomics, biochemistry, and biotechnology. New Phytologist 187: 44-56

Knohl A (2008) Effects of diffuse radiation on canopy gas exchange processes in a forest ecosystem. Journal of Geophysical Research 113: 1-17

Knott AB, Perkins G, Schwarzenbacher R, Bossy-Wetzel E (2008) Mitochondrial fragmentation in neurodegeneration. Nature Reviews Neuroscience 9: 505-518

Ko JH, Kim JH, Jayanty SS, Howe GA, Han KH (2006) Loss of function of COBRA, a determinant of oriented cell expansion, invokes cellular defence responses in *Arabidopsis* thaliana. Journal of Experimental Botany 57: 2923-2936

Kohler RH, Hanson MR (2000) Plastid tubules of higher plants are tissue-specific and developmentally regulated. Journal of Cell Science 113 (Pt 1): 81-89

Kohorn BD, Kobayashi M, Johansen S, Riese J, Huang LF, Koch K, Fu S, Dotson A, Byers N (2006) An *Arabidopsis* cell wall-associated kinase required for invertase activity and cell growth. Plant Journal 46: 307-316

Kolodner RD, Tewari KK (1975) Chloroplast DNA from higher plants replicates by both the Cairns and the rolling circle mechanism. Nature 256: 708-711

Kopriva S (2006) Regulation of sulfate assimilation in *Arabidopsis* and beyond. Annals of Botany 97: 479-495

Korhonen JA, Gaspari M, Falkenberg M (2003) TWINKLE Has 5' -> 3' DNA helicase activity and is specifically stimulated by mitochondrial single-stranded DNA-binding protein. Journal of Biological Chemistry 278: 48627-48632

Korhonen JA, Pham XH, Pellegrini M, Falkenberg M (2004) Reconstitution of a minimal mtDNA replisome in vitro. EMBO Journal 23: 2423-2429

Koumandou VL, Howe CJ (2007) The copy number of chloroplast gene minicircles changes dramatically with growth phase in the dinoflagellate Amphidinium operculatum. Protist 158: 89-103

Koussevitzky S, Nott A, Mockler TC, Hong F, Sachetto-Martins G, Surpin M, Lim J, Mittler R, Chory J (2007) Signals from chloroplasts converge to regulate nuclear gene expression. Science 316: 715-719

Kropat J, Oster U, Rudiger W, Beck CF (1997) Chlorophyll precursors are signals of chloroplast origin involved in light induction of nuclear heat-shock genes. Proceedings of the National Academy of Sciences of the United States of America 94: 14168-14172

Krysan PJ, Young JC, Sussman MR (1999) T-DNA as an insertional mutagen in *Arabidopsis*. Plant Cell 11: 2283-2290

Kubo T, Newton KJ (2008) Angiosperm mitochondrial genomes and mutations. Mitochondrion 8: 5-14

Kumar RA, Bendich AJ (2011) Distinguishing authentic mitochondrial and plastid DNAs from similar DNA sequences in the nucleus using the polymerase chain reaction. Current Genetics 57: 287-295

Lakshmipathy U, Campbell C (1999) The human DNA ligase III gene encodes nuclear and mitochondrial proteins. Molecular and Cellular Biology 19: 3869-3876

Laser B, Mohr S, Odenbach W, Oettler G, Kuck U (1997) Parental and novel copies of the mitochondrial orf25 gene in the hybrid crop-plant triticale: predominant transcriptional expression of the maternal gene copy. Current Genetics 32: 337-347

Lavrov DV (2010) Rapid proliferation of repetitive palindromic elements in mtDNA of the endemic Baikalian sponge Lubomirskia baicalensis. Molecular Biology and Evolution 27: 757-760

Le J, Vandenbussche F, Cnodder T, Straeten D, Verbelen J-P (2005) Cell Elongation and Microtubule Behavior in the *Arabidopsis* Hypocotyl: Responses to Ethylene and Auxin. Journal of Plant Growth Regulation 24: 166–178

Leegood RC, Lea PJ, Adcock MD, Häusler RE (1995) The regulation and control of photorespiration. Journal of experimental botany 46: 1397-1414

Legros F, Malka F, Frachon P, Lombes A, Rojo M (2004) Organization and dynamics of human mitochondrial DNA. Journal of Cell Science 117: 2653-2662

Leister D (2005) Genomics-based dissection of the cross-talk of chloroplasts with the nucleus and mitochondria in *Arabidopsis*. Gene 354: 110-116

Levi S, Rovida E (2009) The role of iron in mitochondrial function. Biochimica et Biophysica Acta 1790: 629-636

Li Y, Swaminathan K, Hudson ME (2011) Rapid, organ-specific transcriptional responses to light regulate photomorphogenic development in dicot seedlings. Plant Physiology 156: 2124-2140

Lim L, McFadden GI (2010) The evolution, metabolism and functions of the apicoplast. Philosophical Transactions of the Royal Society of London. Series B, Biological Sciences 365: 749-763

Lippok B, Brennicke A, Wissinger B (1994) Differential RNA editing in closely related introns in Oenothera mitochondria. Molecular & General Genetics 243: 39-46

Liu CN, Li XQ, Gelvin SB (1992) Multiple copies of virG enhance the transient transformation of celery, carrot and rice tissues by Agrobacterium tumefaciens. Plant Molecular Biology 20: 1071-1087

Liu P, Qian L, Sung JS, de Souza-Pinto NC, Zheng L, Bogenhagen DF, Bohr VA, Wilson DM, 3rd, Shen B, Demple B (2008) Removal of oxidative DNA damage via FEN1-dependent long-patch base excision repair in human cell mitochondria. Molecular and Cellular Biology 28: 4975-4987

Liu Y, Kao HI, Bambara RA (2004) Flap endonuclease 1: a central component of DNA metabolism. Annual Review of Biochemistry 73: 589-615

Liu Z, Butow RA (2006) Mitochondrial retrograde signaling. Annual Review of Genetics 40: 159-185

Livak KJ, Schmittgen TD (2001) Analysis of relative gene expression data using real-time quantitative PCR and the 2(-Delta Delta C(T)) Method. Methods 25: 402-408

Logan DC (2006) Plant mitochondrial dynamics. Biochimica et Biophysica Acta 1763: 430-441

Logan DC (2010) The dynamic plant chondriome. Seminars in Cell & Developmental Biology 21: 550-557

Logan DC, Leaver CJ (2000) Mitochondria-targeted GFP highlights the heterogeneity of mitochondrial shape, size and movement within living plant cells. Journal of Experimental Botany 51: 865-871

Logan DC, Scott I, Tobin AK (2004) ADL2a, like ADL2b, is involved in the control of higher plant mitochondrial morphology. Journal of Experimental Botany 55: 783-785

Long SP, Bernacchi CJ (2003) Gas exchange measurements, what can they tell us about the underlying limitations to photosynthesis? Procedures and sources of error. Journal of Experimental Botany 54: 2393-2401

MacAlpine DM, Kolesar J, Okamoto K, Butow RA, Perlman PS (2001) Replication and preferential inheritance of hypersuppressive petite mitochondrial DNA. EMBO journal 20: 1807-1817

Macvanin M, Adhya S (2012) Architectural organization in E. coli nucleoid. Biochimica et Biophysica Acta 1819: 830-835

Manchekar M, Scissum-Gunn K, Song D, Khazi F, McLean SL, Nielsen BL (2006) DNA recombination activity in soybean mitochondria. Journal of Molecular Biology 356: 288-299

Mancuso C, Scapagini G, Curro D, Giuffrida Stella AM, De Marco C, Butterfield DA, Calabrese V (2007) Mitochondrial dysfunction, free radical generation and cellular stress response in neurodegenerative disorders. Frontiers in Bioscience 12: 1107-1123

Mancuso M, Coppede F, Migliore L, Siciliano G, Murri L (2006) Mitochondrial dysfunction, oxidative stress and neurodegeneration. Journal of Alzheimer's Disease 10: 59-73

Manter DK, Kerrigan J (2004) A/C(i) curve analysis across a range of woody plant species: influence of regression analysis parameters and mesophyll conductance. Journal of Experimental Botany 55: 2581-2588

Marienfeld J, Unseld M, Brennicke A (1999) The mitochondrial genome of *Arabidopsis* is composed of both native and immigrant information. Trends in Plant Science 4: 495-502

Marin-Garcia J, Damle S, Jugdutt BI, Moe GW (2012) Nuclear-mitochondrial cross-talk in global myocardial ischemia. A time-course analysis. Molecular and Cellular Biochemistry 364: 225-234

Matsunaga F, Norais C, Forterre P, Myllykallio H (2003) Identification of short 'eukaryotic' Okazaki fragments synthesized from a prokaryotic replication origin. EMBO Reports 4: 154-158

McBride HM, Neuspiel M, Wasiak S (2006) Mitochondria: more than just a powerhouse. Current Biology 16: R551-560

Mignotte F, Tourte M, Mounolou JC (1987) Segregation of mitochondria in the cytoplasm of Xenopus vitellogenic oocytes. Biology of the Cell / under the auspices of the European Cell Biology Organization 60: 97-102

Miller G, Suzuki N, Ciftci-Yilmaz S, Mittler R (2010) Reactive oxygen species homeostasis and signalling during drought and salinity stresses. Plant, Cell & Environment 33: 453-467

Miyakawa I, Okamuro A, Kinsky S, Visacka K, Tomaska L, Nosek J (2009) Mitochondrial nucleoids from the yeast Candida parapsilosis: expansion of the repertoire of proteins associated with mitochondrial DNA. Microbiology 155: 1558-1568

Monastyrska I, Klionsky DJ (2006) Autophagy in organelle homeostasis: peroxisome turnover. Molecular Aspects of Medicine 27: 483-494

Monson RK, Edwards GE, Ku MSBK (1984) C3- C4 Intermediate Photosynthesis in Plants. University of California Press on Behalf of the American Institute of Biological Sciences 34: 563-566

Monticone M, Panfoli I, Ravera S, Puglisi R, Jiang MM, Morello R, Candiani S, Tonachini L, Biticchi R, Fabiano A, Cancedda R, Boitani C, Castagnola P (2010) The nuclear genes

Mtfr1 and Dufd1 regulate mitochondrial dynamic and cellular respiration. Journal of Cellular Physiology 225: 767-776

Moraes CT (2001) What regulates mitochondrial DNA copy number in animal cells? Trends in Genetics 17: 199-205

Moriyama T, Terasawa K, Fujiwara M, Sato N (2008) Purification and characterization of organellar DNA polymerases in the red alga Cyanidioschyzon merolae. FEBS journal 275: 2899-2918

Moriyama T, Terasawa K, Sato N (2011) Conservation of POPs, the plant organellar DNA polymerases, in eukaryotes. Protist 162: 177-187

Mosig G (1998) Recombination and recombination-dependent DNA replication in bacteriophage T4. Annual Review of Genetics 32: 379-413

Mullet JE (1988) Chloroplast development and gene expression. Annual Review of Plant Physiology and Plant Molecular Biology 39: 475–502

Munwes I, Geffen E, Friedmann A, Tikochinski Y, Gafny S (2011) Variation in repeat length and heteroplasmy of the mitochondrial DNA control region along a core-edge gradient in the eastern spadefoot toad (Pelobates syriacus). Molecular Ecology 20: 2878-2887

Nakagawa CC, Jones EP, Miller DL (1998) Mitochondrial DNA rearrangements associated with mF plasmid integration and plasmodial longevity in Physarum polycephalum. Current Genetics 33: 178-187

Neff MM, Fankhauser C, Chory J (2000) Light: an indicator of time and place. Genes & Development 14: 257-271

Nielsen BL, Cupp JD, Brammer J (2010) Mechanisms for maintenance, replication, and repair of the chloroplast genome in plants. Journal of Experimental Botany 61: 2535-2537

Nobusawa T, Umeda M (2012) Very-long-chain fatty acids have an essential role in plastid division by controlling Z-ring formation in *Arabidopsis* thaliana. Genes to Cells : Devoted to Molecular & Cellular Mechanisms

Nomura H, Komori T, Uemura S, Kanda Y, Shimotani K, Nakai K, Furuichi T, Takebayashi K, Sugimoto T, Sano S, Suwastika IN, Fukusaki E, Yoshioka H, Nakahira Y, Shiina T (2012) Chloroplast-mediated activation of plant immune signalling in *Arabidopsis*. Nature Communications 3: 926

Nosek J, Kosa P, Tomaska L (2006) On the origin of telomeres: a glimpse at the pre-telomerase world. BioEssays : News and Reviews in Molecular, Cellular and Developmental Biology 28: 182-190

Nosek J, Tomaska L (2003) Mitochondrial genome diversity: evolution of the molecular architecture and replication strategy. Current Genetics 44: 73-84

Nowack MK, Harashima H, Dissmeyer N, Zhao X, Bouyer D, Weimer AK, De Winter F, Yang F, Schnittger A (2012) Genetic framework of cyclin-dependent kinase function in *Arabidopsis*. Developmental Cell 22: 1030-1040

Nowikovsky K, Reipert S, Devenish RJ, Schweyen RJ (2007) Mdm38 protein depletion causes loss of mitochondrial K+/H+ exchange activity, osmotic swelling and mitophagy. Cell Death and Differentiation 14: 1647-1656

O'Connor TR, Dyreson C, Wyrick JJ (2005) Athena: a resource for rapid visualization and systematic analysis of *Arabidopsis* promoter sequences. Bioinformatics 21: 4411-4413

Oda K, Yamato K, Ohta E, Nakamura Y, Takemura M, Nozato N, Akashi K, Kanegae T, Ogura Y, Kohchi T, et al. (1992) Gene organization deduced from the complete sequence of

liverwort Marchantia polymorpha mitochondrial DNA. A primitive form of plant mitochondrial genome. Journal of Molecular Biology 223: 1-7

Ögren E, Evans JR (1993) Photosynthetic light-response curves. Planta 189: 182-190

Ohta E, Oda K, Yamato K, Nakamura Y, Takemura M, Nozato N, Akashi K, Ohyama K, Michel F (1993) Group I introns in the liverwort mitochondrial genome: the gene coding for subunit 1 of cytochrome oxidase shares five intron positions with its fungal counterparts. Nucleic Acids Research 21: 1297-1305

Okada S, Brennicke A (2006) Transcript levels in plant mitochondria show a tight homeostasis during day and night. Molecular Genetics and Genomics 276: 71-78

Okamoto K, Shaw JM (2005) Mitochondrial morphology and dynamics in yeast and multicellular eukaryotes. Annual Review of Genetics 39: 503-536

Oldenburg DJ, Bendich AJ (2004) Changes in the structure of DNA molecules and the amount of DNA per plastid during chloroplast development in maize. Journal of Molecular Biology 344: 1311-1330

Oldenburg DJ, Bendich AJ (2004) Most chloroplast DNA of maize seedlings in linear molecules with defined ends and branched forms. Journal of Molecular Biology 335: 953-970

Ono Y, Sakai A, Takechi K, Takio S, Takusagawa M, Takano H (2007) NtPolI-like1 and NtPolI-like2, bacterial DNA polymerase I homologs isolated from BY-2 cultured tobacco cells, encode DNA polymerases engaged in DNA replication in both plastids and mitochondria. Plant & Cell Physiology 48: 1679-1692

Osteryoung KW, Stokes KD, Rutherford SM, Percival AL, Lee WY (1998) Chloroplast division in higher plants requires members of two functionally divergent gene families with homology to bacterial ftsZ. Plant Cell 10: 1991-2004

Paeschke K, McDonald KR, Zakian VA (2010) Telomeres: structures in need of unwinding. FEBS Letters 584: 3760-3772

Parent J-S, Lepage E, Brisson N (2011) Divergent roles for the two PolI-like organelle DNA polymerases of *Arabidopsis*. Plant Physiology 156: 254–226

Park JH, Halitschke R, Kim HB, Baldwin IT, Feldmann KA, Feyereisen R (2002) A knock-out mutation in allene oxide synthase results in male sterility and defective wound signal transduction in *Arabidopsis* due to a block in jasmonic acid biosynthesis. Plant Journal 31: 1-12

Peeters N, Small I (2001) Dual targeting to mitochondria and chloroplasts. Biochimica et Biophysica Acta 1541: 54-63

Pesaresi P, Masiero S, Eubel H, Braun HP, Bhushan S, Glaser E, Salamini F, Leister D (2006) Nuclear photosynthetic gene expression is synergistically modulated by rates of protein synthesis in chloroplasts and mitochondria. Plant cell 18: 970-991

Pfannschmidt T (2003) Chloroplast redox signals: how photosynthesis controls its own genes. Trends in Plant Science 8: 33-41

Pham XH, Farge G, Shi Y, Gaspari M, Gustafsson CM, Falkenberg M (2006) Conserved sequence box II directs transcription termination and primer formation in mitochondria. Journal of Biological Chemistry 281: 24647-24652

Poburko D, Demaurex N (2012) Regulation of the mitochondrial proton gradient by cytosolic Ca(2+) signals. European Journal of Physiology 464: 19-26

Ponce G, Rasgado FA, Cassab GI (2008) Roles of amyloplasts and water deficit in root tropisms. Plant, Cell & Environment 31: 205-217

Preuten T, Cincu E, Fuchs J, Zoschke R, Liere K, Borner T (2010) Fewer genes than organelles: extremely low and variable gene copy numbers in mitochondria of somatic plant cells. Plant Journal 64: 948-959

Raturi A, Simmen T (2012) Where the endoplasmic reticulum and the mitochondrion tie the knot: The mitochondria-associated membrane (MAM). Biochimica et Biophysica Acta

Reddy PH, McWeeney S, Park BS, Manczak M, Gutala RV, Partovi D, Jung Y, Yau V, Searles R, Mori M, Quinn J (2004) Gene expression profiles of transcripts in amyloid precursor protein transgenic mice: up-regulation of mitochondrial metabolism and apoptotic genes is an early cellular change in Alzheimer's disease. Human Molecular Genetics 13: 1225-1240

Reyes A, Yang MY, Bowmaker M, Holt IJ (2005) Bidirectional replication initiates at sites throughout the mitochondrial genome of birds. Journal of Biological Chemistry 280: 3242-3250

Rhee SY, Beavis W, Berardini TZ, Chen G, Dixon D, Doyle A, Garcia-Hernandez M, Huala E, Lander G, Montoya M, Miller N, Mueller LA, Mundodi S, Reiser L, Tacklind J, Weems DC, Wu Y, Xu I, Yoo D, Yoon J, Zhang P (2003) The *Arabidopsis* Information Resource (TAIR): a model organism database providing a centralized, curated gateway to *Arabidopsis* biology, research materials and community. Nucleic Acids Research 31: 224-228

Rhoads DM, Subbaiah CC (2007) Mitochondrial retrograde regulation in plants. Mitochondrion 7: 177-194

Robberson DL, Kasamatsu H, Vinograd J (1972) Replication of mitochondrial DNA. Circular replicative intermediates in mouse L cells. Proceedings of the National Academy of Sciences of the United States of America 69: 737-741

Rodriguez-Villalon A, Gas E, Rodriguez-Concepcion M (2009) Phytoene synthase activity controls the biosynthesis of carotenoids and the supply of their metabolic precursors in dark-grown *Arabidopsis* seedlings. Plant Journal 60: 424-435

Ropp PA, Copeland WC (1996) Cloning and characterization of the human mitochondrial DNA polymerase, DNA polymerase gamma. Genomics 36: 449-458

Rossi ML, Pike JE, Wang W, Burgers PM, Campbell JL, Bambara RA (2008) Pif1 helicase directs eukaryotic Okazaki fragments toward the two-nuclease cleavage pathway for primer removal. Journal of Biological Chemistry 283: 27483-27493

Rowan BA, Bendich AJ (2009) The loss of DNA from chloroplasts as leaves mature: fact or artefact? Journal of Experimental Botany 60: 3005-3010

Rowan BA, Oldenburg DJ, Bendich AJ (2004) The demise of chloroplast DNA in *Arabidopsis*. Current Genetics 46: 176-181

Rowan BA, Oldenburg DJ, Bendich AJ (2007) A high-throughput method for detection of DNA in chloroplasts using flow cytometry. Plant Methods 3: 5

Ruckle ME, Burgoon LD, Lawrence LA, Sinkler CA, Larkin RM (2012) Plastids are major regulators of light signaling in *Arabidopsis*. Plant Physiology 159: 366-390

Ruhanen H, Ushakov K, Yasukawa T (2011) Involvement of DNA ligase III and ribonuclease H1 in mitochondrial DNA replication in cultured human cells. Biochimica et Biophysica Acta 1813: 2000-2007

Rumeau D, Peltier G, Cournac L (2007) Chlororespiration and cyclic electron flow around PSI during photosynthesis and plant stress response. Plant, Cell & Environment 30: 1041-1051

Samson F, Brunaud V, Balzergue S, Dubreucq B, Lepiniec L, Pelletier G, Caboche M, Lecharny A (2002) FLAGdb/FST: a database of mapped flanking insertion sites (FSTs) of *Arabidopsis* thaliana T-DNA transformants. Nucleic Acids Research 30: 94-97

Sarzi E, Goffart S, Serre V, Chretien D, Slama A, Munnich A, Spelbrink JN, Rotig A (2007) Twinkle helicase (PEO1) gene mutation causes mitochondrial DNA depletion. Annals of Neurology 62: 579-587

Sato A, Nakada K, Hayashi J (2006) Mitochondrial dynamics and aging: Mitochondrial interaction preventing individuals from expression of respiratory deficiency caused by mutant mtDNA. Biochimica et Biophysica Acta 1763: 473-481

Schaller A, Hahn D, Jackson CB, Kern I, Chardot C, Belli DC, Gallati S, Nuoffer JM (2011) Molecular and biochemical characterisation of a novel mutation in POLG associated with Alpers syndrome. BMC Neurology 11: 4

Scharff LB, Koop HU (2006) Linear molecules of tobacco ptDNA end at known replication origins and additional loci. Plant Molecular Biology 62: 611-621

Schmid J, Amrhein N (1995) Molecular organization of the shikimate pathway in higher plants. Phytochemistry 39: 737–749.

Schwarzlander M, Konig AC, Sweetlove LJ, Finkemeier I (2012) The impact of impaired mitochondrial function on retrograde signalling: a meta-analysis of transcriptomic responses. Journal of Experimental Botany 63: 1735-1750

Segui-Simarro JM, Coronado MJ, Staehelin LA (2008) The mitochondrial cycle of *Arabidopsis* shoot apical meristem and leaf primordium meristematic cells is defined by a perinuclear tentaculate/cage-like mitochondrion. Plant Physiology 148: 1380-1393

Sekito T, Thornton J, Butow RA (2000) Mitochondria-to-nuclear signaling is regulated by the subcellular localization of the transcription factors Rtg1p and Rtg3p. Molecular Biology of the Cell 11: 2103-2115

Shedge V, Arrieta-Montiel M, Christensen AC, Mackenzie SA (2007) Plant mitochondrial recombination surveillance requires unusual RecA and MutS homologs. Plant Cell 19: 1251-1264

Shedge V, Arrieta-Montiel M, Christensen AC, Mackenzie SA (2007) Plant mitochondrial recombination surveillance requires unusual RecA and MutS homologs. Plant Cell 19: 1251-1264

Shedge V, Davila J, Arrieta-Montiel MP, Mohammed S, Mackenzie SA (2010) Extensive rearrangement of the *Arabidopsis* mitochondrial genome elicits cellular conditions for thermotolerance. Plant Physiology 152: 1960-1970

Shutt TE, Gray MW (2006) Bacteriophage origins of mitochondrial replication and transcription proteins. Trends in Genetics 22: 90-95

Shutt TE, Gray MW (2006) Twinkle, the mitochondrial replicative DNA helicase, is widespread in the eukaryotic radiation and may also be the mitochondrial DNA primase in most eukaryotes. Journal of Molecular Evolution 62: 588-599

Sieburth LE, Muday GK, King EJ, Benton G, Kim S, Metcalf KE, Meyers L, Seamen E, Van Norman JM (2006) SCARFACE encodes an ARF-GAP that is required for normal auxin efflux and vein patterning in *Arabidopsis*. Plant Cell 18: 1396-1411

Skulachev VP (2001) Mitochondrial filaments and clusters as intracellular power-transmitting cables. Trends in Biochemical Sciences 26: 23-29

Small I, Suffolk R, Leaver CJ (1989) Evolution of plant mitochondrial genomes via substoichiometric intermediates. Cell 58: 69-76

Smith AM, Stitt M (2007) Coordination of carbon supply and plant growth. Plant, Cell & Environment 30: 1126-1149

Smith MA, Schnellmann RG (2012) Calpains, mitochondria and Apoptosis. Cardiovascular Research

Sokol A, Kwiatkowska A, Jerzmanowski A, Prymakowska-Bosak M (2007) Up-regulation of stress-inducible genes in tobacco and *Arabidopsis* cells in response to abiotic stresses and ABA treatment correlates with dynamic changes in histone H3 and H4 modifications. Planta 227: 245-254

Spelbrink JN, Li FY, Tiranti V, Nikali K, Yuan QP, Tariq M, Wanrooij S, Garrido N, Comi G, Morandi L, Santoro L, Toscano A, Fabrizi GM, Somer H, Croxen R, Beeson D, Poulton J, Suomalainen A, Jacobs HT, Zeviani M, Larsson C (2001) Human mitochondrial DNA deletions associated with mutations in the gene encoding Twinkle, a phage T7 gene 4-like protein localized in mitochondria. Nature Genetics 28: 223-231

Stumpf JD, Copeland WC (2011) Mitochondrial DNA replication and disease: insights from DNA polymerase gamma mutations. Cellular and Molecular Life Sciences 68: 219-233

Sugimoto K, Kohara Y, Okazaki T (1987) Relative roles of T7 RNA polymerase and gene 4 primase for the initiation of T7 phage DNA replication in vivo. Proceedings of the National Academy of Sciences of the United States of America 84: 3977-3981

Swan MK, Johnson RE, Prakash L, Prakash S, Aggarwal AK (2009) Structural basis of high-fidelity DNA synthesis by yeast DNA polymerase delta. Nature Structural & Molecular Biology 16: 979-986

Takada S, Jurgens G (2007) Transcriptional regulation of epidermal cell fate in the *Arabidopsis* embryo. Development 134: 1141-1150

Tang J, Kobayashi K, Suzuki M, Matsumoto S, Muranaka T (2010) The mitochondrial PPR protein LOVASTATIN INSENSITIVE 1 plays regulatory roles in cytosolic and plastidial isoprenoid biosynthesis through RNA editing. Plant Journal 61: 456-466

Tax FE, Vernon DM (2001) T-DNA-associated duplication/translocations in *Arabidopsis*. Plant Physiology 126: 1527-1538

Timm S, Nunes-Nesi A, Parnik T, Morgenthal K, Wienkoop S, Keerberg O, Weckwerth W, Kleczkowski LA, Fernie AR, Bauwe H (2008) A cytosolic pathway for the conversion of hydroxypyruvate to glycerate during photorespiration in *Arabidopsis*. Plant Cell 20: 2848-2859

Tiranti V, Savoia A, Forti F, D'Apolito MF, Centra M, Rocchi M, Zeviani M (1997) Identification of the gene encoding the human mitochondrial RNA polymerase (h-mtRPOL) by cyberscreening of the Expressed Sequence Tags database. Human Molecular Genetics 6: 615-625

Toshoji H, Katsumata T, Takusagawa M, Yusa Y, Sakai A (2011) Effects of chloroplast dysfunction on mitochondria: white sectors in variegated leaves have higher mitochondrial DNA levels and lower dark respiration rates than green sectors. Protoplasma

Tovar J, Leon-Avila G, Sanchez LB, Sutak R, Tachezy J, van der Giezen M, Hernandez M, Muller M, Lucocq JM (2003) Mitochondrial remnant organelles of Giardia function in iron-sulphur protein maturation. Nature 426: 172-176

Townsend JP, Rand DM (2004) Mitochondrial genome size variation in New World and Old World populations of Drosophila melanogaster. Heredity 93: 98-103

Tsukamoto N, Asakura N, Hattori N, Takumi S, Mori N, Nakamura C (2000) Identification of paternal mitochondrial DNA sequences in the nucleus-cytoplasm hybrids of tetraploid and hexaploid wheat with D and D2 plasmons from Aegilops species. Current Genetics 38: 208-217

Tyynismaa H, Sembongi H, Bokori-Brown M, Granycome C, Ashley N, Poulton J, Jalanko A, Spelbrink JN, Holt IJ, Suomalainen A (2004) Twinkle helicase is essential for mtDNA maintenance and regulates mtDNA copy number. Human Molecular Genetics 13: 3219-3227

Ubeda-Tomas S, Beemster GT, Bennett MJ (2012) Hormonal regulation of root growth: integrating local activities into global behaviour. Trends in Plant Science 17: 326-331

Udvardi MK, Czechowski T, Scheible WR (2008) Eleven golden rules of quantitative RT-PCR. Plant Cell 20: 1736-1737

van Bel AJE (2003) The phloem, a miracle of ingenuity. Plant, Cell and Environment 26: 125-149

van der Veen JH, Wirtz P (1968) EMS induced genic male sterility in *Arabidopsis* thaliana: A model selection experiment. Euphytica 17: 371-377

van Meer G, Voelker DR, Feigenson GW (2008) Membrane lipids: where they are and how they behave. Nature Reviews Molecular Cell Biology 9: 112-124

Van Norman JM, Frederick RL, Sieburth LE (2004) BYPASS1 negatively regulates a root-derived signal that controls plant architecture. Current Biology 14: 1739-1746

Van Norman JM, Sieburth LE (2007) Dissecting the biosynthetic pathway for the bypass1 root-derived signal. Plant Journal 49: 619-628

Vandenbussche F, Verbelen JP, Van Der Straeten D (2005) Of light and length: regulation of hypocotyl growth in *Arabidopsis*. BioEssays: News and Reviews in Molecular, Cellular and Developmental Biology 27: 275-284

Verbitskiy D, Hartel B, Zehrmann A, Brennicke A, Takenaka M (2011) The DYW-E-PPR protein MEF14 is required for RNA editing at site matR-1895 in mitochondria of *Arabidopsis* thaliana. FEBS Letters 585: 700-704

von Caemmerer SF, GD (1981) Some relationships between the biochemistry of photosynthesis and the gasexchange of leaves. Planta 153: 376-387

Wagele H, Deusch O, Handeler K, Martin R, Schmitt V, Christa G, Pinzger B, Gould SB, Dagan T, Klussmann-Kolb A, Martin W (2011) Transcriptomic evidence that longevity of acquired plastids in the photosynthetic slugs Elysia timida and Plakobranchus ocellatus does not entail lateral transfer of algal nuclear genes. Molecular Biology and Evolution 28: 699-706

Wagner D, Meyerowitz EM (2011) Switching on Flowers: Transient LEAFY Induction Reveals Novel Aspects of the Regulation of Reproductive Development in *Arabidopsis*. Frontiers in Plant Science 2: 60

Wall MK, Mitchenall LA, Maxwell A (2004) *Arabidopsis* thaliana DNA gyrase is targeted to chloroplasts and mitochondria. Proceedings of the National Academy of Sciences of the United States of America 101: 7821-7826

Wang F, Sanz A, Brenner ML, Smith A (1993) Sucrose Synthase, Starch Accumulation, and Tomato Fruit Sink Strength. Plant Physiology 101: 321-327

Weigel D (2002) *Arabidopsis*: A Laboratory Manual - Detlef Weigel, Jane Glazebrook - Google Books,

Westermann B (2010) Mitochondrial fusion and fission in cell life and death. Nature Reviews Molecular Cell Biology 11: 872-884

Williams L, Fletcher JC (2005) Stem cell regulation in the *Arabidopsis* shoot apical meristem. Current Opinion in Plant Biology 8: 582-586

Williamson D (2002) The curious history of yeast mitochondrial DNA. Nature Reviews Genetics 3: 475-481

Wise RR (2007) The diversity of plastid form and function. Advances in Photosynthesis and Respiration 23: 3-26

Wise RR, Hoober JK (2006) The structure and function of plastids. Advances in Photosynthesis and Respiration 23: 3-26

Woloszynska M (2010) Heteroplasmy and stoichiometric complexity of plant mitochondrial genomes--though this be madness, yet there's method in't. Journal of Experimental Botany 61: 657-671

Woodson JD, Perez-Ruiz JM, Chory J (2011) Heme synthesis by plastid ferrochelatase I regulates nuclear gene expression in plants. Current Biology 21: 897-903

Wroblewski T, Tomczak A, Michelmore R (2005) Optimization of Agrobacterium-mediated transient assays of gene expression in lettuce, tomato and *Arabidopsis*. Plant Biotechnology Journal 3: 259-273

Wu FH, Shen SC, Lee LY, Lee SH, Chan MT, Lin CS (2009) Tape-*Arabidopsis* Sandwich - a simpler *Arabidopsis* protoplast isolation method. Plant Methods 5: 16

Wullshleger SD (1993) Biochemical Limitations to Carbon Assimilation in C3 Plants—A Retrospective Analysis of the A/Ci Curves from 109 Species. Journal of Experimental Botany

Xu B, Clayton DA (1996) RNA-DNA hybrid formation at the human mitochondrial heavy-strand origin ceases at replication start sites: an implication for RNA-DNA hybrids serving as primers. EMBO Journal 15: 3135-3143

Xu YZ, Arrieta-Montiel MP, Virdi KS, de Paula WB, Widhalm JR, Basset GJ, Davila JI, Elthon TE, Elowsky CG, Sato SJ, Clemente TE, Mackenzie SA (2011) MutS HOMOLOG1 is a nucleoid protein that alters mitochondrial and plastid properties and plant response to high light. Plant Cell 23: 3428-3441

Yamato K, Nozato N, Oda K, Ohta E, Takemura M, Akashi K, Ohyama K (1993) Occurrence and transcription of genes for nad1, nad3, nad4L, and nad6, coding for NADH dehydrogenase subunits 1, 3, 4L, and 6, in liverwort mitochondria. Current Genetics 23: 526-531

Yamtich J, Sweasy JB (2010) DNA polymerase family X: function, structure, and cellular roles. Biochimica et Biophysica Acta 1804: 1136-1150

Yang MY, Bowmaker M, Reyes A, Vergani L, Angeli P, Gringeri E, Jacobs HT, Holt IJ (2002) Biased incorporation of ribonucleotides on the mitochondrial L-strand accounts for apparent strand-asymmetric DNA replication. Cell 111: 495-505

Yasukawa T, Reyes A, Cluett TJ, Yang MY, Bowmaker M, Jacobs HT, Holt IJ (2006) Replication of vertebrate mitochondrial DNA entails transient ribonucleotide incorporation throughout the lagging strand. EMBO Journal 25: 5358-5371

Yoo SD, Cho YH, Sheen J (2007) *Arabidopsis* mesophyll protoplasts: a versatile cell system for transient gene expression analysis. Nature Protocols 2: 1565-1572

Zhang J, Jia J, Breen J, Kong X (2011) Recent insertion of a 52-kb mitochondrial DNA segment in the wheat lineage. Functional & Integrative Genomics 11: 599-609

Zhang W, Murphy C, Sieburth LE (2010) Conserved RNaseII domain protein functions in cytoplasmic mRNA decay and suppresses *Arabidopsis* decapping mutant phenotypes. Proceedings of the National Academy of Sciences of the United States of America 107: 15981-15985

Zhang X, Hu J (2010) The *Arabidopsis* chloroplast division protein DYNAMIN-RELATED PROTEIN5B also mediates peroxisome division. Plant Cell 22: 431-442

Zhao JH, Curtis D, Sham PC (2000) Model-free analysis and permutation tests for allelic associations. Human Heredity 50: 133-139

Zheng L, Zhou M, Guo Z, Lu H, Qian L, Dai H, Qiu J, Yakubovskaya E, Bogenhagen DF, Demple B, Shen B (2008) Human DNA2 is a mitochondrial nuclease/helicase for efficient processing of DNA replication and repair intermediates. Molecular Cell 32: 325-336

Zoschke R, Liere K, Borner T (2007) From seedling to mature plant: *Arabidopsis* plastidial genome copy number, RNA accumulation and transcription are differentially regulated during leaf development. Plant Journal 50: 710-722

APPENDIX

Plant Material

Seed lines containing T-DNA insertional mutations within the *Arabidopsis* DNA polymerase IB (At3g20540: polIB) gene were obtained either from the *Arabidopsis* Biological Resource Center (ABRC) or the INRA. Three of the four obtained allelic insertion lines had exon insertions: Salk_134274 (polIb-1), WiscDsLoxHs02109D (polIb-2), Flag_463C09 (polIb-3). The fourth T-DNA line (Flag_419G10) was an intron insertion. Each allelic line was backcrossed to wild type (Col-0) at least two times to eliminate any additional genomic T-DNA insertion(s) not within the polIB gene. F2 homozygous polIb-2 mutants were then forward crossed into mtGFP (Logan and Leaver, 2000; Jazayeri et al., 2003) and CycB1:1::GFP (obtained from Leslie Sieburth) reporter lines. Genetic screening and genotypic analysis was conducted to isolate both reporter constructs and mutants with a homozygous allelic confirmation. F3 generation plants were used for experimentation and phenotypic analysis.

Plant Growth Conditions

Seeds were surface sterilized and plated on growth medium consisting of 0.5 x Murashige and Skoog salts (Caisson Labs), 0.5 g/L MES (Sigma-Aldrich), 1% sucrose, and 0.8% agar with a final adjusted pH of 5.7 (Sieburth et al., 2006). Seeds were then imbibed and underwent vernalization at 4°C for 3-5 days. Once removed from the cold or at 0 days post-imbibition (dpi) the seedlings were germinated vertically on plates in a controlled environment growth chamber at constant temperature and continuous light (22°C, and 100 to 120 mE m^2 s). After 5 dpi seedling root phenotypes were scored and genotypes were confirmed by a PCR based method prior to transfer to the soil between 10 - 12 dpi. Watering was closely monitored to prevent water stress on younger plants and for consistent development of seeds and embryos.

DNA Isolation Protocol

DNA extraction Buffer consisted of 200mM Tris-HCl (pH 8.0), 25mM EDTA (pH 8.0), 250mM NaCl, and 0.5% SDS. Other reagents required are 100% ice cold 2-Propanol, 70% ice cold ethanol, and diH2O.

1. Add 500µl of DNA extraction buffer to a micro-centrifuge tube with plant tissue that has previously been pulverized to a fine powder with liquid nitrogen.
2. Vortex samples briefly and centrifuge at 3000 rpm for 10 minutes.
3. Remove supernatant and place into a new micro-centrifuge tube. Add 500µl of ice cold 2-propanol. Invert tube to mix.
4. Centrifuge at 13,000 rpm for 10 minutes.
5. Remove supernatant and add 500µl of ice cold 70% ethanol. Centrifuge for 5 minutes at 14,000 or max rpm.
6. Remove supernatant and allow tubes to dry completely.
7. Suspend DNA by adding 100µl TE buffer or PCR water. Continue with DNA to further applications, like PCR.

Protocal was adapted from Sieburth Lab protocol (Otsuga/ Christensen) and Weigel/ Glazebrook protocol

RTqPCR Gene Expression Analysis and qPCR Relative DNA Abundance

Total RNA was isolated from 7 dpi seedlings as directed from the manufacturer using a Qiagen RNA mini prep kit. RNA quality was confirmed by agarose gel electrophoresis and spectrophotometry. Total RNA was treated with DNAse (Qiagen) prior to performing cDNA synthesis reactions using 2 ug of total RNA as directed by the manufacturer using the Promega cDNA synthesis kit. cDNA was diluted 1000 fold prior to setting up qPCR as directed by the

manufacturer using the Roche 480 light cycler master mix. Quantitative reactions were set up as directed by the manufacturer and conducted using an Epindorf Mastercycler® ep Realplex thermocycler. To measure the relative DNA abundance, 20 ng of genomic DNA was added to each qPCR setup as previously described. All reactions were conducted with technical replicates and in biological triplicates. Calculations for relative gene expression and DNA abundance were conducted using the ΔΔCT equations (Livak and Schmittgen, 2001; Sieburth et al., 2006). Relative gene expression experiments were normalized to Actin 2 gene expression (Zhang et al., 2010). Relative DNA abundance experiments were normalized to plastid RNA polymerase gene (AtRpo) (Preuten et al., 2010).

Chloroplast Counts

To determine chloroplast counts we isolated mesophyllic protoplasts (Yoo et al., 2007) from epidermis leaf peels (Wu et al., 2009) of 4 week old rosette leaf numbers 4 and 5. Protoplasts were isolated from biological triplicates and pooled together prior to examination with an Olympus FluoView FV 300 confocal laser scanning microscope. A red Helium-Neon laser source at 633 nm was used to excite chloroplast for detection. Chloroplasts at the cell midline (greatest area point) were used as our initial focal point. We continued with a Z-scan of 6 to 8 virtual sections at fixed distance intervals down from the midpoint of the cell. We counted chloroplasts and measured the cell planer area using NIH Image J software within the third virtual section down from the cell midpoint.

Mitochondria Counts

Both live wild type and polIb-2 mutant seedlings that contained the mtGFP reporter and were germinated in the dark were sampled at 2 dpi to examine mitochondrial numbers within the hypocotyl epidermis cells. Plants were sampled at an early age to minimize light scatter from

hypocotyl tissue thickness and plants were germinated in the dark to prevent the development of autoflorescent chlorophyll. Cells were counted from the hypocotyl root-shoot junction up to the cotyledons and overlapping DIC and epiflorescence GFP images were acquired using an Olympus BX50 microscope with a 20x objective (NA 0.5) for wild type and 40x objective (NA 0.75) for polIb-2 mutants for each cell position. A composite image of the hypocotyl was made from the individual micrographs using Adobe Photoshop. DIC micrographs were annotated and stacked on top of fluorescent micrographs using NIH Image J as a template to count mitochondria. Image J was used to trace cell borders and transposed to the matching florescent image where Image J measured the cell planer area. For mitochondrial GFP detection and counts Image J was calibrated with a preset "mean" threshold prior to using the particle counter function. Mitochondrial count within the cell planer area in addition to relative size of mitochondria from the GFP signal were obtained in four to eight technical replicates of epidermis cells at each position per hypocotyl. Three biological replicates were examined.

Photosynthesis and Respiration

Seedlings were germinated in glass scintillation with 5 ml of growth medium. Gas exchange experiments were conducted using a Li-Cor 6400XT Portable Photosynthesis System equipped with a 6400-22L Lighted Conifer Chamber (Li-Cor, Inc.) after 3 weeks plant growth. Individual plants (in scintillation vials) were placed in the conifer chamber where light levels, carbon dioxide levels, humidity levels, and leaf temperature could be controlled to generate a light response curve and a carbon assimilation curve (A/Ci). Plants were examined prior to four weeks growth to prevent canopy (shadowing) effect from rosette leaf overgrowth. Data was collected for the generation of the light response curve when conductance, carbon dioxide, and flow rate became stable. Technical replicate readings were recorded (every 5 seconds for 25

seconds) and then averaged based on changing chamber light intensity (PARi: 1.3, 200, 400, 600, 800, 1000, 1200, 1400, 1600, 1800, 2000). Carbon assimilation experiments were conducted in a similar manner except chamber light remained constant (PARi: 1000) and carbon dioxide concentrations were adjusted (45, 100, 200, 300, 400, 600, 800, 1000 μmol). Calculation and the plotting of both the light response and carbon assimilation curves were generated following the manufacturer's directions (Li-Cor) and from the literature (Farquhar, 1980; von Caemmerer, 1981; Donahue, 1997).